DISSERTATION

Reg3β restricts the spatiotemporal accumulation of neutrophil granulocytes within the ischemic heart

Julia Detzer

2020

Max-Planck-Institute
for Heart and Lung Research
W.G. Kerckhoff-Institute

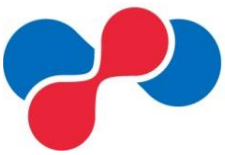

JUSTUS-LIEBIG-
UNIVERSITÄT
GIESSEN

Reg3β restricts the spatiotemporal accumulation of neutrophil granulocytes within the ischemic heart

INAUGURALDISSERTATION

Zur Erlangung des Doktorgrades der Naturwissenschaften

-Doctor rerum naturalium-
(Dr. rer. nat.)

Eingereicht am Fachbereich Biologie und Chemie
der Justus-Liebig-Universität Gießen

Vorgelegt von

Julia Detzer

Bad Nauheim, 2020

Die vorliegende Arbeit wurde am Max-Planck-Institut für Herz- und Lungenforschung in Bad Nauheim angefertigt.

Titel englisch:

Reg3β restricts the spatiotemporal accumulation of neutrophil granulocytes within the ischemic heart

Titel deutsch:

Reg3β schränkt die räumliche und zeitliche Anreicherung von neutrophilen Granulozyten im ischämischen Herz ein

Erstgutachter:
Prof. Dr. Dr. Thomas Braun
Abteilung für Entwicklung und Umbau des Herzens
Max-Planck-Institut für Herz- und Lungenforschung
Ludwigstraße 43
61231 Bad Nauheim

Zweitgutachter:
Prof. Dr. Michael Martin
Institut für Immunologie
Justus-Liebig-Universität Gießen
Heinrich-Buff-Ring 17
35392 Gießen

Für Hans

Table of contents

1 Abstract

The onset of myocardial infarction (MI) promptly activates the innate immune system to initiate endogenous repair processes. However, the initially beneficial effects of the inflammatory response can rapidly become injurious for the heart and promote infarct expansion. Neutrophils are the first immune cells that infiltrate the infarcted heart. They clear the injured area from necrotic cardiomyocytes and matrix debris by phagocytosis and the release of degrading enzymes, promoting cardiac remodeling. If not tightly regulated in a spatiotemporal manner, an excessive and prolonged immune response of neutrophils results in an impaired remodeling process. Hence, a timely resolved clearance of neutrophils is fundamental for the resolution of inflammation and wound healing.

This project reveals a novel mechanism for the removal of cardiac neutrophils from the site of inflammation by the cardiomyocyte-derived C-type lectin Reg3β after the onset of experimental MI. Reg3β co-localized and directly bound to a subpopulation of inflammatory active cardiac neutrophils inducing an aponecrotic-like cell death. In this context, loss of Reg3β led to an increased accumulation of neutrophils in the remote zone of the infarcted heart at day 4 post-MI, which is presumably associated with the destabilization the left ventricular wall causing cardiac rupture. Reg3β-mediated cell death of inflammatory active neutrophils was confirmed by LDH release, intracellular ATP decrease and incorporation of Cytotox Green within the first hour of stimulation in vitro. Morphological changes were characterized by cytoplasmic vacuolization and degradation of intracellular organelles without the formation of apoptotic bodies. Resting or unprimed neutrophils from the bone marrow, blood and spleen were not responsive to Reg3β. Reg3β binding on primary neutrophils was dependent on the recognition of the carbohydrate residues N-Acetylgalactosamin, N-acetylglucosamine and mannose on the cell surface. Consequently, Reg3β was internalized by clathrin-mediated endocytosis and transported to azurophilic granules or rather primary lysosomes presumably via the endolysosomal pathway. Concurrently with Reg3β engulfment, intracellular ROS production rapidly increased and primary lysosomes were destabilized resulting in cytosolic cathepsin release and lysosomal-dependent cell death. Finally, Reg3β binding and induction of cell death facilitated efferocytosis of neutrophils by macrophages in vivo.

In summary, Reg3β mediates a ROS-dependent lysosomal cell death in neutrophils, representing a novel clearing mechanism of inflammatory active neutrophils from the site of cardiac damage after the onset of MI contributing to the resolution of inflammation.

2 Zusammenfassung

Unmittelbar nach einem Herzinfarkt wird das angeborene Immunsystem, welches endogene Reparaturprozesse einleitet, aktiviert. Die zu Beginn förderlichen Auswirkungen der inflammatorischen Reaktion können jedoch bald schädlich für das Herz werden und den Infarktbereich vergrößern. Neutrophile Granulozyten wandern als erste Immunzellen in das infarzierte Herz ein. Durch Phagozytose und Freisetzung von degradierenden Enzymen entfernen sie nekrotische Kardiomyozyten und Matrixtrümmer und begünstigen so das kardiale Remodeling. Eine exzessive und anhaltende Immunantwort von neutrophilen Granulozyten kann jedoch zu einem beeinträchtigten Remodeling führen. Daher ist eine räumlich und zeitlich regulierte Entfernung von neutrophilen Granulozyten von grundlegender Bedeutung für ein Abklingen der Inflammation und Förderung von Wundheilung.

Diese Arbeit beschreibt einen neuen Mechanismus zur Entfernung kardialer neutrophile Granulozyten vom Entzündungsort des infarzierten Herzens durch das aus Kardiomyozyten stammende C-Typ Lektin Reg3β. Es konnte gezeigt werden, dass Reg3β mit einer Subpopulation inflammatorisch aktiver kardialer neutrophile Granulozyten kolokalisiert und direkt an diese bindet, was zu einem aponekrotischen Zelltod führte. In diesem Zusammenhang verursachte der Verlust von Reg3β eine erhöhte Akkumulation von neutrophilen Granulozyten im nicht-infarzierten Bereich 4 Tage nach experimentellem Herzinfarkt, was vermutlich eine Destabilisierung der linksventrikulären Wand und eine Herzruptur zur Folge hatte. Der durch Reg3β-vermittelte Zelltod der neutrophilen Granulozyten wurde durch LDH-Freisetzung, intrazelluläre ATP-Abnahme und der Aufnahme von Cytotox Green innerhalb der ersten Stunde nach Stimulation in vitro bestätigt. Morphologische Veränderungen waren gekennzeichnet durch Vakuolenbildung im Zytoplasma und Degradierung intrazellulärer Organellen ohne die Ausbildung von Apoptosekörperchen. Ruhende oder inflammatorisch inaktive neutrophile Granulozyten aus dem Knochenmark, Blut und Milz waren nicht responsiv auf Reg3β. Die Reg3β-Bindung an kultivierte neutrophile Granulozyten aus der Maus erfolgte über Erkennung der Kohlenhydratreste N-acetylgalactosamine, N-Acetylglucosamin und Mannose auf der Zelloberfläche. Daraufhin wurde Reg3β durch Clathrin-vermittelte Endozytose internalisiert und vermutlich über den endolysosomalen Weg zu azurophilen Granula bzw. primären Lysosomen transportiert. Zeitgleich mit der Aufnahme von Reg3β stieg die intrazelluläre ROS-Produktion rasch an und die primären Lysosomen wurden destabilisiert, was eine Freisetzung von Cathepsin ins Zytosol zur Folge hatte und somit einen lysosomalen Zelltod auslöste. Außerdem förderte Reg3β durch die Induktion des Zelltods die Efferozytose von neutrophilen Granulozyten durch Makrophagen in vivo.

Zusammengefasst stellt die Induktion des ROS-abhängigen lysosomalen Zelltodes durch Reg3β einen neuen Mechanismus zur Entfernung inflammatorisch aktiver neutrophiler Granulozyten aus dem geschädigten Herzen nach Infarkt dar.

3 Introduction

3.1 The neutrophil

3.1.1 Biological characteristics

The family of granulocytes, also known as polymorphonuclear (PMN) leukocytes, comprises several cell types including neutrophils, basophils and eosinophils, which are characterized by a distinctive morphological feature, the cytoplasmic granules (Dancey, Deubelbeiss, Harker, & Finch, 1976). Of them, neutrophils represent the most abundant cell type with about 50-70 % of circulating leukocytes under homeostatic conditions (Bartneck & Wang, 2019). Mature neutrophils differentiate from hematopoietic stem cells in the bone marrow with a turnover rate of 10^{11} cells per day (Cannistra & Griffin, 1988). In order to retain the cells within the bone marrow and form a neutrophil reservoir, the bone marrow stromal cell-derived factor 1 (SDF-1) interacts with its major receptor C-X-C chemokine receptor type 4 (CXCR4) on neutrophils (Q. Ma, Jones, & Springer, 1999). The granulocyte colony-stimulating factor (G-CSF) disrupts the SDF-1/CXCR4 axis and initiates neutrophil mobilization into the blood stream. Circulating neutrophils are relatively short lived cells with a life span of about 5 days in humans and 18 hours in mice (Pillay et al., 2010). Once they become senescent or aged cells, they have been shown to upregulate CXCR4 and migrate back to the bone marrow where the cells undergo apoptosis and are phagocytosed by stromal macrophages (Furze & Rankin, 2008). This in turn stimulates the production of G-CSF creating a positive feedback loop to maintain neutrophils homeostasis (Martin et al., 2003; Rankin, 2010). Hence, CXCR4 elicits a dual role in neutrophil homeostasis by serving as retention signal for neutrophils in the bone marrow and homing signal back to the bone marrow for aged cells from the circulation. Apart from the bone marrow, neutrophil clearance from the circulation also occurs in the liver (Hong et al., 2012) and spleen (Shi, Gilbert, Kokubo, & Ohashi, 2001).

Fully differentiated neutrophils possess four types of granules that are sequentially formed during granulopoiesis in the bone marrow (Borregaard & Cowland, 1997; Borregaard, Sehested, Nielsen, Sengelov, & Kjeldsen, 1995) and contain microbicidal proteins and proteolytic enzymes. Primary or azurophilic granules enclose myeloperoxidase (MPO), serine proteases, defensins and acidic hydrolases and are considered as primary lysosomes or lysosome-related organelles (Bainton, 1999; Dell'Angelica, Mullins, Caplan, & Bonifacino, 2000). Secondary or specific granules are smaller than azurophilic granules and contain lactoferrin, neutrophil gelatinase-associated lipocalin (NGAL) and cathelicidin (Yonggang Ma et al., 2016). The third type, gelatinase granules, are the smallest granules and contain several matrix

metalloproteinases (Faurschou & Borregaard, 2003). Finally, secretory vesicles function as storage organelles for membrane proteins, e.g. integrins and selectins.

3.1.2 Neutrophils under inflammatory conditions

Tissue resident immune cells including macrophages and mast cells function as sentinels for tissue injury or pathogens. Once they come in contact with danger-associated molecular pattern (DAMPs) or pathogen-associated molecular pattern (PAMPs), the resident cells get activated and release pro-inflammatory cytokines to activate endothelial cells and recruit neutrophils and monocytes from the circulation (Kono, Karmarkar, Iwakura, & Rock, 2010; McDonald et al., 2010; Miller et al., 2006). Of them, neutrophils are the first immune cells that infiltrate the site of inflammation and represent key players during the early immune response (Kolaczkowska & Kubes, 2013).

The initial exposure to inflammatory mediators such as DAMPs, PAMPs, chemokine (C-X-C motif) ligand 8 (CXCL8), lipopolysaccharide (LPS) or granulocyte-macrophage colony-stimulating factor (GM-CSF) augments the responsiveness of neutrophils for activating stimuli without gene transcription or translation, a process called priming (Doerfler, Danner, Shelhamer, & Parrillo, 1989). Priming allows a rapid and full activation of neutrophils transforming the cells from senescent circulating to effector cells (Borregaard et al., 1995) with an increased life span to ensure an efficient immune response (Colotta, Re, Polentarutti, Sozzani, & Mantovani, 1992). Priming also stimulates neutrophil degranulation that is the mobilization of cytoplasmic granules to the plasma membrane und subsequent release of their content. Gelatinase and specific granules are the first granules to be exocytosed followed by azurophilic granules (Sengeløv, Kjeldsen, & Borregaard, 1993). Secretory vesicles, in contrast, incorporate into the plasma membrane resulting in the expression of integrins and selectins on the cell surface essential for chemotaxis to the site of inflammation (Borregaard, Kjeldsen, Lollike, & Sengeløv, 1993; Borregaard, Miller, & Springer, 1987). Neutrophil recruitment and transmigration requires adhesive interaction with the activated endothelial cells and involves several molecular steps (N. G. Frangogiannis, 2012) (Figure 1). The first step of capturing neutrophils from the blood stream is predominantly mediated by selectins (Buscher et al., 2010) followed by firm adhesion and crawling through the interaction of integrins and adhesion molecules (Phillipson et al., 2006). Eventually, cell polarization and deformability facilitate infiltration to the site of injury, which is achieved via inter- or paracellular transendothelial migration (Lou, Alcaide, Luscinskas, & Muller, 2007; Wegmann et al., 2006). By continuous release of inflammatory mediators such as leukotriene B4 (LTB4) and CXCL8, the neutrophil recruitment and immune response is amplified and maintained (Lämmermann et al., 2013).

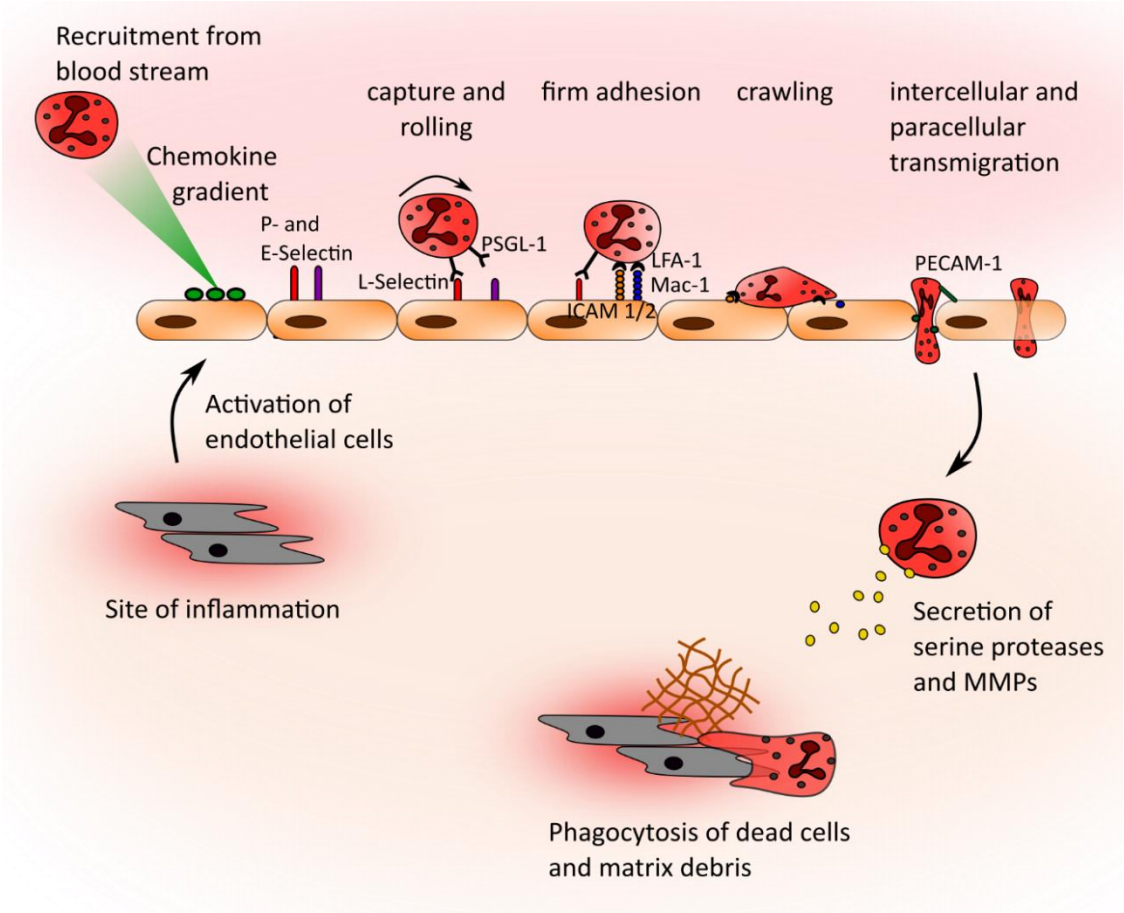

Figure 1: Neutrophil recruitment at the site of sterile injury

Transmigration of neutrophils is carried out by a series of sequential steps. Initially, the release of DAMPs by necrotic cells and pro-inflammatory cytokines by resident immune cells initiates the activation of endothelial cells in the heart. Activated endothelial cells bind chemokines on glycosaminoglycans on their cell surface generating a chemokine gradient to attract neutrophils from the circulation (Kumar et al., 1997). Additionally, endothelial cells upregulate the expression of P- and E-selectins to capture neutrophils onto their cell surface (Butcher, 1991; Lasky, 1992; McEver, Moore, & Cummings, 1995). These selectins bind to P-selectin ligand 1 (PSGL-1) and L-selectin which are expressed by most leukocytes, including neutrophils (Buscher et al., 2010). Rolling motion of the cells emerges from breaking old and forming new bonds of selectins with their ligands (Alon, Hammer, & Springer, 1995; Yago, Zarnitsyna, Klopocki, McEver, & Zhu, 2007). Firm adhesion and crawling on activated endothelial cells is executed by the β-integrins LFA-1 and Mac-1 expressed by neutrophils and their ligands, intercellular adhesion molecule (ICAM) -1 and -2 present on activated endothelial cells (Phillipson et al., 2006). Next, neutrophils start to transmigrate either directly through endothelial cells (intercellular) or through the junctions of endothelial cells (paracellular). The latter is mediated by integrins, adhesion molecules platelet/endothelial cell adhesion molecule 1 (PECAM-1), CD99, and the endothelial cell-selective adhesion molecule (ESAM) (Lou et al., 2007; Wegmann et al., 2006). After transmigration into the inflamed tissue, neutrophils start to secrete degrading enzymes to digest extracellular matrix components and phagocytose necrotic cells (Dehn & Thorp, 2018; Esmann et al., 2010). (Adapted from (Yuan, Shen, Rigor, & Wu, 2012))

Both, under infectious and sterile inflammation, primed and activated neutrophils exhibit four key pro-inflammatory functions. First, increased degranulation and associated release of antimicrobial peptides and serine proteases (Guthrie, McPhail, Henson, & Johnston, 1984) to

digest extracellular matrix components or attack microorganisms. Second, phagocytosis of necrotic cells or microbes to clear the inflamed tissue (Sørensen et al., 2001) and third, enhanced reactive oxygen species (ROS) generation by phosphorylation of cytosolic NADPH oxidase 2 (NOX2) components (Dewas, Dang, Gougerot-Pocidalo, & El-Benna, 2003). Recently, a fourth defense mechanism of neutrophils was identified, called neutrophil extracellular traps or NETs (Brinkmann et al., 2004). NETs are extracellular complexes of chromosomal DNA, citrullinated histones and granule proteins such as MPO or neutrophil elastase (NE), released by neutrophils to trap and kill invading microorganism. Nowadays, NETs are also known to be involved in several non-infectious diseases, as post-injury sterile inflammation and chronic sterile inflammation (Eszter, Gabrielle, & Zsolt, 2017) (Figure 2).

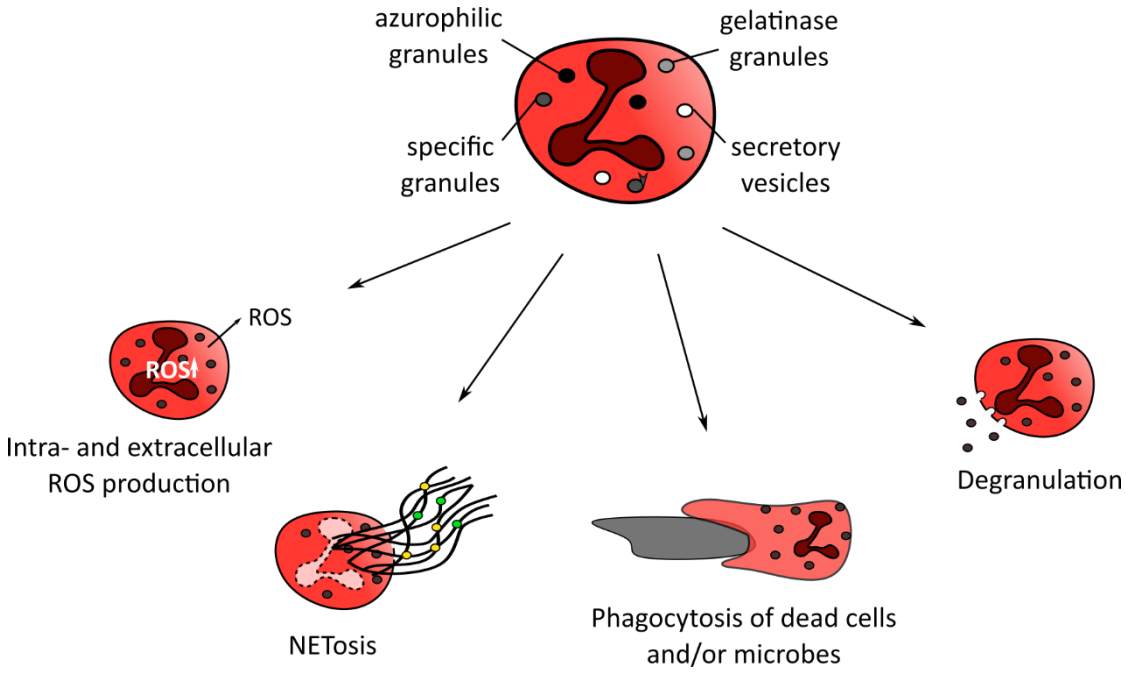

Figure 2: Effector functions of activated neutrophils at the site of inflammation
The main effector functions of primed and activated neutrophils comprise degranulation, phagocytosis, ROS production and the recently added NETosis. Degranulation or exocytosis of granules results in the release of proteolytic enzymes and bactericidal peptides (Guthrie et al., 1984). Phagocytosis of dead cells clears the inflamed tissue and paves the way for healing, whereas removal of pathogens limits tissue injury (Sørensen et al., 2001). NOX2-derived ROS generation at the plasma membrane supports the clearance of bacteria at the site of infection (Dewas et al., 2003) while intracellular ROS generation into phagolysosome lumen ensures the elimination of phagocytosed microbes (Rothe, Oser, & Valet, 1988). The term NETosis is referred to the release of net-like DNA structures armed with neutrophilic granule proteins as MPO and NE to trap and kill bacteria in the tissue (Brinkmann et al., 2004). Two types of NETosis have been described. The suicidal form involves nuclear decondensation, disruption of the membrane and subsequent release of DNA. During the vital NETosis, the nucleus becomes decondensed but the membrane stays intact upon NET release (de Buhr & Köckritz-Blickwede, 2016). (Adapted from (LeBlanc, 2020))

In addition to generating extra- and intracellular ROS, the phagocyte NADPH oxidase NOX2 is known to fulfill diverse functions in neutrophil activity, depending on its cellular location. The enzyme complex consists of several proteins (Figure 3). In resting cells, the heterodimer cytochrome b_{558} composed of the two membrane proteins $gp91^{phox}$ and $p22^{phox}$ resides rather in the membrane of specific granules and secretory vesicles than in the plasma membrane (Borregaard, Heiple, Simons, & Clark, 1983; Nguyen, Green, & Mecsas, 2017) while $p47^{phox}$, $p67^{phox}$, $p40^{phox}$ and the small G-protein Rac2 are cytosolic proteins (Vignais, 2002). Upon neutrophil activation, the cytosolic granules are mobilized to the plasma membrane, resulting in the increased of the cytochrome b_{558} content (Borregaard et al., 1983; Nguyen et al., 2017). In parallel the cytosolic NOX2 components are phosphorylated to enable the assembly with the membrane proteins thereby forming the NOX2 complex (Groemping & Rittinger, 2005). The fully activated NOX2 is now capable of producing ROS by reducing oxygen using cytosolic NADPH as electron donor to superoxide ($O_2^{-\cdot}$), a processed referred to as respiratory burst (Chanock, el Benna, Smith, & Babior, 1994). Together with hydrochlorous acid (HOCl) converted from H_2O_2 by MPO, extracellular ROS production serves as highly effective anti-microbial agent by modifying or damaging bacterial molecules and represent a major defense mechanism of neutrophil immune response (Klebanoff, 1970; Rosen & Klebanoff, 1979). Upon phagocytosis of pathogens, however, specific granules incorporating NOX2 in their membrane fuse with the phagosome and produce ROS into the phagosomal lumen contributing to an antimicrobial milieu (Root, Metcalf, Oshino, & Chance, 1975). Consequently, patients that suffer from chronic granulomatous diseases (CGD) are more susceptible to many infections due to an impaired NOX2 activity in neutrophils (Seger, 2010). Beyond its antimicrobial effects, intracellular ROS has been shown to modify cell signaling (Veal, Day, & Morgan, 2007) including cell death (Akahoshi et al., 1997; Blomgran, Zheng, & Stendahl, 2007; Geering & Simon, 2011; Mihalache et al., 2011; von Gunten et al., 2005), neutrophil migration (Nguyen et al., 2017) and angiogenesis (Zhao, Zhao, Chen, Ahokas, & Sun, 2009).

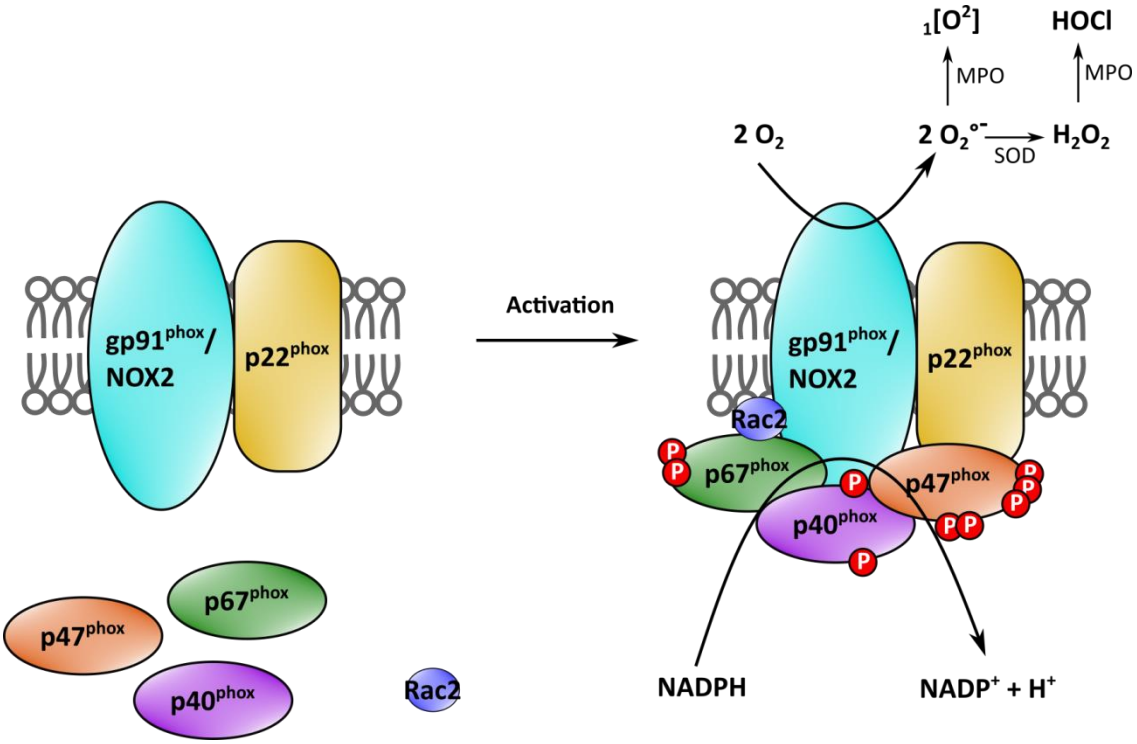

Figure 3: Activation of NOX2 in neutrophils

The NOX2 complex consists of several transmembrane and cytosolic proteins. In resting neutrophils, the components $p47^{phox}$, $p67^{phox}$, $p40^{phox}$ and the small G-protein Rac2 are dispersed in the cytosol, the transmembrane components $gp91^{phox}$ and $p22^{phox}$ are located in the membrane of specific and secretory vesicles and to a small amount in the plasma membrane (Borregaard et al., 1993). Upon priming and activation of neutrophils, the cytosolic proteins are phosphorylated by protein kinase C (PKC) and mitogen-activated protein kinases (MAPK) (Sheppard et al., 2005), which is a prerequisite for the translocation to the membrane and assembly with the transmembrane proteins $gp91^{phox}$ and $p22^{phox}$. $gp91^{phox}$ represents the redox center by transferring electrons from NADPH in the cytosol across the membrane to oxygen thereby generation the $O_2^{\cdot-}$ (Smith, Connor, Chen, & Babior, 1996). To prevent intoxication by ROS, the antioxidant scavenging enzyme superoxide dismutase (SOD) transforms two $O_2^{\cdot-}$ into the less toxic H_2O_2 (Imlay, 2008). MPO in azurophilic granules further converts H_2O_2 into HOCl or directly converts $O_2^{\cdot-}$ into singlet oxygen (Klebanoff, 1970). (Adapted from (Beaumel et al., 2017))

3.1.3 Neutrophil heterogeneity

There is growing evidence that beside their pro-inflammatory activity, distinct neutrophil subsets fulfill different roles during infection, inflammation and cancer (Tsuda et al., 2004) such as modulation of adaptive immunity, resolution of inflammation (Tsuda et al., 2004), neoangiogenesis (Massena et al., 2015) and tumor-associated immune response (Fridlender et al., 2009). Under homeostatic conditions, neutrophil subsets with specific gene and transcription factor expression profiles already exist in the bone marrow (Velten et al., 2017): proliferative precursor cells or pre-neutrophils expressing CD117 and CXCR4, which differentiate into non-proliferative immature $CXCR2^{neg}$ $CD101^{neg}$ and mature $CXCR2^{pos}$ and $CD101^{pos}$ neutrophils (Evrard et al., 2018). Once released from the bone marrow, neutrophil ageing associated with

phenotypical changes of decreased CD62L as well as increased CD11b and CXCR4 expression (Adrover, Nicolás-Ávila, & Hidalgo, 2016; Casanova-Acebes et al., 2013), hypersegmented nucleus and enhanced integrin activation (Casanova-Acebes et al., 2013) contributes to heterogeneity in the circulation. Moreover, mass spectrometry analysis provided hints for tissue specific subsets (Becher et al., 2014) that may be differentially stimulated by tissue-derived signals, i.e. a large population of $CXCR4^{pos}$ neutrophils were found in the lungs to rapidly initiate an immune response against pathogens (L. G. Ng, Ostuni, & Hidalgo, 2019; Yipp et al., 2017).

The phenotypic and functional diversity of neutrophils under inflammatory conditions has been explored in the last years, as well. Here, inflammatory mediators like DAMPs, PAMPs, cytokines and growth factors released from the site of infection or inflammation induce the expression of surface receptors, the secretion of various cytokines (Kolaczkowska & Kubes, 2013; Nourshargh, Renshaw, & Imhof, 2016) and increase the life span of neutrophils by apoptosis inhibition (Geering, Stoeckle, Conus, & Simon, 2013), indicating phenotypic changes of neutrophils upon exposure to external stimuli. Interestingly, aged neutrophils were found to be more effective as first line of defense compared to young neutrophils by means of enhanced bactericidal functions i.e. increased ROS generation and phagocytosis (Uhl et al., 2016). In the context of resolution of inflammation, neutrophil populations with a reparative phenotype have been identified. $CD49d^{+}CXCR4^{+}VEGFR1^{+}$ pro-angiogenic neutrophils produce matrix metalloproteinase 9 (MMP9) in response to vascular endothelial growth factor A (VEGF-A) and contribute to vascular growth (Massena et al., 2015). Another source for neutrophil plasticity and heterogeneity is represented by reverse migrating neutrophils out of the inflamed tissue, which exhibit an increased life span and capacity for ROS generation and express $ICAM1^{high}$ $CXCR1^{low}$ (Buckley et al., 2006). Neutrophils migrating to secondary lymphoid organs, on the other hand, express an activated phenotype with $CD11b^{high}$ $CD62^{low}$ and $CXCR2^{low}$ (H. R. Hampton, Bailey, Tomura, Brink, & Chtanova, 2015). Whether the different phenotypes under inflammatory conditions arise from tissue specific environmental stimuli, pre-existing subsets in the bone marrow and circulation or both, remains elusive (Kolaczkowska & Kubes, 2013).

3.2 Cardiac remodeling after acute myocardial infarction

The onset of acute MI triggers intrinsic repair mechanisms based on biochemical, molecular, cellular and structural changes, a process referred to as cardiac or left ventricular (LV) remodeling (Gaudron et al., 2001; Hochman & Bulkley, 1982; McKay et al., 1986; Pfeffer, Pfeffer, Fletcher, & Braunwald, 1991) (Figure 4). Immediately after cardiac injury, necrotic cardiomyocytes release DAMPs such as high-mobility group box 1 (HMBG1), interleukin- (IL-) 1α,

RNA or heat shock proteins (HSP). In both humans and mice, DAMPs function as pro-inflammatory mediators and promptly activate the innate immune system to clear dead cells and degraded matrix components from the infarct area within the first days post-MI (Dewald et al., 2004; Nikolaos G. Frangogiannis, 2014; Yang et al., 2002). Thereafter an anti-inflammatory phase follows to initiate resolution of inflammation, fibroblast proliferation and neovascularization, which lasts for about one to two weeks in mice (Nikolaos G. Frangogiannis, 2014) and for several weeks in humans (Dewald et al., 2004; Yang et al., 2002). Owing to a very low regeneration capacity of cardiomyocytes in mammals (Bergmann et al., 2009), the massive loss of contractile tissue is eventually compensated by the formation of a collagenous scar to maintain cardiac architecture and functionality (Cohn, Ferrari, & Sharpe, 2000; Hochman & Bulkley, 1982). Scar maturation is completed within three to four weeks in mice (Nikolaos G. Frangogiannis, 2014) and in humans within weeks to months (Dewald et al., 2004; Yang et al., 2002).

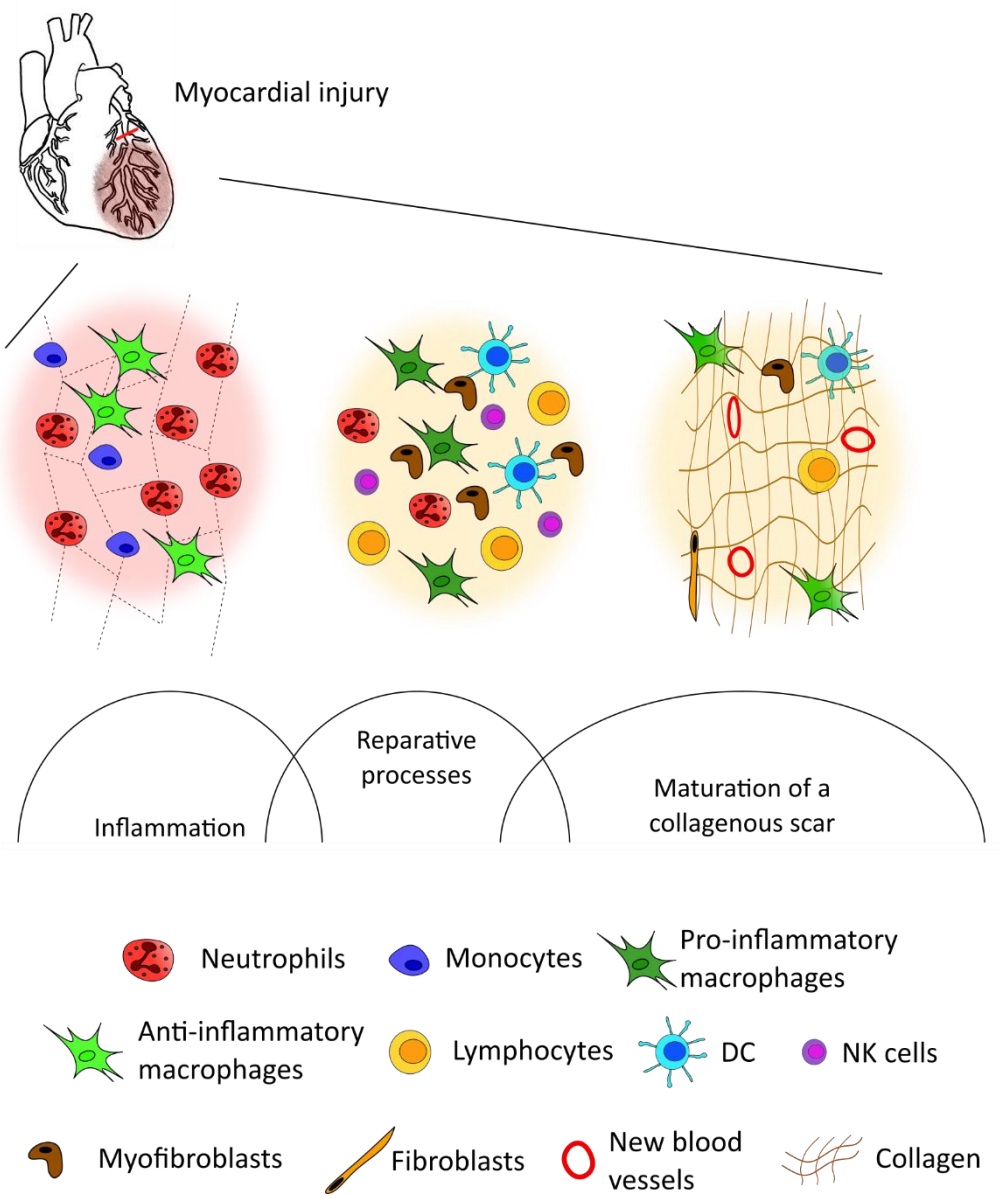

Figure 4: Cardiac remodeling after the onset of MI

The sudden loss of myocardial tissue initiates endogenous repair mechanisms characterized by three overlapping phases. DAMPs released by necrotic cardiomyocytes activate the innate immune system and attract leukocytes to the site of injury (N. G. Frangogiannis, 2012; van Hout, Arslan, Pasterkamp, & Hoefer, 2016). The inflammatory phase is dominated by infiltrating neutrophils followed by monocytes that differentiated into macrophages within the tissue (Y. Ma, Yabluchanskiy, & Lindsey, 2013). Both cell types pave the way for cardiac healing by phagocytosing dead cardiomyocytes and matrix debris (N. G. Frangogiannis, 2012). However, subsequent resolution of inflammation is essential for cardiac healing is the resolution of inflammation. Pro-inflammatory macrophages are replaced by anti-inflammatory or reparative macrophages. They remove apoptotic neutrophils from the site of inflammation via efferocytosis, secrete anti-inflammatory mediators and promote angiogenesis and tissue healing (Nahrendorf et al., 2007; Ortega-Gómez, Perretti, & Soehnlein, 2013). Fibroblasts transdifferentiate into myofibroblasts, the main source of collagen, which contributes to scar formation (Nikolaos G. Frangogiannis, Mendoza, Smith, Michael, & Entman, 2000). Finally, neovascularization (Abbott et al., 2004) and the formation of a collagenous scar to maintain cardiac architecture and functionality is initiated (Dobaczewski, Gonzalez-Quesada, & Frangogiannis, 2010; N. G. Frangogiannis, 2012). (Adapted from (Westman et al., 2016))

The outcome of cardiac repair is dependent on a finely balanced and timely coordinated transition between these three healing processes and is executed by a complex interaction amongst tissue-resident cells (cardiomyocytes, endothelial cells, fibroblasts, macrophages, dendritic cells (DC) and mast cells) and invading immune cells (neutrophils, monocytes, macrophages, natural killer (NK) cells and B- and T-lymphocytes) (Burchfield, Xie, & Hill, 2013; N. G. Frangogiannis, 2012; Humeres & Frangogiannis, 2019; Prabhu & Frangogiannis, 2016; Segers, Brutsaert, & De Keulenaer, 2018; Talman & Kivelä, 2018). Finally, chemokines as key players for the orchestration of reparative processes in the heart complete the complexity of cardiac remodeling (B. Chen & Frangogiannis, 2020). Chemokines in general can be distinguished based on the arrangement of their conserved N-terminal cysteine residues namely CC, CXC and CX_3C chemokines whereas the X represents any other amino acid than cysteine (Wilbanks et al., 2001; Zhu, Han, Peng, Qin, & Wang, 2012). Besides their main function of regulating leukocyte recruitment, they also modulate the phenotype of immune cells, angiogenesis and fibroblast proliferation (B. Chen & Frangogiannis, 2020).

Although the early inflammatory response attenuates noxious processes (N. G. Frangogiannis, 2012), inflammation can also harm the host tissue if not tightly regulated. An excessive immune cell infiltration and activation results in adverse cardiac remodeling with the consequence of infarct size expansion and left ventricular wall thinning (Ong et al., 2018; Panizzi et al., 2010). On the other hand, suppression of inflammation by inhibition of the complement system or immune cell infiltration can result in the accumulation of granulation tissue, poor wound healing and increased fibrosis (Horckmans et al., 2017; van Amerongen, Harmsen, van Rooijen, Petersen, & van Luyn, 2007).

3.2.1 The role of inflammation in cardiac remodeling

After the onset of MI, DAMPs and ROS generation in the ischemic heart are involved in cardiac remodeling. DAMPs released by necrotic and stressed myocardial cells in the infarct area activate the complement system (Christia & Frangogiannis, 2013; Hill & Ward, 1971) and bind to pattern recognition receptors (PRRs) of endothelial cells and tissue resident DCs, monocytes, macrophages, lymphocytes and fibroblasts. The activated tissue resident immune cells in turn augment the pro-inflammatory response by releasing inflammatory mediators comprising IL-6, IL-8, IL-1β and tumor necrosis factor (TNF)α (Nikolaos G. Frangogiannis et al., 1998) (Gordon, Shaw, & Kirshenbaum, 2011; Gwechenberger et al., 1999). They further mediate the recruitment of leukocytes to the site of injury (N. G. Frangogiannis, 2012; van Hout et al., 2016) by releasing chemokines that bind to glycosaminoglycans on endothelial cell surfaces in the heart (Kumar et al., 1997; Zarbock, Ley, McEver, & Hidalgo, 2011) resulting in locally high chemokine

concentrations. In mice, macrophage inflammatory protein-2α (MIP-2α) also known as CXCL2, LTB4, CXCL1, and complement component 5a (C5a) are the main drivers for neutrophil chemotaxis and activation under pathological conditions (Bejjani et al., 2020; Ivey, Williams, Collins, Jose, & Williams, 1995; Sanz & Kubes, 2012). Shortly after neutrophil accumulation, Ly6C^{hi} pro-inflammatory monocytes infiltrate the injured heart in response to CCL2 and differentiate into macrophages within the tissue (Leuschner et al., 2012; Nahrendorf et al., 2007). Both cell types primarily remove dead cells by phagocytosis and secrete degrading enzymes i.e. proteases and MMPs to clear the infarcted heart from extracellular matrix and cell debris (Dehn & Thorp, 2018; Esmann et al., 2010). Moreover, elevated ROS levels, generated by NOX2 of infiltrating neutrophils and macrophages (Zhao, Zhao, Yan, & Sun, 2009) and by the cardiomyocyte NOX4 (Infanger et al., 2010), mediate heart failure by exerting deleterious effects on cardiomyocytes and vascular cells (Dhalla, Elmoselhi, Hata, & Makino, 2000). However, some data demonstrated that ROS production stimulates signal transduction to activate and regulate chemotaxis and cytokine production of leukocytes (Dhalla, Elmoselhi, Hata, & Makino, 2000; Lefer & Granger, 2000; Sellak, Franzini, Hakim, & Pasquier, 1994). In contrast to neutrophils, which are rapidly removed from the infarction area within 7 days, macrophages acquire a reparative phenotype and remain in the damaged tissue during the reparative phase (N. G. Frangogiannis, 2012; Y. Ma et al., 2013).

3.2.2 Resolution of inflammation and initiation of reparative processes

After clearing the infarction area from necrotic cardiomyocytes and degraded extracellular matrix, new structures are required to maintain tissue integrity and heart function. Here, the resolution of inflammation is an essential to initiate the proliferative phase and goes along with the restriction of neutrophil activity and clearance of the cells from the inflamed tissue. Most neutrophils are thought to undergo constitutive or spontaneous apoptosis, a non-inflammatory cell death accompanied with decreased cell function (Savill et al., 1989). However, recent findings proved the ability of neutrophils to migrate back into the vasculature in sterile inflammation (J. Wang et al., 2017). Whether apoptosis is the most relevant pathway for neutrophil removal or other still unknown mechanisms are equally important, is not fully understood.

Apoptotic neutrophils release so called ‘find me’ signals and flip phosphatidylserine (PS) on the outside of the plasma membrane facilitating subsequent efferocytosis by macrophages (Rather, 1970). The term efferocytosis was defined by deCathelineau and Henson as ‘to carry to the grave’ and refers to the recognition and engulfment of dead cells by phagocytes (deCathelineau & Henson, 2003; Shi et al., 2001). Efferocytosis of neutrophils triggers a phenotypical change of

macrophages into anti-inflammatory cells and the secretion of IL-10 and transforming growth factor (TGF) β (Ortega-Gómez et al., 2013). Additionally, pro-inflammatory macrophages are replaced by newly recruited Ly6C^{high} monocytes that give rise to locally proliferating and reparative Ly6C^{low} macrophages (Hilgendorf et al., 2014). Together with monocytes, other leukocytes such as DCs and NK cells infiltrate the damaged heart. They mediate the phenotypic switch of the pro-inflammatory to the reparative phase by secreting anti-inflammatory mediators such as TGFβ and IL-10 and directly interacting with monocytes (Anzai et al., 2012; Knorr, Münzel, & Wenzel, 2014; Zouggari et al., 2013). Besides the cells from the innate immune system, B- and T-lymphocytes also contribute to early myocardial healing. After MI, the number of B- and T-cells immediately increases in the injured area and peaks around day 7 (Yan et al., 2013). CD4^{+} T-lymphocytes regulate the infiltration of pro-inflammatory Ly6C^{high} monocytes (Hofmann et al., 2012) whereas regulating T-cells (T_{regs}) promote their differentiation into reparative macrophages by the secretion of IL-10, IL-13 and TGFβ (Weirather et al., 2014). The direct influence of B-cells to cardiac healing, though, remains unclear, yet (Keppner et al., 2018). TGFβ is a pleiotropic cytokine with complex functions during cardiac healing. It possesses potent anti-inflammatory properties by modulating the phenotypical activity of leukocytes (Fan, Ruan, Sensenbrenner, & Chen, 1992; Werner et al., 2000) and attenuates further neutrophil infiltration by the suppressing the expression of adhesion molecules on endothelial cells (Gamble & Vadas, 1988). Additionally, TGFβ suppresses CXCL10, which is upregulated after infarction and inhibits angiogenesis (Nikolaos G. Frangogiannis et al., 2000). Angiogenesis is critical for cardiac healing since the formation of new blood vessel can rescue injured or stressed cardiomyocytes thereby avoiding infarct expansion and adverse remodeling (Cochain, Channon, & Silvestre, 2013). Neovascularization is further initiated by VEGF and CXCL12 that regulate the recruitment of endothelial progenitor cells and modulate the formation of new blood vessels (Abbott et al., 2004; Liehn, Postea, Curaj, & Marx, 2011). Together with CCL2 (Morimoto et al., 2006), TGFβ also modulates the transdifferentiation of fibroblasts into myofibroblasts (Desmoulière, Geinoz, Gabbiani, & Gabbiani, 1993), which are the dominant source of collagen (Nikolaos G. Frangogiannis et al., 2000). Together with proteoglycans and glycoproteins, collagen constitute the extracellular matrix for scar formation (Liehn et al., 2011; Lindsey, Mann, Entman, & Spinale, 2003). An additional important anti-inflammatory cytokine IL-10 prevents excessive inflammation by inhibiting the production of pro-inflammatory cytokines and chemokines. Furthermore, it promotes the synthesis of tissue inhibitor of metalloproteinase (TIMP), that contribute to extracellular matrix stabilization important for functional recovery of the heart (N. G. Frangogiannis et al., 2000; Steenbergen & Frangogiannis, 2012).

3.2.3 Maturation of a collagenous scar

Lastly, the maturation phase, determined by an attenuated inflammation, neovascularization, and the formation of a collagenous scar, completes the wound healing processes (Dobaczewski et al., 2010; N. G. Frangogiannis, 2012). The majority of myofibroblasts and macrophages are removed from the site of inflammation presumably via apoptosis, though a small population of myofibroblasts persists within the infarction area (Dobaczewski et al., 2010; Takemura et al., 1998; van den Borne et al., 2009). Subsequently, the provisional matrix and granulation tissue are gradually replaced by scar tissue scar tissue that consists of collagen type I, II, IV and VI with the most abundant components being collagen type I and type III (Bishop, Greenbaum, Gibson, Yacoub, & Laurent, 1990; Swift et al., 2013). MMPs including MMP-2 (gelatinase A), MMP-9 (gelatinase B) and MMP-13 (type I collagenase) are major regulators of collagen deposition and matrix organization. They are present in the myocardial interstitium and are activated by free radicals, hypoxia and cytokines such as TNFα and IL-1β (Creemers, Cleutjens, Smits, & Daemen, 2001; Nian, Lee, Khaper, & Liu, 2004; Siwik, Chang, & Colucci, 2000) that are known to be upregulated in MI (Spinale et al., 2000). The final maturation of the scar is modulated by fibronectin and collagen through TNF, TGFβ and osteopontin (or Eta-1) (Deten et al., 2001; Nian et al., 2004) and includes collagen crosslinking and alignment to stabilize the heart structure and maintain cardiac function. To restore the supply of oxygen and nutrients via the formation of new blood vessels, angiogenesis is activated immediately after the onset of MI and mediated by VEGF, IL-8 and interferon-inducible protein 10 (IP10) which are secreted by mast cells, macrophages and myofibroblasts (Nian et al., 2004).

3.2.4 Therapies for cardiovascular diseases

Nowadays, improvements in clinical therapies for heart attacks have resulted in a decrease in mortality (Moran et al., 2014; Mozaffarian et al., 2015; Nichols, Townsend, Scarborough, & Rayner, 2014). The most successful current therapies including percutaneous coronary intervention (PCI), thrombolysis and coronary artery bypass graft (CABG) surgery aim to restore the occluded blood vessel as early as possible to minimize the ischemia-induced loss of the contractile myocardium (Dalen et al., 1988; Markis et al., 1981). Although improving short-time survival after MI, this strategy can extent tissue damage and infarct size by myocardial reperfusion injury (Jennings, Sommers, Smyth, Flack, & Linn, 1960; Keeley & Hillis, 2007; Yellon & Hausenloy, 2007). The reperfusion of the infarcted tissue maintains intact cardiomyocytes but augments the disruption of already damaged cells (Reimer, Lowe, Rasmussen, & Jennings, 1977). Moreover, it leads to interstitial hemorrhage from injured vessels, which in turn increases the

interstitial pressure and activates signaling pathways resulting in apoptotic and necrotic tissue injury (Yellon & Hausenloy, 2007). However, there are currently no alternative strategies that show a comparable progress in terms of survival rates. Beyond that, long-term mortality due to myocardial infarction-related heart insufficiency or recurrence of MI remains high or is even increasing (Chamberlain et al., 2015; Moran et al., 2014; Smolina, Wright, Rayner, & Goldacre, 2012), making cardiovascular diseases still one of the most common cause of death worldwide (Roth et al., 2018).

The development of novel cardioprotective strategies has gained more interest in recent years. The importance of the early pro-inflammatory phase for reparative processes in the heart has been recognized since early clinical studies attempt to ameliorate cardiac healing by using of broad immunosuppression but turned out to be fatal in terms of functional recovery post-MI (Giugliano, Giugliano, Gibson, & Kuntz, 2003). Further clinical immunomodulatory therapeutic approaches attempted to target specific cell types or early initiators of inflammation while maintaining the beneficial aspects of the initial immune response. They included the included the antibody-mediated inhibition of leukocyte infiltration via the integrin adhesion receptor (Baran et al., 2001), suppression of complement activation via C5a inhibitors (_ENREF_83Mahaffey et al., 2003), depletion of inflammatory cytokines as IL-1, IL-6 and TNFα (Mann et al., 2004) and the inhibition of an excessive inflammation by blocking mast cell degranulation (Holmes et al., 2002). Additionally, some trials focused on the late phase of cardiac healing by modulating B- and T-lymphocytes (Zouggari et al., 2013). However, most of these studies were not effective in reducing infarct size and failed to improve cardiac function or are still conflicting because of a high variability in the study populations, study design and outcome measures (Panahi et al., 2018). Due to the complex and dynamic nature of the immune response as well as the pleiotropic effects of inflammatory cytokines, the target cells, timing and dosage of medication should be carefully considered to avoid severe side effects and optimize infarct healing (Panahi et al., 2018).

3.2.5 The role of neutrophils in cardiac repair and resolution of inflammation

Neutrophils have long been considered detrimental for cardiac repair by promoting tissue injury (Wright, Moots, Bucknall, & Edwards, 2010). However, several clinical studies attempting to suppress neutrophil infiltration and activity failed to improve the reparative processes of the heart (Baran et al., 2001; Faxon, Gibbons, Chronos, Gurbel, & Sheehan, 2002; Harlan & Winn, 2002). Recent findings proved neutrophils to be crucial for cardiac healing, as depletion of neutrophils in the early phase of cardiac remodeling caused a pronounced pro-inflammatory phenotype of macrophages, increased fibrosis and impaired cardiac function resulting in heart

failure of infarcted mice (Horckmans et al., 2017). Furthermore, a study of Daseke et al. could imply different functions of neutrophils at different stages during post-MI cardiac repair based on proteomic findings. Day 1 neutrophils displayed an increased degranulation activity and enhanced MMP secretion whereas neutrophils at day 3 upregulated apoptotic pathways and modulated extra cellular matrix (ECM) organization. Day 5 neutrophils amplified the ECM remodeling and switched to a reparative phenotype contributing to scar formation at day 7 (Daseke et al., 2019). It has been demonstrated, that neutrophils possess reparative functions by directly contributing to endothelial repair (Alard et al., 2015) and promoting angiogenesis via the release of MMPs and VEGF (Massena et al., 2015; J. Wang et al., 2017) (Figure 5). In addition to directly controlling the growth of new blood vessels, neutrophils secrete annexin A1 to promote macrophage polarization towards a pro-angiogenic phenotype with increased VEGF secretion (Ferraro et al., 2019). The polarization of macrophages towards a reparative phenotype is further initiated by NGAL released by apoptotic neutrophils (Mishra et al., 2005). These macrophages are characterized by the expression of proto-oncogene tyrosine-protein kinase MER (MerTK) (Horckmans et al., 2017) and the secretion of anti-inflammatory mediators as TGFβ, IL-10 and VEGF (Ortega-Gómez et al., 2013). Lastly, neutrophil granules are filled with MMPs and serine proteases that degrade collagens (M. Lin et al., 2008) and extracellular matrix components (L. L. Ng et al., 2011) to pave the way for leukocyte infiltration and wound healing. An excessive accumulation and prolonged persistence on the other hand contribute to adverse remodeling and further tissue injury (Panizzi et al., 2010). Hence, a spatiotemporal accumulation of distinct neutrophil phenotypes that do not only regulate the early inflammatory phase, but also modulate the resolution of inflammation is fundamental cardiac healing processes and restoration of heart structure and function (Soehnlein, Steffens, Hidalgo, & Weber, 2017).

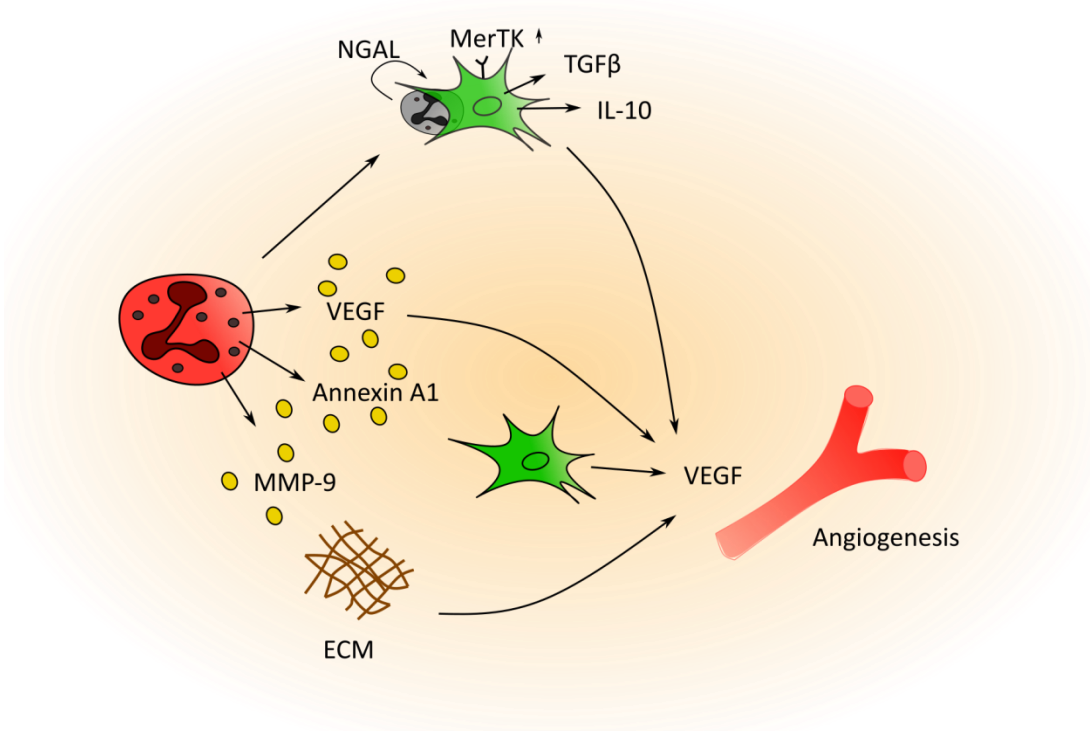

Figure 5: Neutrophils contributing to wound healing after MI

Next to their pro-inflammatory response, neutrophils also contribute to tissue restoration after injury by contributing to angiogenesis and polarization of macrophages. Apoptotic neutrophils release NGAL to induce the polarization of macrophages towards a reparative phenotype characterized by the expression of the efferocytosis maker MerTK and the production of the anti-inflammatory mediators TGFβ and IL-10 (Horckmans et al., 2017; Ortega-Gómez et al., 2013). Annexin A1 and MMP-9 are released by neutrophils and promote the secretion of the pro-angiogenetic factor VEGF by macrophages (Ferraro et al., 2019) and the ECM (Nozawa, Chiu, & Hanahan, 2006). In addition, neutrophils also secrete VEGF by themselves.

Neutrophils are primarily removed by spontaneous apoptosis (Savill et al., 1989) or by death receptor-mediated apoptosis via the secretion of the ligands TNFα and Fas-ligands by macrophages (Renshaw et al., 2000). The trigger for spontaneous apoptosis remains elusive, though. Apoptotic neutrophils in turn secrete annexin A1 and lactoferrin, which suppress neutrophil infiltration by disrupting the neutrophil-endothelium interaction and attract phagocytosing macrophages (X. Liu et al., 2012). The removal of neutrophils is influenced by 'find-me' (lipid mediators and nucleotides) (Truman et al., 2008) and 'eat-me' signals (externalized phosphatidylserine, altered lipids), which are expressed by dying neutrophils and are important for the recognition by phagocytosing cells (Scannell et al., 2007).

Beside the clearance via cell death, new findings demonstrated a reverse migration of neutrophils from the tissue back to the circulation in zebrafish (Mathias et al., 2006), mice (J. Wang et al., 2017) and even humans (Buckley et al., 2006). Neutrophils migrating out of the inflamed tissue featured a phenotype of 'aged' neutrophils with $CXCR4^{hi}$ expression and low

inflammatory activity and promoted the resolution of inflammation and (J. Wang et al., 2017). Nevertheless, the removal of neutrophils from the site of inflammation must be tightly regulated to avoid an increased susceptibility to infections due to an accelerated removal (Seger, 2010) or to avoid enhanced tissue injury due to a delayed clearance (Panizzi et al., 2010). The mechanisms for a timely restriction of neutrophil accumulation into the ischemic heart are not yet fully understood, though.

3.3 Regenerating islet-derived protein (Reg) 3β

Reg3β is a C-type lectin that belongs to the Reg protein family. The Reg family in general consists of four groups: Reg1, Reg2, Reg3 and Reg4 (Okamoto, 1999). Reg proteins were independently discovered in the context of pancreatic diseases like pancreatic stones formation (De Caro, Lohse, Sarles, & communications, 1979), regenerating islets after a pancreatectomy in rats (Terazono et al., 1988), acute pancreatitis samples (Keim, Rohr, Stöckert, & Haberich, 1984) and hepatocellular carcinomas (Z. Chen, Downing, & Tzanakakis, 2019; Lasserre, Christa, Simon, Vernier, & Bréchot, 1992).

Humans express five Reg protein members, REG1A, REG1B, REG3A, REG3B and REG4 while in rodents seven Reg protein orthologues are detectable, namely Reg1, Reg2, Reg3α, Reg3β, Reg3γ, Reg3δ and Reg4 (Z. Chen et al., 2019; Hartupee et al., 2001). Most Reg proteins share high homologous similarities between two different species, i.e. mouse and human, or within one species (Z. Chen et al., 2019) (Figure 6). Reg encoding genes from humans and rodents are approximately 3kb in size with six exons and five introns and share the same chromosomal locus (2p12), except for Reg4. (Abhirath, Anne-Fleur, & Emmanuel, 2012; Hartupee et al., 2001) Reg4 is the last discovered Reg protein and differs from the other Reg proteins with seven introns and a chromosomal locus of 1p11 (Violette et al., 2003).

A

	REG1A	REG1B	REG3A	REG3G	REG4
Reg1	74.53%	72.05%	47.53%	48.47%	34.07%
Reg2	65.12%	63.37%	42.61%	40.68%	32.59%
Reg3a	43.53%	44.51%	61.85%	65.52%	35.25%
Reg3b	41.72%	42.28%	69.54%	68.79%	31.88%
Reg3g	44.87%	44%	67.05%	64.94%	36.23%
Reg3d	43.29%	44.58%	49.71%	51.15%	26.62%
Reg4	32.69%	33.97%	35.03%	32.28%	66.24%

B

	Reg1	Reg2	Reg3a	Reg3b	Reg3g	Reg3d	Reg4
Reg1		75.74%	41.10%	41.06%	46%	42.42%	31.37%
Reg2			39.55%	40.26%	41.22%	40.94%	27.59%
Reg3a				59.54%	58.62%	50%	33.54%
Reg3b					71.68%	54.22%	36.88%
Reg3g						50%	35.85%
Reg3d							27.85%
Reg4							

High similarity — Low similarity

Figure 6: Sequence homology of human and mouse Reg proteins

(A) Sequence homology between Reg proteins of humans (capital letters) and mice (small letters) and (B) between murine Reg proteins to each other. (Adapted from (Z. Chen et al., 2019))

The superfamily of C-type lectins, which comprises more than 1000 proteins subdivided into 17 groups, characterized by one distinctive feature, the C-type-like lectin domain (CTLD) (Dieckgraefe et al., 2002). They exhibit a binding affinity to mannose-containing and galactose containing carbohydrates, respectively through conserved residues in the CTLD comprising EPN (Glu-Pro-Asn) and OPD (Gln-Pro-Aps) motifs (Brown, Willment, & Whitehead, 2018; Weis, Drickamer, & Hendrickson, 1992; Zelensky & Gready, 2005). C-type lectins exist as free or transmembrane proteins and are involved in diverse physiological and pathophysiological conditions. Soluble C-type lectins function as growth factors, opsonins, antimicrobial proteins, components of the ECM and as regulators of processes such as development, respiration, coagulation, angiogenesis and inflammation (Brown et al., 2018).

Reg proteins belong to the subgroup 6 and are secreted C-type lectins (Dieckgraefe et al., 2002). In contrast to common C-type lectins, they selectively bind to carbohydrate structures on glycoproteins through the EPN motif (Dieckgraefe et al., 2002; Lehotzky et al., 2010) in a Ca^{2+}-independent manner (Drickamer, 1999). Another feature of the Reg proteins, except of Reg4 (Ho et al., 2010), is a trypsin cleavage site near the N-terminus followed by a putative signal peptide. Trypsin digestion results in a soluble short peptide and a remaining insoluble fragment that forms fibrils whose functions are not clear, yet (Z. Chen et al., 2019; Graf et al., 2001). Although the discovery of Reg proteins was about half a century ago, the regulation of their expression, function und physiological and pathophysiological conditions and signal transduction is still relatively unknown. Reg proteins appear to be pleiotropic with overlapping functions under normal conditions (Z. Chen et al., 2019). However, most studies focused on one particular Reg protein, resulting in many different functions of individual Reg proteins lacking a common basis.

Certain Reg3 proteins, including Reg3β, Reg3γ and the human HIP/PAP proved to be bactericidal by binding to specific peptidoglycans on the bacteria wall. The murine Reg3γ and human HIP/PAP homologue were capable to control gut microbiota in mice by spatially segregating gram-positive bacteria from the surface of the small intestine epithelium (Z. Chen et al., 2019; Mukherjee et al., 2014; Vaishnava et al., 2011). The bactericidal mechanism was based on the formation of an oligomeric pore in the bacterial wall and was completely blocked by the addition of soluble N-acetylglucosamine polymers (Mukherjee et al., 2014). Reg3β was shown to have antimicrobial effects on both, gram-negative and gram-positive bacteria (Farinholt, Dinh, & Kuspa, 2019; Miki, Holst, & Hardt, 2012; Stelter et al., 2011) by binding to N-acetylglucosamine and mannose polysaccharides on the bacteria cell wall via the EPN motif in a Ca^{2+} independent manner (Cash, Whitham, Hooper, & purification, 2006; Lehotzky et al., 2010). Mutations in the EPN motif resulted in reduced binding to the cell wall and diminished bactericidal effects (Lehotzky et al., 2010). Therefore, murine Reg3α is unable to bind carbohydrate residues due to an EPN motif deficiency. Despite their bactericidal role in the intestine, Reg proteins are implicated in different pathologies such as cancer (Cavard et al., 2006; Violette et al., 2003), diabetes (Astorri et al., 2010) and inflammation or injury not only in the pancreas but also in other tissues, including the digestive tract (Hervieu et al., 2006), brain (Duplan et al., 2001), and heart (Loerchner et al., 2015). The murine Reg3β in particular is reported to be upregulated in the early phase of pancreatitis (Dieckgraefe et al., 2002), to modify cell tumor function by interfering the uptake of extracellular vesicles (Bonjoch, Gironella, Iovanna, & Closa, 2017) and to mediate macrophage recruitment into the ischemic heart (Loerchner et al., 2015).

4 Objective of the work

Understanding the dynamics and intercellular communication of tissue-specific and infiltrating immune cells that contribute to cardiac repair is essential for the development of novel therapeutic strategies in cardiovascular diseases. On the basis of a comprehensive knowledge of these cellular interactions, new concepts need to be derived, in particular to maintain the beneficial effects of a well-coordinated immune response for optimized functional recovery of the infarcted heart while preventing excessive inflammation and impaired wound healing.

In this context, Lörchner et al. have identified the C-type lectin Reg3beta (Reg3β) which was secreted by cardiomyocytes within the ischemic heart upon myocardial infarction (Loerchner et al., 2015). The loss of Reg3β provoked in their study a delayed recruitment of macrophages accompanied with a prolonged persistence of neutrophils. According to the authors, this inflammatory dysbalance led to an impaired wound healing culminating in an increased mortality due to cardiac ruptures around day 4 after permanent LAD ligation in mice. Mechanistically, it was shown that Reg3β directed the recruitment of macrophages to the site of inflammation (Loerchner et al., 2015). The role of Reg3β on restricting neutrophil accumulation, however, remained to be determined.

Accordingly, the present work aimed to investigate the possible influence of Reg3β on the resolution of inflammation upon experimental myocardial infarction in mice by regulating the infiltration, accumulation and removal of neutrophils at the site of cardiac injury. For this purpose, a direct interaction of Reg3β with neutrophils via specific binding sites has been investigated. Of particular interest here was the impact of Reg3β on neutrophil motility, viability and inflammatory activity. Furthermore, this project intended to uncover the molecular mechanisms of Reg3β-mediated neutrophil clearance. By deciphering specific signaling pathways and effector proteins downstream of Reg3β that modulate neutrophil function and persistence, new targets for a cell-specific therapy should be identified.

5 Materials and Methods

5.1 Materials

5.1.1 Chemical reagents

Chemical	Catalog Number	Company
1,4- Dithiothreitol (DTT)	6908.1	Carl Roth
4-(2-hydroxyethyl)-1-piperazineethanesulfonic acid (HEPES)	6763.3	Carl Roth
Acetic acid	KK62.1	Carl Roth
Agar 100 resin	AGR1031	Agar scientific Ltd. UK
Agarose	A9539	Sigma-Aldrich
Ampotericin B (Fungizone)	11510496	Gibco
Aprotinin	A6106	Sigma-Aldrich
autoMACS Rinsing Solution	130-091-222	Miltenyi Biotec
BenchMark™ Protein Ladder	10747012	Invitrogen
Benzamidine	B6506	Sigma-Aldrich
Bicine	B3876	Sigma-Aldrich
Bovine Serum Albuminutes(BSA)	A9576	Sigma-Aldrich
Brewer Thioglycollate medium	B2551	Sigma-Aldrich
Bromphenol blue	114391	Merck
Calcium chloride ($CaCl_2$)	CN93.1	Carl Roth
Casein from bovine milk	C3400	Sigma-Aldrich
Dimethylsulfoxide (DMSO)	D8418	Sigma-Aldrich
Dulbecco`s Modified Eagle`s Medium, high glucose	11971025	ThermoFisher Scientific™
Ethanol, absolute	5054.1	Carl Roth
Ethanol, denaturated	T913.1	Carl Roth
Ethylcinnamate (ECi)	112372	Sigma-Aldrich
Fetal Calf Serum (FCS)	F2442	Sigma-Aldrich
Fibronectin Solution, bovine	C-43050	PromoCell
Galactose	59-23-4	Sigma-Aldrich
Glucoside	I3750	Sigma-Aldrich
Glutaraldehyde solution	354400	Merck
Hydrogenperoxide (H_2O_2) 30 %	CP26.1	Roth

Leupeptin	103476-89-7	Sigma-Aldrich
MACS BSA Stock Solution	130-091-376	Miltenyi Biotec
MACS Columns MS	130-042-201	Miltenyi Biotec
MACS Separator	130-042-109	Miltenyi Biotec
Magnesium chloride ($MgCl_2$)	7786-30-3	Sigma-Aldrich
Mannan	M3640	Sigma-Aldrich
MES SDS Running buffer 20x	NP0002	Invitrogen
Methanol	8388.1	Carl Roth
Mowiol 4-88	0713.1	Carl Roth
N-acetylgalactosamine	A2795	Sigma-Aldrich
N-acetylglucosamine	A8625	Sigma-Aldrich
N-acetylneuraminic acid	19023	Sigma-Aldrich
Amersham™ Protran™ 0.45 µm NC nitrocellulose blotting membranes	10600002	GE Healthcare Life Sciences®
NuPAGE 4-12% Bis-Tris Gel, 1mm x 17well	NP0329BOX	Novex™
Osmoium tetroxide	O5500	Merck
Paraformaldehyde (PFA)	30525-89-4	Merck
PCR Buffer Without MgCl2, 10x concentrated	11699105001	Merck
Gibco™ Penicillin-Streptomycin (10,000 U/mL)	11528876	ThermoFisher Scientific™
Potassium chloride (KCl)	P9327	Sigma-Aldrich
Pre-Separation Filters 30 µm	130-041-407	Miltenyi Biotec
Red Alert™ 10x Western Blot Stain	71078	Merck
Rotiphhorese® Gel 40 (29:1 acrylamid/bisacrylamid)	A515.1	Carl Roth
Skim Milk Powder	70166	Merck
Sodium Chloride (NaCl)	3957.1	Carl Roth
Sodium Dodecylsulfate (SDS)	5136.2	Carl Roth
Sucrose	S0389	Sigma-Aldrich
SuperSignal West Femto Maximum Sensitivity Substrate	34094	ThermoFisher Scientific™
TEMED	T9281	Sigma-Aldrich
Tissue-Tek® O.C.T. Compound	4583	Sakura
Tris	4855.1	Carl Roth
Triton-X-100	648463	Sigma-Aldrich
Methyl α-D-mannopyranoside	M6882	Sigma-Aldrich

Biogel P6	1504130	BioRad
Uranyl Acetate	E22400-05	Science Services

5.1.2 Inhibitors, enzymes, recombinant proteins, kits

Inhibitors	Catalog Number	Company
Chlorpromazine hydrochloride	C8138	Sigma-Aldrich
Diphenyleneiodonium chloride (DPI)	4673-26-1	Sigma-Aldrich
Imipramine hydrochloride	I7379	Sigma-Aldrich
Methyl-β-cyclodextrin (MβCD)	C4555	Sigma-Aldrich
Monodansylcadaverine (MDAC)	D4008	Sigma-Aldrich
Nystatin	N6261	Sigma-Aldrich

Enzymes	Catalog Number	Company
DNAse I	79254	Qiagen
Endo H	P0702S	New England Biolabs
Liberase DH Research Grade	5401127001	Roche
O-glycosidase	P0733S	New England Biolabs
PNGase	P0707S	New England Biolabs
Protein Deglycosylation Mix II	P6044S	New England Biolabs
Taq polymerase	45705	ThermoFisher Scientific™
α1-2,3,6 Mannosidase	P0768S	New England Biolabs
α2-3,6,8,9 Neuraminidase A	P0722S	New England Biolabs
β-N-acetylhexosaminidase$_f$	P0721S	New England Biolabs
β1-4 Galactosidase S	P0745S	New England Biolabs

Recombinant Proteins	Catalog Number	Company
LPS, E. Coli O111:B4	LPS25	Merck
Recombinant murine MIP-2 (CXCL2)	250-15	Peprotech
Recombinant murine granulocyte-colony stimulating factor (G-CSF)	250-05	Peprotech
Recombinant murine interferon-γ (IFNγ)	315-05	Peprotech
Murine regenerating islet-derived protein 3β (Reg3β)	AF5110	R&D Systems
N-formylmethionyl-leucyl-phenylalanine (fMLP)	F3506	Sigma-Aldrich

Phorbol-12-myristat-13-acetat (PMA)	1652981	Peprotech

Kits	Catalog Number	Company
2-D Clean-Up Kit	GE80-6484-51	Merck
Alexa Fluor® 790 Antibody Labeling Kit	A20189	Invitrogen™
BD Cytofix/Cytoperm™	554714	BD Bioscience
CellTiter-Glo® Luminescent Cell Viability Assay	G7570	Promega
CytoTox 96® Non-Radioactive Cytotoxicity Assay	G1780	Promega
Debris Removal Solution	130-109-398	Miltenyi Biotec
EasySep™ Mouse Neutrophil Enrichment Kit	19762	STEMCELL
Lightning-Link® APC Antibody Labeling Kit	705-0030	Nous Biologicals
Macrophage Isolation Kit (Peritoneum), mouse	130-110-434	Miltenyi Biotec
Phagocytosis assay kit (IgG FITC)	500290	Cayman

5.1.3 Antibodies and cell labeling dyes

Primary Antibodies	Catalog Number	Company
Citr. Histone H3	ab176842	Abcam
Citr. Histone H4	ab51997	Abcam
Goat anti mouse Cathepsin B	AF965	R&D Systems
Goat anti mouse Cathepsin D	AF1029	R&D Systems
Goat anti mouse Galectin 1	AF1245	R&D Systems
Mouse anti mouse CD64 APC	139305	BioLegend
Mouse anti mouse CD64 FITC	139315	BioLegend
Mouse anti mouse α-Sarcomeric Actin	A2172	Sigma-Aldrich
Rabbit anti mouse Beclin-1	3495	Cell Signaling Technology
Rabbit anti mouse Cleaved Caspase-1 (Asp296)	89332	Cell Signaling Technology
Rabbit anti mouse Cleaved caspase-3 (Asp175)	9661	Cell Signaling Technology
Rabbit anti mouse Cleaved caspase-7 (Asp198)	8438	Cell Signaling Technology
Rabbit anti mouse Cleaved Caspase-8 (Asp387)	8592	Cell Signaling Technology

Rabbit anti mouse collagen type II	600-401-104	Rockland
Rabbit anti mouse LC3B	PA1-16930	Invitrogen™
Rabbit anti mouse pMLKL (Ser345)	37333	Cell Signaling Technology
Rabbit anti mouse pRIP3 (Thr231/Ser232)	57220	Cell Signaling Technology
Rat anti mouse Caspase-11	14340	Cell Signaling Technology
Rat anti mouse CD115 PE	135505	BioLegend
Rat anti mouse CD11b APC/Cyanine7	101225	BioLegend
Rat anti mouse CD11b FITC	101205	BioLegend
Rat anti mouse CD11b PE	101207	BioLegend
Rat anti mouse CD31	102501	BioLegend
Rat anti mouse CD45 FITC	103107	BioLegend
Rat anti mouse F4/80 PE	123109	BioLegend
Rat anti mouse LAMP1/CD107a	MAB4320	R&D Systems
Rat anti mouse Ly6G BV421	127627	BioLegend
Rat anti mouse Ly6G FITC	127605	BioLegend
Rat anti mouse Ly6G PE/Cyanine7	127617	BioLegend
Sheep anti mouse Reg3beta	AF5110	R&D Systems

Secondary antibodies	**Catalog Number**	**Company**
Chicken anti goat AF488	A-21467	Invitrogen™
Chicken anti goat AF594	A-21468	Invitrogen™
Donkey anti rat AF488	A-21208	Invitrogen™
Goat anti mouse AF594	A-11005	Invitrogen™
Goat anti mouse HRP	115-035-146	Dianova
Goat anti rabbit AF594	A-11012	Invitrogen™
Goat anti rabbit HRP	111-035-045	Dianova
Rabbit and rat HRP	RbxRt-003-DHRPX	Dianova
Rabbit anti goat HRP	GAR/IgG(Fc)/PO	Dianova
Rabbit anti sheep HRP	HAF016	R&D Systems

Labeling dyes	**Catalog Number**	**Company**
7AAD Viability Staining Solution	420403	BioLegend
Acridine orange base	235474	Sigma-Aldrich
CM-H2DCFDA	C6827	Invitrogen™

DAPI	D9542	Sigma-Aldrich
IncuCyte® Cytotox Green	4633	IncuCyte®
LysoTracker™ Green DND-26	L7526	Invitrogen™
Molecular Probes™ Dihydrorhodamin123	D23806	Invitrogen™
pHrodo™ Red	P36600	Invitrogen™
Po-Pro®-1	P3581	Invitrogen™

5.1.4 Laboratory Equipment

Equipment	Company
1.3ml K3 EDTA Tube	SAI Infusion Technologies
10 cm Petri dishes	Greiner Bio-One®
6-, 12-, 24- and 96-well Cellstar® cell culture plates	Greiner Bio-One®
BD LSRFortessa™ cell analyzer	BD Bioscience
Casting chamber	Hoefer
Cell disruption vessel	Parr Instrument Company
Cell scrapers 25 cm	Sarstedt®
Centrifuge tubes	Beckmann Coulter
ChemiDoc™ MP System	Bio-Rad®
Clean Bench HeraSAFE KS	ThermoFisher Scientific™
Corning™ Costar™ Tranwell™ Permeable Supports	ThermoFisher Scientific™
EasySep™ Magnet	StemCell
Gravity size exclusion column	BioRad
HERAcell™ 150 CO_2 incubator	ThermoFisher Scientific™
Heraeus™ Fresco™ 21 Microcentrifuge	ThermoFisher Scientific™
Heraeus™ Multifuge™ X3R TX-1000	ThermoFisher Scientific™
Hidex Sense Microplate reader	Hidex
Leica TCS SP8 confocal microscope	Leica Microsystems
LS Columns	Miltenyi Biotec
NanoDrop 2000c UV-Vis spectrophotometer	ThermoFisher Scientific™
Neubauer cell counting chamber	Optik Labor®
Nunc™ Lab-Tek™ II Chamber Slide™ System	ThermoFisher Scientific™
Odyssey® 91201 imaging system	LI-COR Biosciences®
Pre-Separation Filters 30 µm	Miltenyi Biotec

ProteomeLab XL-I Analytical Ultracentrifuge	Beckman Coulter
Reichert Ultracut E ultramicrotome	Leica Biosystems
Scanning electron microscope FEI XL30	Philips®
Screen mesh polyamide monofile, mesh width 200 µm	neoLab Migge GmbH
Sonopuls® HD 2070 ultrasonic homogenizer	Bandelin®
Surgical disposable scalpels	B- Braun®
SW41 Ti Swinging-Bucket Rotor	Beckmann Coulter
Synergy H1	BioTek
Tecnai™ Spirit TEM	FEI™
TEM Grids, Carbon Film coated	Science Services
Transmission electron microscope EM 902	Zeiss®
UltraMicroscope II	LaVision BioTec
XCell II™ Blot Modules	Novex™
XCell SureLock™ Mini-Cells	Novex™

Softwares	**Company**
BD FACSDiva v6 Software	BD Bioscience
Cytoscape	Open source
FIJI	Open source
GraphPad Prism 5.0	GraphAd Software, Inc.
Image Lab	Bio-Rad®
Imaris	Bitplane
ImSpector	LaVision BioTec
LAS X Life Science	Leica

5.1.5 Media and solutions

Cell culture solutions and medium	
PEB buffer	PBS 2 mM EDTA 0.5 % BSA
Neutrophil culture medium (500 ml)	DMEM (High-Glucose, 4.5 g/l) 5 ml Penicillin (100 U/ml) and Streptomycin (100 µg/ml) G-CSF (10 ng/ml)

Macrophage culture medium (500 ml)	DMEM (High-Glucose, 4.5 g/l) 5 ml Penicillin (100 U/ml) and Streptomycin (100 µg/ml) 25 ml FCS
Casein solution	9 g Casein in 100 ml 1x PBS (pH 7.2) 0.9 mM $CaCl_2$ 0.5 mM $MgCl_2$ heated up to 60°C while stirring for at least 3 hours
Immunohistochemistry	
Fixation solution	4% PFA in PBS, pH 7.4
Permeabilization solution	0.5 % Triton X-100 in PBS
Mowiol mounting medium	2.4 g Mowiol 6 g glycerol 6 ml H_2O 12 ml of 0.2 M Tris-Cl (pH 8.5)
Cell harvest	
Protein extraction buffer	100 mM Tris, pH 8.8 10 mM EDTA 40 mM DTT 10 % SDS pH adjusted to 8.0 with HCl
Sonification buffer	50 mM Trix, pH 8.0 500 mM NaCl 10 mM Imidazole
Protease inhibitor mix	500 µg/ml Benzamidin 2 µg/ml Aprotinin 2 µg/ml Leupeptin 2 mM PMSF 1 mM Sodium Vanadate 20 mM Sodium Fluoride
Electrophoresis and blotting	
Extraction buffer (EP), proteins	0.1 M Tris-HCl, pH 8.8 0.01 M EDTA

	0.04 M DTT 10 % SDS pH 8
5x Laemmli Buffer	1 M Tris-HCl (pH 6.8) 10 % SDS 50 % Glycerol dissolved in distilled water
10x TBS buffer (5 liter)	400 g NaCl 120.5 g Tris pH to 7.6 Final volume made to 2 L with ddH2O
1x TBS-T (5 liter)	250 ml 20x TBS buffer 5 ml Tween 20 final volume made up with distilled water
1X MES SDS Running buffer (5L)	250ml 20xMES SDS Running buffer final volume made up with distilled water
Blocking solution (Western blot)	5 % skim milk powder in TBS-T
20X Transfer buffer (2L)	163.2 g Bicine 209.3 g Bis Tris 12 g EDTA Final volume made up with ddH2O
1x Transfer buffer (5L)	250 ml 20x Transfer buffer 1000 ml Methanol final volume made up with distilled water
Nitrogen cavitation	
Disruption buffer	100 mM KCl 3 mM NaCl 3.5 mM $MgCl_2$ 19 mM HEPES

5.1.6 Genotyping Primers

Primer	Sequence	WT Allele	Targeted Allele
Reg3β$^{-/-}$	5' GTCCTCCATGGTGAAGAGAAC 3'	600 bp	400 bp
	5' ATTCCCATCCACCTCCATTG 3' (WT)		
	5' AGAGGCTATTCGGCTATGACT 3'		
	5' CCTGATCGACAAGACCGGCTT 3' (Targeted)		
Nox2$^{-/-}$	5' AAGAGAAACTCCTCTGCTGTG AA 3'	240 bp	195 bp
	5' CGCACTGGAACCCCTGAGAAAGG 3'		
	5'GTTCTAATTCCATCAGAAGCTTATCG 3'		

5.1.7 Mice

Throughout the whole study, 8 to 12 weeks old adult mice with a body weight of 25-30 g were used to ensure the reproducibility of the individual experiments.

All animal experimentations were performed in accordance with the German animal protection law and EU ethical guidelines and were approved by the local governmental animal protection authority Regierungspräsidium Darmstadt (TVA B2/1209) as described by Lörchner et al. (Lörchner, Hou, et al., 2018). Mice were sacrificed by CO_2 euthanasia and cervical dislocation.

5.1.7.1 Wild-type mice

C57BL/6J mice were in-house bred and used as controls as indicated.

5.1.7.2 Mice deficient of Regenerating islet-derived protein 3 β (*Reg3b*$^{-/-}$)

Mice with a constitutive knock-out of Reg3β (*Reg3b*$^{-/-}$; B6; 129-Reg2^{tm1Lchr}/H) were originally generated by Lieu et al. (Lieu et al., 2006) and obtained from S. Hunt, University College of London. The region from a position within exon 2 to a position in exon 5 was replaced by a reporter/selection cassette, thus deleting exons 3 and 4. *Reg3b*$^{-/-}$ mice are phenotypically indistinguishable from wild-type mice, develop normally and are fertile.

5.1.7.3 Mice deficient of gp91phox (*Nox2*$^{-/-}$)

Mice with a constitutive knock-out of Cybb (B6.129S-Cybbtm1Din/J), also known as *gp91phox*$^{-/-}$ were originally generated by Pollock et al. ((Pollock et al., 1995)) and kindly provided by R. Brandes, Vascular Research Center Frankfurt a.M. A selection cassette for neomyocin-resistance was placed into the third exon thereby disrupting the Cybb gene. *Nox2*$^{-/-}$ are phenotypically inconspicuously, develop normal and are fertile.

5.2 Methods

5.2.1 Isolation and cultivation of primary neutrophils from the peritoneum

Primary neutrophils were isolated from the peritoneum after the induction of a peritonitis by injecting 1 ml of casein solution intraperitoneal (i.p.) 24 hours and 1 hour prior to the isolation (Swamydas, Luo, Dorf, & Lionakis, 2015). The mice were sacrificed, the peritoneal wall was exposed by removing the abdominal skin and 6 ml of PEB buffer was injected into the peritoneal cavity. After gently massaging the abdomen of the mouse the peritoneal fluid was harvested using a 21G needle and collected in 15 ml tubes on ice. Neutrophils were purified using the EasySep™ Mouse neutrophils enrichment kit from StemCell according to the manufacturer's instructions. Briefly, neutrophils were enriched by negative selection as unwanted cells were targeted with biotinylated antibodies directed against cells other than neutrophils. Labelled cells were crosslinked to magnetic particles using tetrameric antibody complexes and separated with the EasySep™ magnet. Unlabeled, purified neutrophils were poured off into a separate tube and pelleted by centrifugation at 300 x g for 10 min, 4 °C for further experimental procedures.

Purified peritoneal neutrophils were cultivated in fibronectin (1 µg/ml) coated cell culture plates in Dulbecco`s Modified Eagle`s Medium (DMEM), high glucose medium supplemented with 1% Penicillin/Streptavidin (P/S) and 10 ng/ml G-CSF at a density of 6 x 10^5 cells/ml. After the cells adhered to the culture plate, the medium was removed and fresh medium supplemented with 1% P/S and 10 ng/ml G-CSF was added to the cells.

5.2.2 Isolation and cultivation of bone marrow-derived, blood and splenic neutrophils

Bone marrow-derived neutrophils were harvested from femur and tibia as previously described (Yonggang Ma et al., 2016). After removing skin and muscles the bones were flushed with 8 ml of PEB buffer using a 24 G needle and the cell suspension was collected in a 15 ml tube on ice.

Whole blood was harvested by decapitating the mice and collecting the blood in EDTA tubes for 30 minutes rolling at RT to prevent blood clotting.

The spleen was excised, mashed in PEB buffer and filtered through a nylon mesh with 200 µm pore size to obtain a single cell suspension (collected in PEB buffer on ice).

Subsequent to obtaining single cell suspensions of neutrophil populations from different origins, red blood cell lysis was performed with ice cold hypotonic water lysis (hypotonic shock) for 15 sec and restored by adding five times the volume of PEB buffer (Shehadul Islam, Aryasomayajula, & Selvaganapathy, 2017). Neutrophils were purified using the EasySep™ Mouse neutrophils enrichment kit from StemCell and cultured as described above.

5.2.3 Isolation and cultivation of primary macrophages from the peritoneum

Primary macrophages were isolated from the peritoneum after the induction of a peritonitis with 3 % thioglycollate 4 days prior to the isolation. (Ray & Dittel, 2010). The lavage of the peritoneal cavity was performed as described in 5.2.1. Macrophages were purified using the Macrophage Isolation kit from Miltenyi Biotec according to the manufacturer's instructions. Briefly, macrophages isolation is based on negative selection by depleting unwanted cells with biotinylated antibodies directed against non-macrophages. Labeled cells were incubated with anti-biotin antibodies conjugated to MicroBeads and magnetically retained within a MACS Column in the magnetic field of a MACS Separator (Y. Liu et al., 2017). Unlabeled macrophages passed the column and were collected in a separate tube for further experimental procedures. Primary macrophages were cultivated in uncoated 24- and 6-well cell culture plates in DMEM, high glucose medium supplemented with 1% P/S and 5 % FCS at a density of 1 x 10^6 cells/ml. After the cells adhered to the cell culture plate, the medium was removed and fresh medium supplemented with 1% P/S and 5 % FCS was added to the cells.

5.2.4 Experimental myocardial infarction in adult mice

The experimental procedure of permanent LAD Ligation was conducted by Roxanne Wagner according to the TVA B2/1209 and already described by Lörchner et al. (Loerchner et al., 2015). WT and *Reg3b*$^{-/-}$ mice, 10 to 12 weeks of age, were subjected to a permanent left anterior descending coronary artery (LAD) Ligation. Two hours prior to surgery, the mice received a single dose of 0.1 mg/kg body weight (BW) buprenorphine. The mice were anesthetized with 2% isoflurane and cannulated into the trachea using a 20-gauge intravenous catheter with a blunt end (Loerchner et al., 2015). The mice were artificially ventilated at a rate of 150 strokes per minute using a rodent ventilator with a mixture of O_2 and air (80%) to which 2 % isoflurane was added. During the whole surgery, the mice were placed on a heating pad to maintain body temperature. The fur was removed before opening the thorax between 3rd and 4th rib and dissecting tissue and muscle to uncover the heart. A 7-0 silk suture was used to ligate the left anterior descending coronary artery permanently with a single suture. Infarction was confirmed by discoloration of the ventricle and ST-T changes on ECG. Thorax and skin were closed, animals extubated and allowed to recover from surgery. The mice received another dose of 0.1 mg/kg BW buprenorphine directly after the surgery and 24 hours later. Additionally, 200 mg/kg BW of metamizol was administered through the drinking water in the first 3 days post-surgery.

5.2.5 Enzymatic digestion of infarcted heart tissue to isolate cardiac leukocytes

Infarcted hearts were collected and washed with PBS to remove remaining blood in the chambers. The infarction area was mechanically dissected from the atria, right ventricle and septum using scissors and subsequently digested enzymatically with 0.1 mg/ml liberase TH Grade from Roche for 30 minutes at 37°C. The supernatant was collected in PEB buffer on ice and the remaining tissue was digested once more with fresh liberase for 30 minutes at 37°C. After collecting the supernatant, the cell suspension was centrifuged at 300 x g for 10 min, 4°C. The pellet was resuspended in PEB buffer and applied over a 30 µm filter followed by another centrifugation step. Next, cell and matrix debris was removed by resuspending the cell pellet in 4 ml cold PBS and 1 ml of debris removal solution from Miltenyi Biotec. 2 ml of cold PBS were gently layered on top before centrifugation at 3000 x g for 10 min, 4 °C. The debris formed an interphase above the cell pellet, which was aspirated. The cells were washed with 10 ml cold PBS and centrifuged at 1000 x g for 10 min, 4 °C. Finally, red blood cell lysis was performed by hypotonic water lysis followed by a centrifugation step. The isolated and purified leukocytes were resuspended in PEB buffer for further experimental procedures.

5.2.6 Flow cytometry

After the isolation of both, primary cells from the peritoneum and infarcted heart, the concentration was adjusted to 1 x 10^6 cells in 100 µl PEB buffer per sample according to the manufacturer's instruction of the antibodies. The cell suspension was incubated with specific primary antibodies conjugated to fluorescent dyes for 20 minutes on ice in the dark. Thereafter, cells were washed with PEB buffer and centrifuged at 300 x g for 10 min, 4 °C. Finally, the cells were resuspended in 500 µl PEB buffer and analyzed on BD LSRFortessa™. Data analysis was done with the BD FACS Diva v6 Software.

The primary antibody targeting Reg3β was manually labeled with APC using the Lightning-Link® Antibody Labeling Kit according to the manufacturer's instructions. 10 µg of sheep anti mouse Reg3β from R&D was mixed with 1 µl LL-Modifier solution and incubated with 10 µg Lightning-Link® APC O/N at RT. To eliminate free APC dye, 1 µl of LL-Quencher solution was added to the labeled antibody and mixed well. For cell surface detection of Reg3β, the primary antibody manually labeled with APC was added to the cells together with the other antibodies directed against the cell surface antigens of interest.

Intracellular Reg3β staining was conducted with the Fixation/Permeabilization Solution Kit from BD. Briefly, after antibody staining for surface antigens as described above, the cells were fixed in PFA and permeabilized with saponin. The cells were kept in saponin-containing

permeabilization buffer and incubated with Reg3β for 20 minutes on ice. After washing the cells once in permeabilization buffer and once in PEB buffer, the pellet was resuspended in PEB buffer for FACS analysis.

Following antibody staining for surface antigens, apoptosis and necrosis was detected by staining $1x10^6$ cells in 100 µl PEB with 25 µM Po-Pro®-1 and 2.5 µg/ml 7AAD solution. After 20 minutes incubation, the cells were directly analyzed by flow cytometry without an additional washing step.

5.2.7 Immunohistochemistry

Infarcted hearts were collected, washed with PBS and fixed with 4 % PFA for 2 hours at RT. Afterwards, the fixed heart samples were incubated in 15 % and 30 % sucrose solution for at least 4 hours each, before they were mounted in Tissue-Tec® O.C.T.™ compound and stored at -80 °C. Cryosections with a thickness of 7 µm were collected on slides and washed with PBS prior to the antibody staining.

For immunohistochemical analysis of primary neutrophils, cells were cultured on 4-well chamber slides with removable well, were washed with PBS and fixed with 4 % PFA for 10 minutes at RT. For intracellular staining, cells were further permeabilized with 0.1 % Triton X-100 in PBS for 10 minutes at RT followed by PBS wash.

Both, tissue sections and cultured cells were incubated with the primary antibody of interest for 2 hours at RT or overnight at 4 °C depending on the antibody. After washing three times with PBS the secondary antibody conjugated to a fluorescent dye or to biotin was added to the samples and incubated for 1 or 2 hours, respectively, at RT in the dark followed by an PBS wash. In case of a biotinylated secondary antibody, the sample was additionally incubated with Streptavidin conjugated to a fluorescent dye for 1 hour at RT. When detecting more than one antigen of interest, the primary, secondary and, if necessary, tertiary antibodies of each antigen were applied one after another. For a nuclear counterstain, the tissue sections or cells were incubated with 4',6-Diamidin-2-phenylindol (DAPI) for 10 minutes at RT. Finally, the slides were washed with PBS and coverslips were mounted with mowiol. Imaging was performed with the Leica TCS SP8 confocal microscope and LAS X Life Science software. Data analysis was done with the imaging software FIJI.

5.2.8 Light sheet microscopy

Three-dimensional imaging of infarcted hearts with light sheet microscopy was adapted from the BALANCE protocol of Merz et al. (Merz et al., 2019). Adult WT and *Reg3b*$^{-/-}$ were subjected to LAD Ligation. At day 1, 2, 4 and 7 post-MI the mice were anesthetized with 180 mg/kg BW

ketamine and 16 mg/kg BW xylazine. The mice received intravenous injections in the retro-orbital sinus with 10 µg of each antibody diluted in PBS in a total volume of 50 µl. Antibodies directed against the neutrophil marker Ly6G were directly coupled with AlexaFluor647. Antibodies directed against the endothelial marker CD31 (samples from day 1, 2 and 4) and collagen type I (samples from Day 7) were manually labeled with AlexaFluor790 using the antibody labeling kit from ThermoFisher. Accordingly, 100 µg antibody solution was added to the AlexaFluor790 dye and incubated for 1 hour at RT in the dark. The antibody solution was applied to a purification column with 1.5 ml resin bed and centrifuged at 1100 x g for 5 minutes to collect the labeled antibody and remove unbound molecules. After 20 minutes incubation, mice were sacrificed and perfused with PBS through the left atrium by making a small cut in the right atrium. The excised hearts were placed in 4 % PFA for 2 hours at RT for chemical fixation followed by dehydration in an ethanol series in dH_2O of 30%, 50%, 70%, 90% and 2x 100 % for at least 4 hours at 4°C each while rolling. Next, the hearts were bleached in 5% hydrogen peroxide and 5% DMSO in 100 % methanol for 4 hours at 4°C. After washing in 100 % ethanol for 1 hour, the samples were warmed up to RT and transferred in pure ethylcinnamate (ECi). The cleared heart was kept in ECi at RT in the dark. Light sheet imaging was performed with the Ultramicroscope II and ImSpector software both from LaVision BioTec. The microscope is based on a MVX10 zoom body from Olympus with a 2x objective and equipped with a Zyla 4.2 PLUS sCMOS camera from Andor.

3D reconstruction and data analysis was done using Imaris Software from Bitplane. Based on the autofluorescence of the heart itself, heart surface area and volume were quantified using the automated Contour Surface tool. The $CD31^{neg}$ area or rather Collagen type II^{pos} area identified the infarction zone and was traced manually using the Contour Surface tool. The surface of the $CD31^{pos}$ or rather Collagen Typ II^{neg} RZ was calculated by subtracting the IZ area from the whole heart area. Infiltrating tissue neutrophils were identified and quantified using the Spot Detection tool based on the size and round shape. Spotted neutrophils located within the infarct or RZ, respectively, were quantified with the Spots split into surface objects tool. Finally, the sum of detected neutrophils in the whole heart, infarct or RZ was normalized to the respective surfaces.

5.2.9 Transwell migration assay

Primary neutrophils from the peritoneum were cultured on permeable polycarbonate membrane inserts with a pore size of 3 µm. 100 ng/ml of recombinant murine Reg3β, 100 ng/ml of recombinant murine CXCL2 as positive control and PBS as control were added to the lower chamber each. After 2.5 hours, cells migrated to the lower chamber were fixed with 4 % PFA

and stained with DAPI for 10 minutes at RT. Cell migration towards PBS, Reg3β and CXCL2 was assessed from cell counts from five random field per well compared to control cells.

5.2.10 Incucyte® Systems for Live-Cell Imaging

Casein-elicited neutrophils from the peritoneum were cultured in 24-well plates in culture medium with 250 nM IncuCyte™ Cytotox Green Reagent. Next, cells were stimulated with Reg3β in different concentrations: 10 ng/ml, 100 ng/ml and 1000 ng/ml. Control cells were treated with PBS. The number of Cytotox Green positive dead neutrophils was recorded using the Incucyte™ System every hour for a total of 6 hours.

5.2.11 LDH assay

The CytoTox 96® Non-Radioactive Cytotoxicity Assay from Promega based on the release of lactate dehydrogenase (LDH) was performed with isolated primary neutrophils from the bone marrow, blood, spleen and peritoneum according to the manufacturer's instructions. The cells were cultured in 24-well plates and stimulated with 100 ng/ml of recombinant murine Reg3β. Control cells were equally stimulated with 100 ng/ml IFNγ or PBS, respectively.
LDH release was measured after 15 min, 30 min, 45 minutes and 60 minutes post stimulation by transferring 3 x 50 µl supernatant of each sample into a 96-well plate. The samples were incubated with the LDH substrate tetrazolium salt, which is converted into a red formazan product in the presence of LDH. The absorbance signal of the red formazan product was recorded at 490 nm in the Hidex sense microplate reader, which is proportional to the number of dead cells.

5.2.12 ATP assay

The CellTiter-Glo® Luminescent Cell Viability Assay from Promega based on the quantitation of intracellular ATP was performed with casein-elicited neutrophils from the peritoneum according to the manufacturer's instructions. The cells were cultured in 24-well plates and stimulated with 100 ng/ml of recombinant murine Reg3β. Positive and negative controls were stimulated with 100 ng/ml IFNγ and PBS, respectively. Intracellular ATP content was measured after 30 minutes and 60 minutes post stimulation by adding the CellTiter-Glo® Reagent to cells resulting in cell lysis and release of intracellular ATP. The assay reaction mix comprises Ultra-GloTM recombinant luciferase catalyzing the mono-oxygenation from luciferin in the presence of ATP. The generation of the luminescent signal was measured by the luminometer from LI-COR Biosciences® and is proportional to the number of viable cells.

5.2.13 Transmission electron microscopy

Sample preparation of Reg3β stimulated neutrophils and transmission electron microscopy (TEM) was performed in cooperation with PD Dr. Ulrich Gärtner at the University of Giessen.
TEM was conducted with casein-elicited and bone-marrow-derived neutrophils. The cells were adjusted to 1 x 10^6 cells/ml culture medium and stimulated with 100 ng/ml Reg3β in 1.5 ml Eppendorf tubes. Control cells were equally treated with PBS. After 15 min, 30 minutes and 60 minutes the cells were spun down at 300 x g for 10 min, 4 °C and the cell pellet was resuspended in 4 % PFA. The samples were post-fixed in 1 % osmium tetroxide in dH_2O and dehydrated in an ethanol series (25%, 50%, 70%, 90% and 100%) as described by (Dhandapani et al., 2019). Thereafter, the cells were embedded in agar 100 resin (Agar scientific Ltd. UK) and cut in ultrathin section using the ultramicrotome from Leica. Image acquisition was done with the Zeiss EM 902.

5.2.14 Scanning electron microscopy

Sample preparation of Reg3β stimulated neutrophils and scanning electron microscopy (SEM) was performed in cooperation with Anika Seipp at the University of Giessen.
Casein-elicited peritoneal and bone marrow-derived neutrophils were cultured on fibronectin coated cover glasses of 10 mm diameter. When attached, cells were stimulated with 100 ng/ml Reg3β or PBS as control for 15 min, 30 minutes and 60 min. Next, the cells were fixed in 2.5 % glutaraldehyde and post-fixed in 1 % osmium tetroxide. Following a washing step in dH_2O, the samples were dehydrated in an ethanol series, dried by critical point CO_2 treatment and subsequently sprayed with gold as described by (Zhou et al., 2019). Cells were examined using the Phillips XL30 SEM.

5.2.15 Negative stain electron microscopy

Negative stain electron microscopy (EM) was conducted in cooperation with Saskia Mehlmann and Dr. Özkan Yildiz from the MPI of Biophysics in Frankfurt. Casein-elicited neutrophils from the peritoneum were disrupted by nitrogen decompression to obtain membrane vesicles. This detergent-free method breaks the cells via pressure and shear stress whereupon cell membrane fragments spontaneously form vesicles. About 50 million neutrophils were collected in 5 ml disruption buffer and placed in the pressure vessel. Nitrogen cavitation was performed at 40 bar for 10 min. EGTA was directly added to the cavitate to a final concentration of 1.5 mM before centrifugation at 400 x g for 15 min, 4 °C to remove nuclei and unbroken cells. Next, the vesicles were pelleted by ultracentrifugation at 43 000 x g for one hour. To further purify the vesicle solution from unwanted debris, the vesicles were applied on a gravity size exclusion column. The

column was manually filled with P-6 resin by adding ~1.5 ml of the resin and centrifugation at 1500 x g for 2 min. The vesicles were added on top of the resin and centrifuged at 1500 x g for 2 minutes. The flow through contains the vesicles whereas the debris remains in the column. Synthetic vesicles composed of 85 % zwitterionic phospholipid (PC) and 15 % acidic phospholipid (PS) were kindly provided by Saskia Mehlmann according to the protocol of Mukherjee et al. (Mukherjee et al., 2014). The purified vesicles and synthetic liposomes were stimulated with 300 ng of recombinant Reg3β for 30 minutes. Pre-coated carbon grids were prepared for sample application by placing it into a glow charging unit for 30 seconds at 10 mÅ. Two µl of sample were applied to the grid and allowed to adsorb to the grid surface for 30 seconds. The liquid was removed by touching the edge of the grid with a sheet of filter paper. Next, two µl of 1% uranyl acetate staining reagent were placed on the grid and immediately removed with the sheet of filter paper. This step was repeated twice (van Pee et al., 2017). Imaging of potential pore formation by Reg3β was performed with the Tecnai™ Spirit TEM from FEI™.

5.2.16 Western blot analysis

To extract total proteins, adherent neutrophil cultures from the peritoneum were lysed in extraction buffer containing protease inhibitors, homogenized by sonification and centrifuged at 10 000 x g for 5 minutes to remove insoluble material. Protein concentration was determined using the DC protein assay from BioRad. Finally, dithiothreitol (DTT) at a final concentration of 40 mM was added to the samples followed by a boiling step at 99 °C for 1 min. Protein samples were mixed with 5X Laemmli buffer and bromphenol blue in a ratio of 3:2 and boiled at 99 °C for 1 min. Approximately 15 µg of protein were applied on Gradient NuPAGE 4-12 % Bis-Tris gels and SDS-PAGE was run at 75 V for 15 minutes and 165 V until the bromphenol blue reached the bottom of the gel. Separated proteins were blotted to a nitrocellulose membrane at 30 V for 2 hours and visualized afterwards by incubating the membrane with RedAlert™ for 5 min. After blocking with 5 % skim milk for 1 hour at RT, the membrane was immunolabeled with specific primary antibodies of interest in 3 % skim milk solution overnight (O/N) at 4°C. The membranes were washed with TBS-T and incubated with the corresponding secondary antibodies conjugated to horseradish peroxidase (HRP) for 1 hour at RT. Visualization was performed by using SuperSignal West Femto Maximum Sensitivity Substrate in a ChemiDoc™ MP System. Quantification of protein expression was based on the mean volume pixel density of the corresponding bands (Lörchner, Widera, et al., 2018).

5.2.17 Intracellular ROS measurement

Intracellular ROS levels were detected using the cell permeable dyes Dihydrorhodamine (DHR) 123 and the chloromethyl derivative of 2',7'-dichlorodihydrofluorescein diacetate (CM-H_2DCFDA) (Rothe et al., 1988). In the presence of ROS, both dyes are oxidized resulting in the formation of fluorescent adducts that are trapped inside the cell and thereby serve as intracellular ROS indicator. Cells from WT mice were stimulated with 100 ng/ml of recombinant murine Reg3β for 15 min, 30 min, 45 minutes and 60 minutes and labeled with 150 µM DHR123 or rather 1 µM CM-H_2DCFDA in medium 10 minutes before Reg3β stimulation stop. Cells were washed with cold PEB, centrifuged for 10 minutes at 300 x g, 4 °C and resuspended in PEB. Intracellular ROS levels were determined by analyzing the mean fluorescent intensity (MFI) of both dyes by flow cytometry. For the investigation of the role of NOX2 in Reg3β-mediated cell death of neutrophils, intracellular ROS levels were detected in peritoneal neutrophils from *Nox2*$^{-/-}$ mice after Reg3β stimulation using DHR123 as described above. Additionally, casein-elicited neutrophils WT mice were pretreated with 1 µM diphenyleneiodonium chloride (DPI) (Buck et al., 2019) for 10 minutes at 37 °C, washed with medium, centrifuged for 10 minutes at 300 x g, RT and resuspended in medium for intracellular ROS analysis with DHR123.

5.2.18 Assessment of lysosomal membrane permeabilization

Lysosomal membrane permeabilization (LMP) was investigated in casein-elicited peritoneal neutrophils post Reg3β stimulation and cardiac neutrophils post-MI (Figure 7).

The galectin puncta assay detects the translocation of cytosolic galectin to leaky lysosomes (Aits et al., 2015) resulting in a dot like pattern of galectin. Peritoneal cells were cultivated and stimulated with 100 ng/ml of recombinant murine Reg3β for 30 minutes at 37 °C. Control cells were treated with PBS. The cells were washed with PBS and fixed with 4% PFA for 10 minutes at RT followed by permeabilization with 0.1 % Triton X-100 for 10 minutes at RT. Neutrophils were stained for intracellular Galectin-1 and the lysosomal marker LAMP1 (J. W. Chen, Murphy, Willingham, Pastan, & August, 1985). Galectin translocation was analyzed using fluorescence microscopy.

The release of lysosomal enzymes upon LMP into the cytosol was examined by analyzing the co-localization of cathepsin B and D with primary lysosomes in peritoneal neutrophils. The cells were cultivated and stimulated with Reg3β for 30 minutes at 37 °C. Subsequently, the cells were washed with PBS, fixed with 4% PFA for 10 minutes at RT and permeabilized with 0.1 % Triton X-100 for 10 minutes at RT followed by an intracellular staining for cathepsin B, D and the lysosomal marker LAMP1. Co-localization of lysosomal enzymes and lysosomes as well as diffuse

staining of cathepsins throughout the entire cells upon LMP (Boya et al., 2003) was determined by fluorescence microscopy.

The lysosomotropic dyes acridine orange (A/O) and LysoTracker (LTR) Green accumulate in acidic organelles as lysosomes and endosomes (Repnik, Česen, & Turk, 2016). Upon destabilization of the lysosomal membrane the lysosomal pH increases resulting in a decreased A/O and LTR staining. Peritoneal neutrophils were cultivated and stimulated with Reg3β for 15 min, 30 min, 45 minutes and 60 min. 15 minutes before stimulation stop the cells were labeled with 5 µg/ml A/O at 37 °C. After washing the cells with PEB, pale cells that lost their A/O staining were quantified using flow cytometry. Cardiac neutrophils were isolated from infarcted hearts at day 1, 2, 4 and 7 post-MI and labeled with 5 µg/ml A/O for 15 minutes at 37 °C and 50 nM LTR for 30 minutes at 37 °C. The cells were washed and stained for CD45, CD11b, CD64 and Ly6G to identify neutrophils. Decrease of lysosomal staining was assessed with flow cytometry.

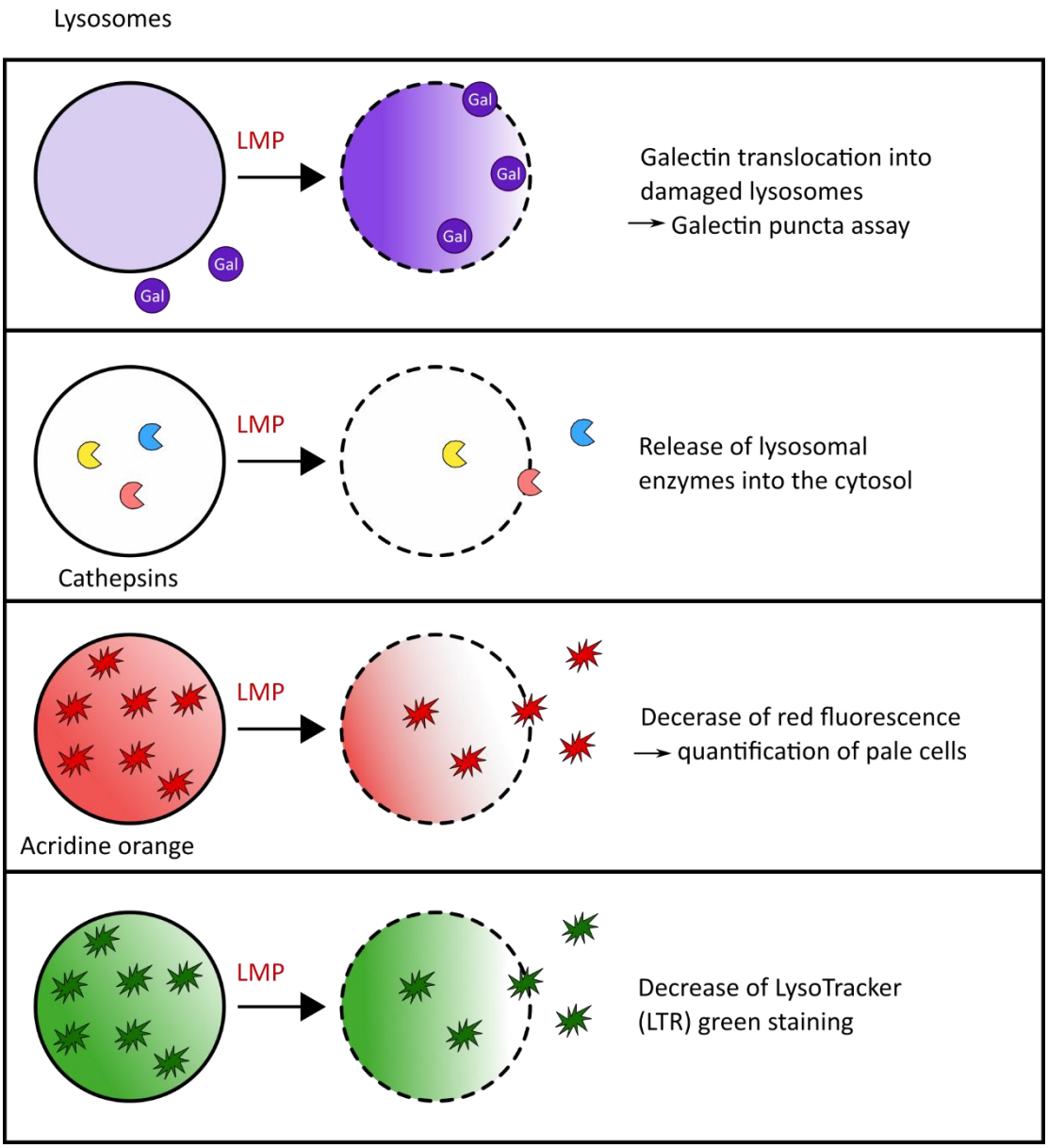

Figure 7: Methods to detect LMP
The scheme illustrates different methods to investigate the destabilization of the lysosomal membrane. The translocation of galectins to leaky lysosomes (= galectin puncta assay), the release of cathepsins from lysosomes into the cytosol, the quantification of pale cells that lost their A/O staining and finally, the decrease of the LTR staining. (Adapted from (F. Wang, Gómez-Sintes, & Boya, 2018))

5.2.19 Deglycosylation of glycoproteins

Reg3β binding to carbohydrate residues of peptidoglycans on the cell surface of neutrophils was assessed by treating the cells with different exoglycosidases which break the glycosidic bond at terminal carbohydrate residues prior to Reg3β treatment. Casein-elicited peritoneal neutrophils were cultured and treated with α2-3,6,8,9 Neuraminidase A (8 mU), β1-4 Galactosidase S (16 mU), β-N-acetylhexosaminidase f (6 mU) and α1-2,3,6 Mannosidase (0.04 mU) for 30 minutes at

37 °C. The protein deglycosylation mix II contains all enzymes and reagents to remove the most common N- and O-linked glycans and was applied as positive control. Following enzymatic pretreatment, the medium was removed, the cells were cultured in fresh cell culture medium and stimulated with Reg3β (100 ng/ml) for additional 30 minutes at 37 °C. Next, Reg3β-mediated cell death upon binding was estimated by LDH assay as described above. Basal cytotoxicity of deglycosidases was excluded by former dose-response studies.

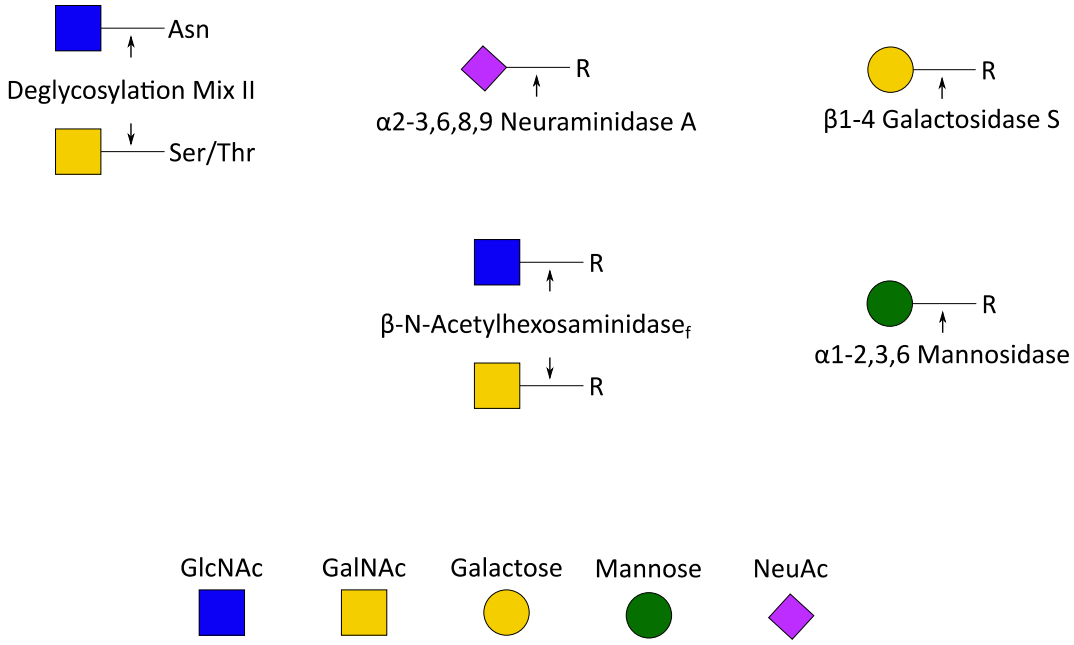

Figure 8: Protein deglycosidases

To assess the binding capacities of Reg3β to carbohydrate residues of glycoproteins on the cell surface of neutrophils, the cells were pre-treated with different exoglycosidases prior to Reg3β stimulation. The protein Deglycosylation Mix II contains all enzymes and reagents to remove common N- and O-linked glycans without protein degradation. N-linked glycans are removed from asparagin residues on the core protein by PNGase F. O-linked glycans are removed by a series of exoglycosidases from the serine or threonine residue of the core protein. The exoglycosidase α2-3,6,8,9 Neuraminidase A cleaves linear and branched terminal neuraminic acid residues, β1-4 Galactosidase S catalyzes the hydrolysis of terminal β1-4 linked galactose residues from oligosaccharides, β-N-acetylhexosaminidase$_f$ cleaves β-N-acetylgalactosamine and glucosamine residues and α1-2,3,6 Mannosidase removes α1-2, α1-3 and α1-6 linked mannose residues from glycans.

Asn = Asparagine; Ser/Thr = Serine or Threonine; R = residue; GlcNAc = N-acetylglucosamine; GalNAc = N-acetylgalactosamine; NeuAc = neuraminic acid

5.2.20 Carbohydrate competition binding assay

A competitive binding assay of Reg3β interacting with neutrophils in the presence of the mono-, di- and polysaccharides was performed with the aim to inhibit Reg3β binding to its potential targets on the cell surface. N-acetylneuraminic acid (400 mM), Galactose (400 mM), N-acetylgalactosamine (100 mM), lactose (400 mM), N-acetylglucosamine (400 mM), Glucose (400 mM), α-methyl mannoside (400 mM) and mannan (30 mM) were each incubated with Reg3β for 30 minute sat 37 °C. Next, the Reg3β-carbohydrate mix was added to cultured primary neutrophils isolated from the peritoneum for 30 minutes at 37 °C. Inhibition of Reg3β binding was assessed by LDH assay as described before. Basal cytotoxicity of inhibitors was saccharides by former dose-response studies.

5.2.21 Inhibition of endocytosis

Casein-elicited neutrophils from the peritoneum were cultured and treated with inhibitors for different endocytosis pathways. The inhibitors and their mechanism of action are summarized in Table 1.

Inhibitor	Mechanism	Pathway
Chlorpromazine	Causes the depletion of adaptor proteins and clathrin from the plasma membrane (L. H. Wang, Rothberg, & Anderson, 1993).	Clathrin-mediated endocytosis
Monodansylcadaverine (MDAC)	Affects the function of clathrin and clathrin-coated vesicles (Schlegel, Dickson, Willingham, & Pastan, 1982).	Clathrin-mediated endocytosis
Methyl-β-cyclodextrin (MβCD)	Cholesterol extraction from the membrane (Holz, 1974; Kilsdonk et al., 1995).	Caveolae-mediated endocytosis
Nystatin	Cholesterol extraction from the membrane (Holz, 1974; Kilsdonk et al., 1995).	Caveolae-mediated endocytosis
Imipramine	Inhibits membrane ruffle formation (H. P. Lin et al., 2018).	Macropinocytosis

Table 1: Endocytosis inhibitors and their mechanism of action

Clathrin-mediated endocytosis was inhibited with chlorpromazine (1 µM) and MDAC (1 µM), caveolae-mediated endocytosis with MβCD (1 µM) and nystatin (1 µM) and micropinocytosis with imipramine (1 µM). All inhibitors were added to the cultured cells and incubated for 30 minutes at 37 °C directly followed by stimulation with Reg3β (100 ng/ml) for 30 minutes at 37 °C. Inhibition of endocytosis was monitored by measuring LDH release. Basal cytotoxicity of inhibitors was excluded by former dose-response studies.

5.2.22 In vivo efferocytosis assay

Efferocytosis of neutrophils by macrophages in the peritoneum was analyzed using the pH sensitive rhodamine-based pHrodo™ Red dye according to the manufacturer's instructions. This cell labeling dye is non-fluorescent at neutral pH but turns bright red upon acidification in the phagosome following phagocytosis. Casein-elicited neutrophils from the peritoneum were labeled with 1 µg/ml pHrodo™ Red for 30 minutes at 37°C. After washing with PEB buffer, the cells were incubated with 100 ng/ml Reg3β or PBS as control for another 30 minutes at 37 °C. The cells were washed with PEB and 15 million labeled neutrophils, Reg3β stimulated and unstimulated control cells, respectively, were injected i.p. into a WT mouse with accumulated macrophages in the peritoneum 4 days after thioglycollate injection. After one hour, the peritoneal cells were isolated and stained for CD11b and F4/80 to identify macrophages. Efferocytosis of neutrophils by macrophages was determined by the quantification of RFP^+ macrophages with flow cytometry.

5.2.23 In vitro phagocytosis assay

Phagocytotic activity of primary macrophages from the peritoneum was detected using FITC labeled IgG-coated latex beads from Cayman. Isolated and purified macrophages from the peritoneum were cultivated in 6-well plates. When adherent, the cells were stimulated with 100 ng/ml Reg3β and IgG FITC latex beads were directly added to the cultured cells and incubated for 2.5 hours at 37 °C. Control cells were equally treated with 1 µg/ml LPS or PBS. Cells were detached using accutase and centrifuged at 300 x g for 10 min, 4°C. The cell pellet was resuspend in PEB buffer and tryphan blue was added to quench surface bound IgG FITC followed by another washing step with PEB buffer. Phagocytotic activity was determined by analyzing FITC positive macrophages with flow cytometry.

5.2.24 Statistical analysis

Statistical analysis and graphical illustrations were elaborated using Graph Pad Prism 5.0.
Differences between two groups were assessed using the Wilcoxon-Mann-Whitney Houston test. For the comparison of more than two groups One-Way ANOVA followed by Bonferroni's post test was applied. Two-Way ANOVA followed by Bonferroni's correction was used for the comparison of two independent groups over time. Correlation analysis was performed with linear regression and calculating Pearson's correlation coefficient r_p or Spearman correlation coefficient r_s as indicated. A p-value of $p < 0.05$ was considered significant in all evaluations unless otherwise indicated.

6 Results

6.1 The role of Reg3β in restricting neutrophil persistence after the onset of myocardial infarction

6.1.1 Neutrophil persistence in *Reg3b*$^{-/-}$ mice is restricted to the heart after the onset of myocardial infarction

Initially, the dynamics of neutrophil persistence within the infarcted heart in *Reg3b*$^{-/-}$ mice compared to WT mice was investigated. Kinetic studies concerning the number of neutrophils in WT and *Reg3b*$^{-/-}$ mice subjected to permanent LAD Ligation were performed with flow cytometry (Figure 9). Neutrophils were defined as CD45^{hi} CD11b^{hi} CD64^{lo} Ly6G^{hi} as shown in the gating scheme (Figure 9A) (Lörchner, Widera, et al., 2018). In line with previous findings (N. G. Frangogiannis, 2012; Yan et al., 2013) a massive and rapid accumulation of neutrophils at the site of injury of approximately 3 x 10^3 cells/mg infarct tissue was observed within the first two days post-MI equally in both mouse strains. At day 4, however, the neutrophil numbers in WT mice substantially declined to ~ 0.8 x 10^3 cells/mg whereas in *Reg3b*$^{-/-}$ mice the numbers remained significantly higher with 2 x 10^3 cells/mg, confirming the results of Lörchner et al. (Loerchner et al., 2015). At day 7, neutrophils were equally cleared/removed from the infarcted heart in both mouse strains (Figure 9B).

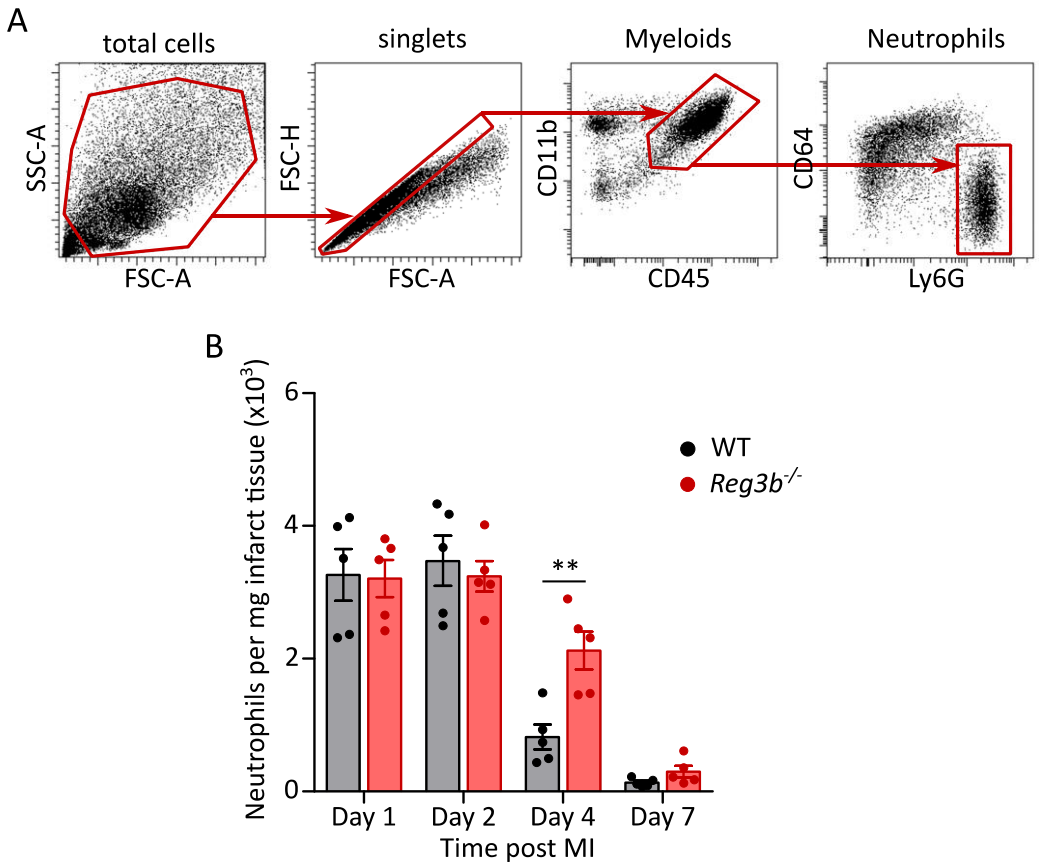

Figure 9: Neutrophils persist in the ischemic heart at day 4 post-MI in *Reg3b*$^{-/-}$ mice
(A) Infarcted hearts were enzymatically digested and cardiac leukocytes were isolated. By plotting the forward scatter (= cell size) against the sideward scatter (= cell granularity), the total cell population is defined and small cell debris is excluded. Following doublet exclusion, the leukocyte marker CD45 and myeloid marker CD11b identify the myeloid cell population. Finally, the cell population negative for the macrophage marker CD64 and positive for the neutrophil marker Ly6G represents the cardiac neutrophils. FSC = forward scatter; SSC = sideward scatter; A = area; H = height
(B) Purified cell suspensions from the infarct area of WT and *Reg3b*$^{-/-}$ mice at day 1, 2, 4 and 7 post LAD ligation were analyzed by flow cytometry. Neutrophils were identified as CD45^{hi} CD11b^{hi} CD64^{lo} Ly6G^{hi}. Cells per mg infarct tissue were calculated by normalization of the percentage of neutrophils to the weight of infarct tissue. Data are shown as mean ± SEM and are representative of eight independent experiments. WT and *Reg3b*$^{-/-}$ n = 5. **p ≤ 0.01 was determined by regular two-way ANOVA followed by Bonferroni post-tests.

Under inflammatory conditions, granulopoiesis in the bone marrow is increased and high numbers of neutrophils are released into the circulation and migrate to the site of injury (Kolaczkowska & Kubes, 2013). In order to dissect the impact of Reg3β deficiency on neutrophils from the periphery, the number of cells from the bone marrow, blood and heart of WT and *Reg3b*$^{-/-}$ mice were compared by means of flow cytometry 4 days post-MI (Figure 10). Bone marrow-derived and blood neutrophil subsets were identified as CD45^{hi} C11b^{hi} CD115^{lo} Ly6G^{hi}

and determined as cells per femur+tibia and cells/ml blood, respectively. Cardiac neutrophils were identified and counted as described above. Interestingly, the persistence of neutrophils at day 4 post-MI due to the loss of *Reg3b*$^{-/-}$ was not observed in the bone marrow and peripheral blood but restricted to the heart after the onset of MI.

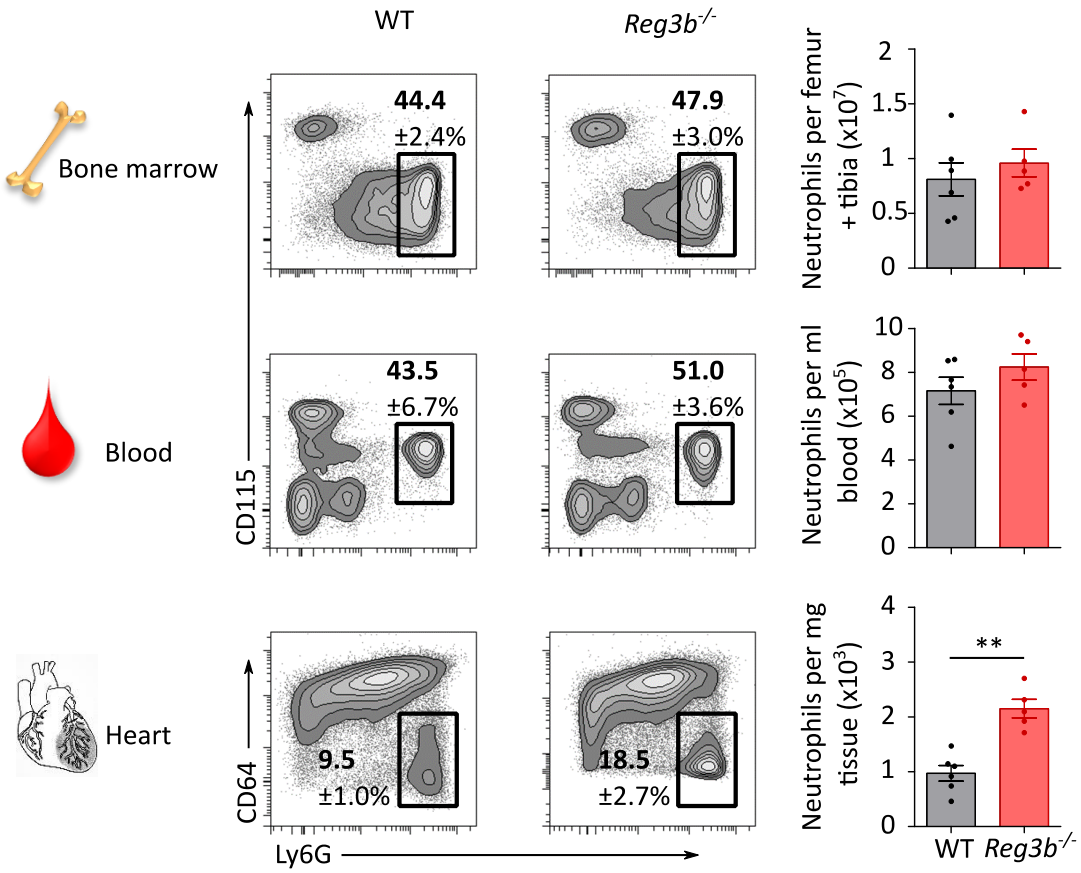

Figure 10: Neutrophil persistence in *Reg3b*$^{-/-}$ mice is restricted to the heart post-MI
Flow cytometric quantification of neutrophils derived from the bone marrow, peripheral blood and cardiac infarct tissue of WT and *Reg3b*$^{-/-}$ mice at day 4 post-MI. Representative contour plots from individual WT and *Reg3b*$^{-/-}$ mice display gated neutrophil populations from indicated tissues. Percentage of cells are shown as mean ± SEM. Corresponding calculations of total neutrophils per femur and tibia, per ml blood or per mg infarct tissue are shown as mean ± SEM. Data represent the results of two independent experiments. WT n = 6, *Reg3b*$^{-/-}$ n = 5. **p ≤ 0.01 was determined by two-tailed Mann-Whitney test.

6.1.2 Reg3β has no impact on neutrophil migration

Since Reg3β functions as chemoattractant for macrophages, a transwell migration assay was performed to examine potential chemotactic effects of Reg3β on neutrophils. As expected,

neutrophils did not exhibit an increased migration rate in response to Reg3β compared to control cells, whereas the migration activity in response to the positive control CXCL2 was ~ 4.6 fold higher (Figure 11).

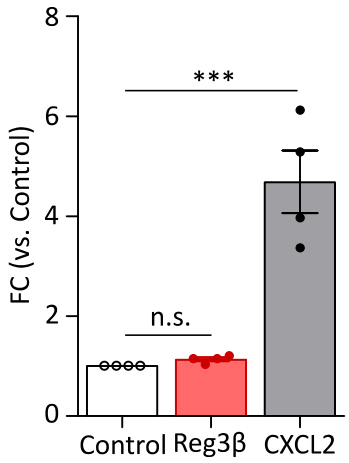

Figure 11: Neutrophils do not exhibit migratory effects in response to Reg3β
Casein-elicited neutrophils from the peritoneum were cultured on transwell inserts to analyze cell migration in response to Reg3β (100 ng/ml) by counting the cells migrated on the cell culture plate after 2.5 hours. CXCL2 (100 ng/ml) was used as positive control. Data represent the fold change of cell migration in response to Reg3β or rather CXCL2 vs. control and are shown as mean ± SEM of two individual experiments. n = 4. ***p ≤ 0.001; n.s. = not significant was determined by one-way ANOVA followed by Bonferroni's post test.

The migration assay implies a different role and effector mechanism of Reg3β for neutrophils than for macrophages and reaffirms the concept of its role in neutrophil clearance from the site of inflammation.

6.1.3 Loss of Reg3β promotes an accumulation and persistence of neutrophils within the remote zone of the infarcted heart

Reg3b$^{-/-}$ mice display an increased mortality rate due to an increased incidence of fatal acute cardiac rupture (Loerchner et al., 2015). The continuous secretion of tissue degrading enzymes by persisting neutrophils may contribute or even expand to further tissue damage (Haslett, 1992; Zimmerli, Seligmann, & Gallin, 1986). To verify the role of neutrophils on left ventricular wall instability in *Reg3b*$^{-/-}$ mice, 3-dimensional (3D) imaging using light sheet microscopy combined with in-vivo antibody labeling was applied. Antibodies directed against the neutrophils marker Ly6G, endothelial cell marker CD31 and collagen type III were used.

A permanent LAD ligation provokes the collapse of coronary arteries inside the infarct area visible by a $CD31^{neg}$ area in the first days post-MI (Merz et al., 2019). At day 7, the infarct area was identified based on the collagenous content of the mature scar. The cellular distribution within the whole heart was assessed by calculating and comparing the number of neutrophils located in the infarct zone (IZ) and the non-infarcted remote zone (RZ) of WT and *Reg3b*$^{-/-}$ mice. On top, the determination of heart and infarct surface area provided information about the effect of Reg3β on heart dilation and expansion of infarct injury.

The size of the heart after the onset of MI as well as the size of the infarction area was not affected by the loss of Reg3β (Figure 12A). Similar to previous findings obtained with flow cytometry, detection of neutrophils in the whole heart revealed a persistence at day 2 post-MI in *Reg3b*$^{-/-}$ mice (Figure 12B). However, considering RZ and IZ separately, differences became apparent. The dynamics of neutrophil accumulation within the $CD31^{neg}$ or rather Collagen type III^{pos} IZ after permanent LAD Ligation was similar in both mouse strains despite a slight but not significant increase of neutrophils in the IZ of *Reg3b*$^{-/-}$ mice at day 1 and 2 (Figure 12B).

In contrast, mice deficient of Reg3β depicted an increased infiltration of neutrophils in the RZ peaking at day 2 and 4 with ~2 x 10^{-4} neutrophils/µm^2 RZ in *Reg3b*$^{-/-}$ vs. ~1 x 10^{-4} neutrophils/µm^2 RZ in WT mice. At day 7, WT and *Reg3b*$^{-/-}$ mice displayed a similar reduction of neutrophils in the RZ with ~3 x 10^{-5} in *Reg3b*$^{-/-}$ and ~2 x 10^{-5} in WT mice (Figure 12B).

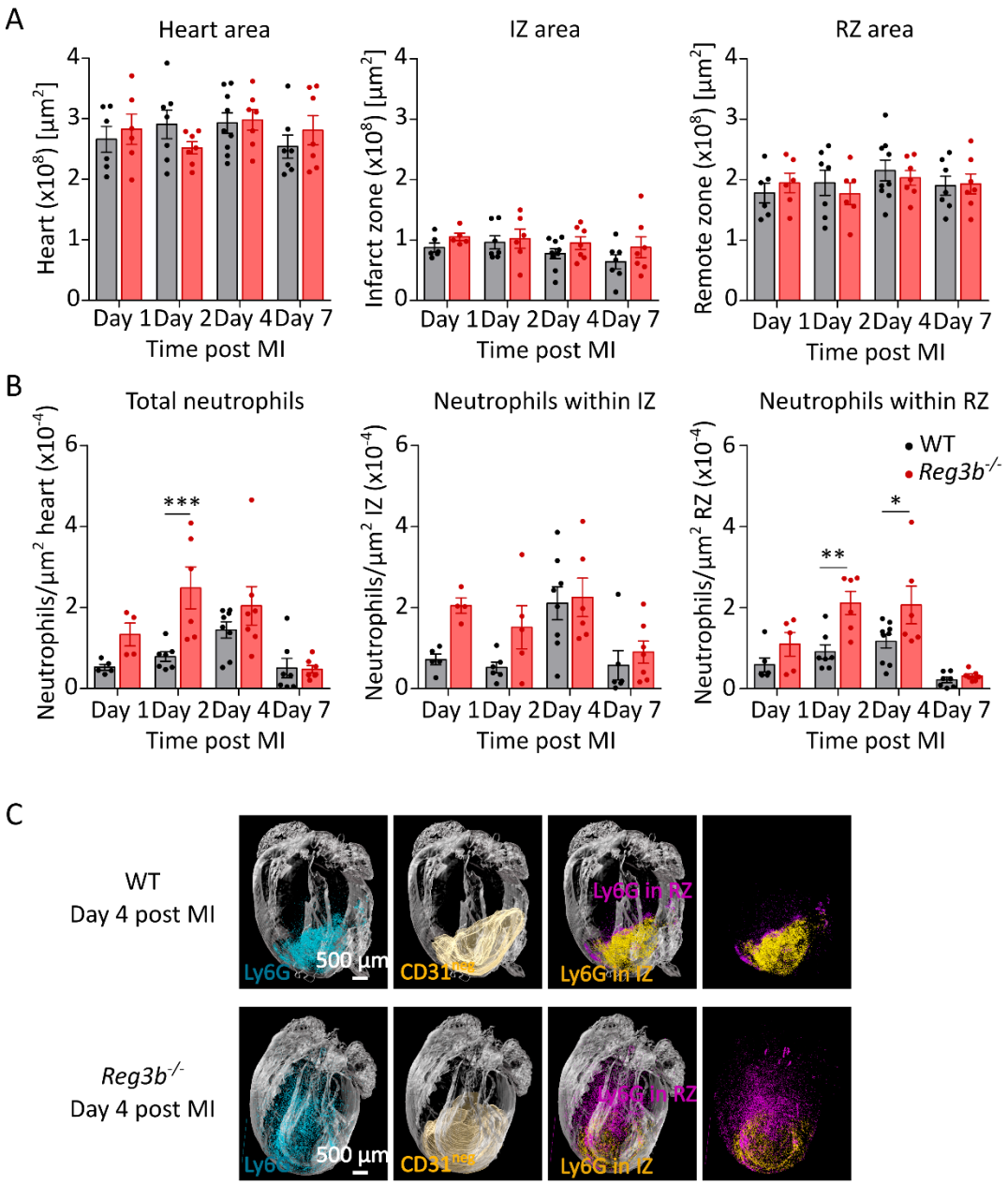

Figure 12: Neutrophils accumulate in the remote zone of *Reg3b*$^{-/-}$ mice at day 2 and 4 post-MI

Infarcted hearts of WT and *Reg3b*$^{-/-}$ mice were stained for the neutrophil marker Ly6G conjugated to AF647, the endothelial cell marker CD31 conjugated to AF790 and collagen type III conjugated to AF790, respectively, by in vivo antibody staining i.v. prior to ECi clearing. Image processing and analysis was done with Imaris. (A) The heart size was calculated by means of the autofluorescence of the heart itself. The IZ was identified by CD31^{neg} area at day 1, 2 and 4 and by collagen^{pos} area at day 7. The RZ was calculated by subtracting the IZ from the heart surface. (B) Total neutrophil counts, neutrophils located in the CD31^{neg} or rather Collagen type II^{pos} IZ and in the CD31^{pos} or rather Collagen type II^{neg} RZ were normalized to the heart surface area, IZ or rather RZ area. Data are shown as mean ± SEM and represent the results of eight independent experiments. WT and *Reg3b*$^{-/-}$ n = 4-8. *p ≤ 0.05; **p ≤ 0.01 was determined by regular two-way ANOVA followed by Bonferroni post-tests. (C) Representative 3D reconstruction display the total neutrophils (cyan) within the whole heart (grey) as well as neutrophils located in the IZ (yellow) and neutrophils located in the RZ (magenta) from individual WT and *Reg3b*$^{-/-}$ mice at day 4 post-MI.

To evaluate the inflammatory activity of persisting neutrophils in *Reg3b*$^{-/-}$ *mice*, the expression of neutrophilic granule proteins was analyzed in the IZ and RZ of WT and *Reg3b*$^{-/-}$ mice at day 4 post-MI. The expression of NE, MPO, NGAL and MMP-9 was increased in the RZ of *Reg3b*$^{-/-}$ mice compared to WT mice. Contrary, the IZ displayed equal expression levels of all proteins (Figure 13).

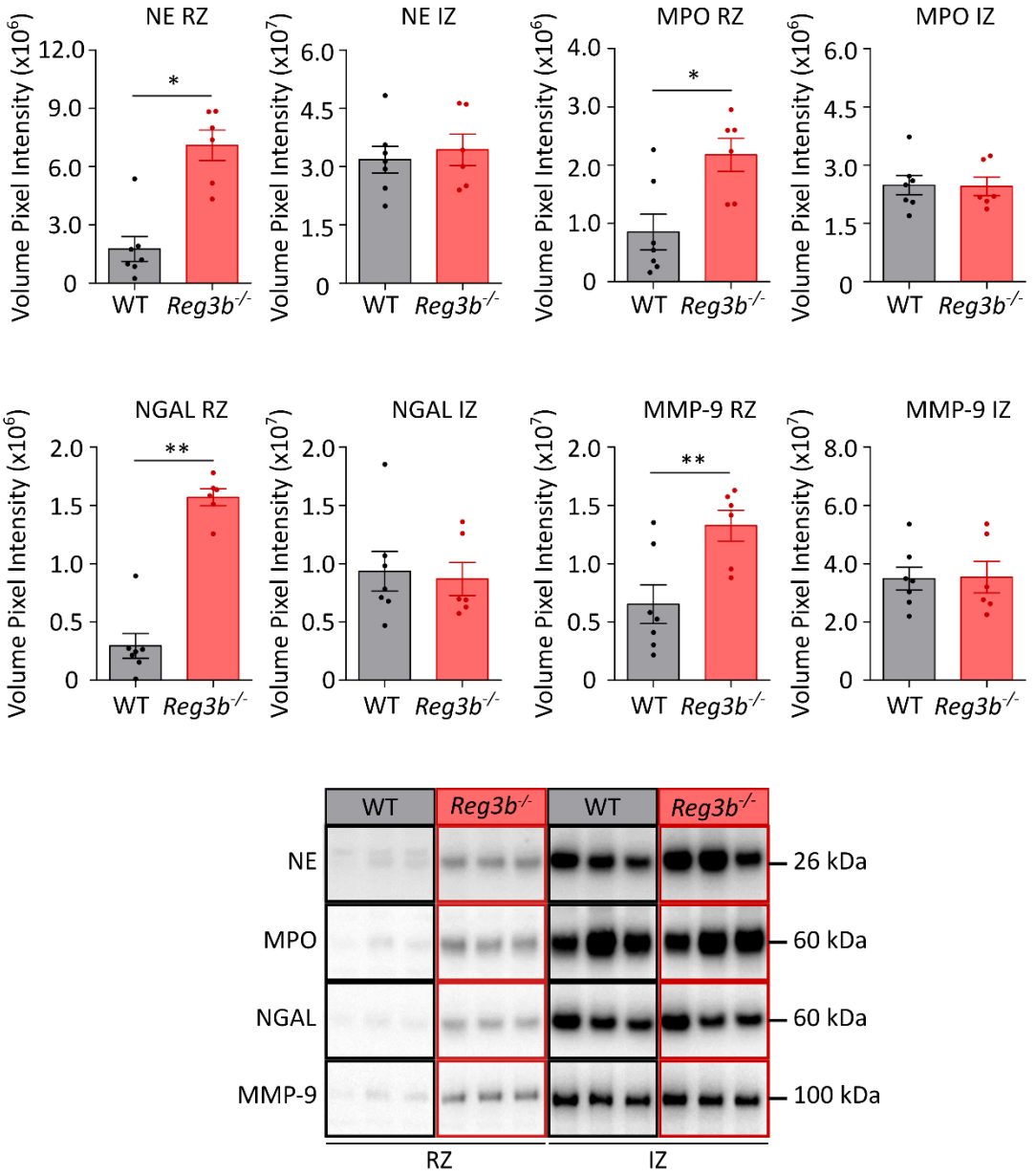

Figure 13: Loss of Reg3β results in an increased expression of neutrophilic granule proteins in the remote zone at day 4 post-MI

Western blot analysis of neutrophilic granule protein expression in infarcted heart samples of WT and *Reg3b*$^{-/-}$ mice fractionated for RZ and IZ 4 days post MI. Quantitative analysis of the volume pixel intensity of NE, MPO, NGAL and MMP-9 in the RZ and IZ of myocardial tissue and representative western blots. Data are shown as mean ± SEM. WT n= 7, *Reg3b*$^{-/-}$ n = 6. *p ≤ 0.05; **p ≤ 0.01 was determined by two-tailed Mann-Whitney test.

Conclusively, genetic loss of Reg3β caused a neutrophil persistence restricted to the heart at day 4 after permanent LAD ligation in mice without affecting the heart and infarct size. Three-dimensional imaging of the whole heart revealed an infiltration of persisting neutrophils in the RZ of *Reg3b*$^{-/-}$ mice. Furthermore, the accumulation of inflammatory active neutrophils in the intact myocardium is believed to be associated with cardiac rupture observed at day 4 post-MI (Loerchner et al., 2015).

6.1.4 Reg3β co-localizes with neutrophils in the ischemic heart

The findings so far have shown the impact of Reg3β deficiency on the overall presence and spatial distribution of neutrophils within the ischemic heart. The direct contribution of Reg3β on neutrophil clearance required further investigations. Immunohistochemical analysis of infarcted hearts of WT mice 4 days post-MI revealed a close proximity of infiltrated neutrophils and Reg3β within the border zone of the infarct area suggesting a direct interaction (Figure 14). Moreover, fluorescence labelling of cardiomyocytes and Reg3β is indicative of cellular origin of Reg3β by stressed but not fully necrotic cardiomyocytes within the ischemic area as already stated by Lörchner et al. (Loerchner et al., 2015).

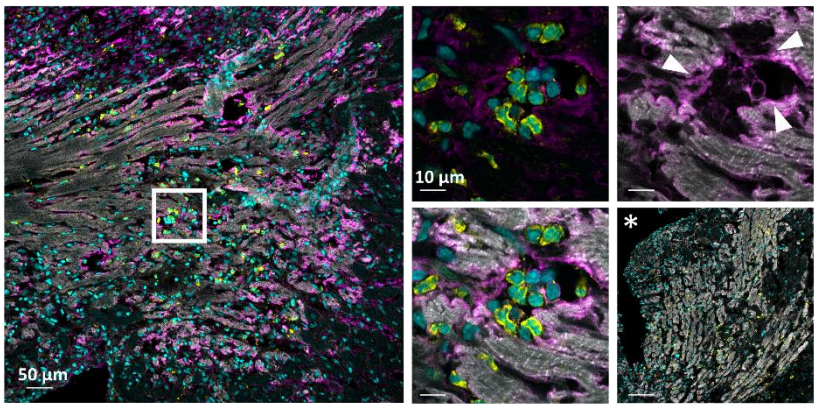

Figure 14: Reg3β and neutrophils directly interact in the infarcted tissue
Frozen tissue sections of WT infarcted hearts 4 days post-MI were stained for cardiomyocytes with sarcomeric actinin (grey), neutrophils with Ly6G (yellow), Reg3β (magenta) and counterstained with DAPI (cyan). Representative images demonstrate a direct interaction of Reg3β and infiltrated neutrophils within the border zone. White arrows indicate the secretion of Reg3β by stressed cardiomyocytes at the border zone. * displays a frozen tissue section of an infarcted heart 4 days post-MI of *Reg3b*$^{-/-}$ mice as staining control for Reg3β. Scale bar as indicated.

Next, 3D imaging using light sheet microscopy combined with in vivo antibody staining was applied to validate the direct interplay of neutrophils and Reg3β in the whole heart. 3D reconstructions of infarcted hearts stained for Ly6G and Reg3β displayed a comparable distribution of neutrophils and Reg3β in the left ventricle (Figure 15A), whereas the non-infarcted control heart did not indicate any neutrophil infiltration or Reg3β expression as expected (Figure 15C). To further examine the direct interaction of neutrophils and Reg3β, both signals were merged in 2D image stacks. A partial co-localization of cells and protein was observed primarily in the border zone of the left ventricular wall (Figure 15B). By plotting the intensity signals of Ly6G and Reg3β obtained from the 3D images, against each other in a density scatter plot, a Pearson's correlation coefficient of 0.55 confirmed the moderate co-localization. An additional cross correlation analysis verified the accuracy of the co-localization analysis. By shifting the Ly6G image pixel by pixel in x/y (grey) and z (black) direction relative to the Reg3β image and calculating the respective Pearson's R, the correlation coefficients constantly decreased (Figure 15D).

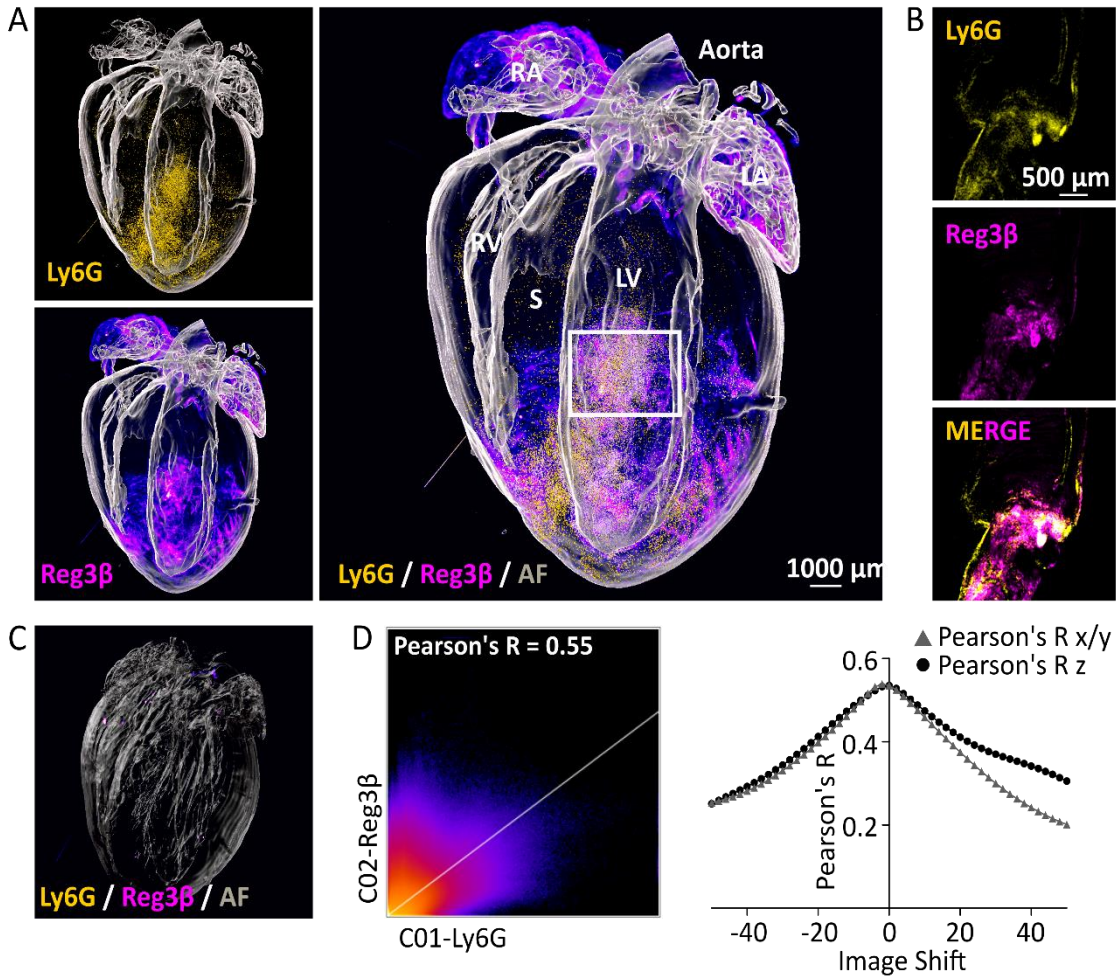

Figure 15: Reg3β and neutrophils partially co-localize within the ischemic heart
Infarcted hearts of adult WT mice were stained for the neutrophil marker Ly6G conjugated to AF647 and Reg3β conjugated to AF790 in vivo prior to ECi clearing 4 days post-MI. (A) Representative 3D reconstructions show the distribution of neutrophils (Ly6G in yellow) and Reg3β (magenta) within the whole heart. (B) The enlarged image section of the left ventricular wall visualizes the partial co-localization of neutrophils and Reg3β (white) in the border zone. (C) A non-infarcted WT heart was used as staining control. (D) Co-localization analysis using the Coloc2 plugin from ImageJ displays the scatter plot of the Ly6G and Reg3β signal intensities and the calculated correlation coefficient by linear regression. The cross correlation function was obtained by plotting the respective Pearson's R as a function of the pixel shift in x/y and z direction. WT n = 3.

Taken together, these results indicate that cardiomyocyte-derived Reg3β co-localized with and bound to a certain proportion of infiltrating neutrophils in the ischemic heart, assuming a direct impact on neutrophil accumulation and clearance by Reg3β.

6.2 Underlying mechanisms of Reg3β-mediated neutrophil clearance

6.2.1 Reg3β binding to neutrophils coincides with decreased cell viability

Following the evidence of co-localizing neutrophils and Reg3β in the injured heart, a direct binding of Reg3β to cardiac neutrophils was further examined by flow cytometry. Reg3β was detected via antibody staining on the cell surface of cardiac neutrophils from day 1 until day 7 post-MI. According to the isotype control, Reg3β bound to a subpopulation of neutrophils that constantly increased from 11 % at day 1 up to 20 % at day 7. In this context, the Reg3β unbound or Reg3β negative binding subpopulation significantly decreased from 88 % at day 1 to 70 % at day 7 post-MI (Figure 16).

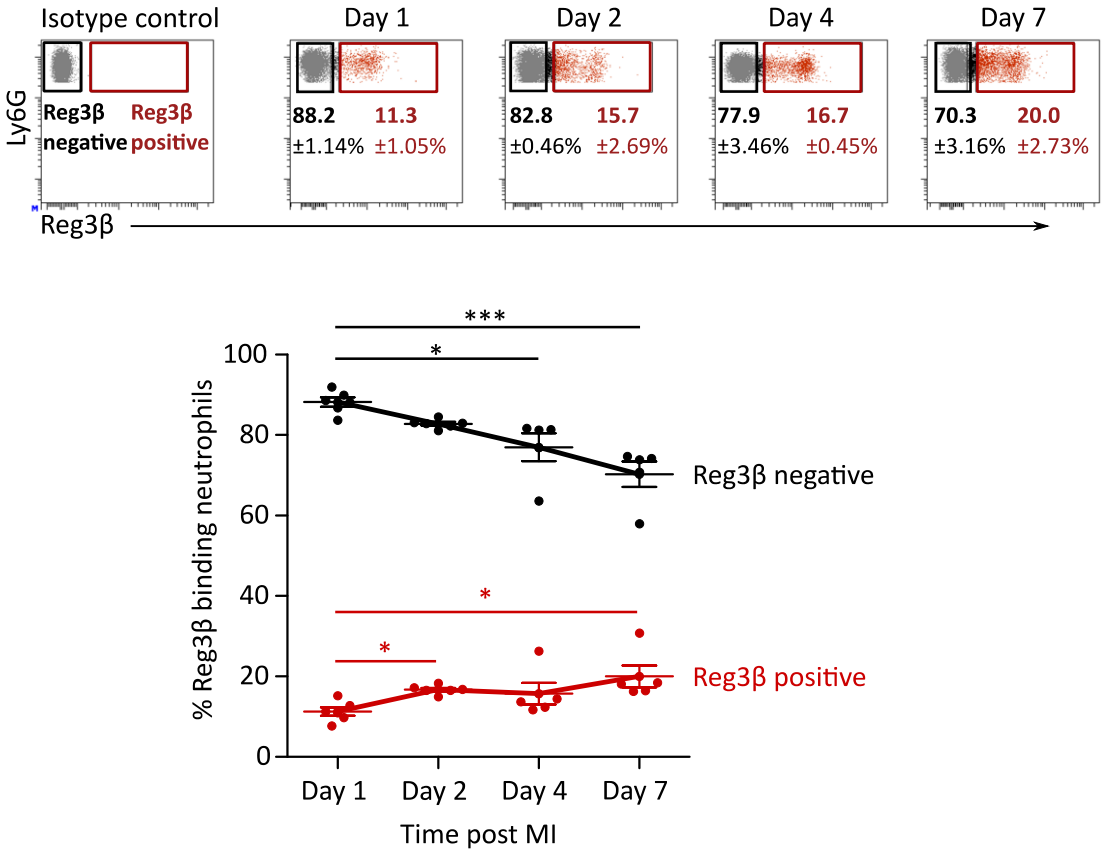

Figure 16: The Reg3β-binding neutrophil subpopulation increases over time post-MI
Infarcted hearts of WT mice were digested at indicated time-points post-MI and analyzed with flow cytometry. Neutrophils were identified as CD45^{hi} CD11b^{hi} CD64^{lo} Ly6G^{hi} and examined for cell surface binding of Reg3β at each time-point. Representative dot plots display the dynamics of Reg3β positive and negative binding neutrophil population post-MI. The gate determining the Ly6G^{hi} and Reg3β-binding population was set according to the corresponding isotype control of the Reg3β antibody. Percentage of cells are shown as mean ± SEM of four independent experiments. Day 1 and 2 n = 6; day 4 and 7 n = 5. *p ≤ 0.05; ***p ≤ 0.001 was determined by regular two-way ANOVA followed by Bonferroni post-tests.

Regarding the potential role of Reg3β on neutrophil removal, both populations were analyzed for apoptotic and necrotic cell death events 4 days post-MI using flow cytometry with the intention to study the consequences of Reg3β binding to the cell viability of neutrophils (Figure 17). Due to the changes in permeability of the cell membrane during apoptosis, the cyanine dye Po-Pro1 can enter the cell whereas the cell impermeant dye 7AAD cannot (Idziorek, Estaquier, De Bels, & Ameisen, 1995; D. Wlodkowic, Telford, Skommer, & Darzynkiewicz, 2011). Cells with a pronounced loss of membrane integrity are permeable to both, Po-Pro1 and 7AAD, and are termed aponecrotic (Idziorek et al., 1995; Donald Wlodkowic, Skommer, & Pelkonen, 2007). The relative number of Po-Pro1^{neg} and 7AAD^{neg} viable neutrophils was around 80 % in the Reg3β negative binding population and dropped to ~ 40 % in the Reg3β positive-binding population. The percentage of Po-Pro1^{pos} and 7AAD^{pos} aponecrotic neutrophils was 40 % in the Reg3β positive-binding fraction but nearly absent with ~ 1.5 % in the Reg3β negative binding population. Contrary, the relative number of Po-Pro1^{pos} and 7AAD^{neg} apoptotic cells was comparable with ~15 % in both populations, suggesting that Reg3β binding induces aponecrotic cell death but not apoptosis to cardiac neutrophils (Figure 17).

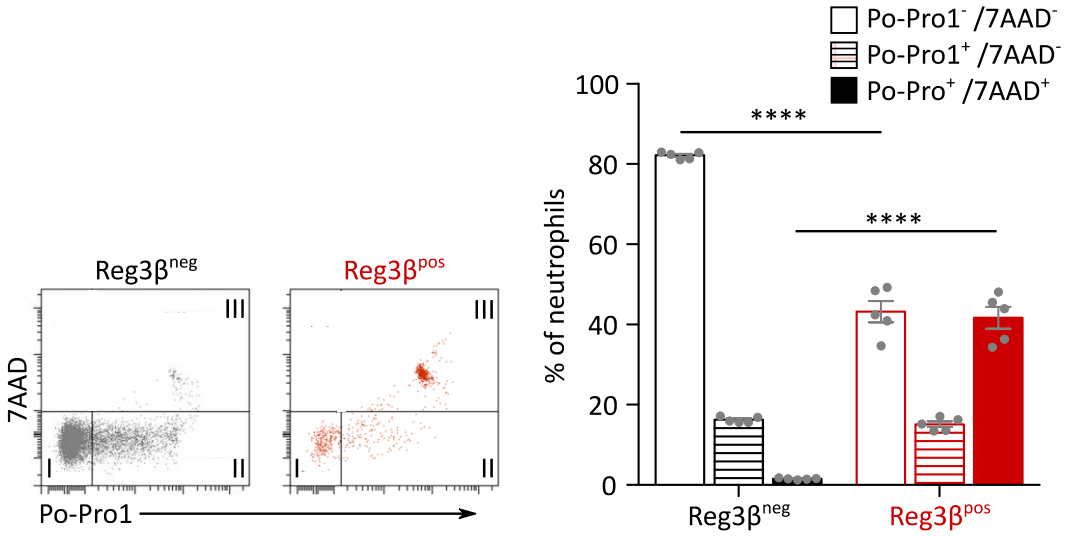

Figure 17: Reg3β positive-binding neutrophils display an increased aponecrotic phenotype
Infarcted hearts of WT mice were enzymatically digested 4 days post-MI and analyzed for neutrophil cell death by flow cytometry. Neutrophils were identified as CD45^{hi} CD11b^{hi} CD64^{lo} Ly6G^{hi} and cell death was determined using the apoptotic marker Po-Pro1 and the necrotic marker 7AAD. Representative dot plot illustrates the identification of viable cells in quadrant I (Po-Pro1^{neg} / 7AAD^{neg}), apoptotic cells in quadrant II (Po-Pro1^{pos} / 7AAD^{neg}) and aponecrotic cells in quadrant III (Po-Pro1^{pos} / 7AAD^{pos}) of Reg3β negative binding (grey) and Reg3β positive-binding cardiac neutrophils (red). Relative numbers of viable, apoptotic and aponecrotic neutrophils are shown as mean ± SEM. N = 5. ****p ≤ 0.0001 was determined by regular two-way ANOVA followed by Bonferroni post-tests.

Next, a correlation analysis was performed to test the association between Reg3β binding to cardiac neutrophils and the concurrence of aponecrotic cell death. Relative numbers of Reg3β negative binding or rather Reg3β positive-binding neutrophils were plotted against the respective numbers of Po-Pro1^{pos} / 7AAD^{pos} aponecrotic cells obtained from day 1, 2, 4 and 7 post-MI (Figure 18). Reg3β positive-binding neutrophils exhibited a strong and positive correlation of 0.63 (Pearson's), or rather 0.78 (Spearman's) with aponecrotic cells. In contrast Reg3β negative binding neutrophils negatively correlated with aponecrotic neutrophils with a correlation coefficient of -0.24 (Pearson's) and -0.11 (Spearman's), respectively, substantiating that Reg3β binding is associated with the induction of an apoptosis-necrosis like cell death to a subpopulation of cardiac neutrophils.

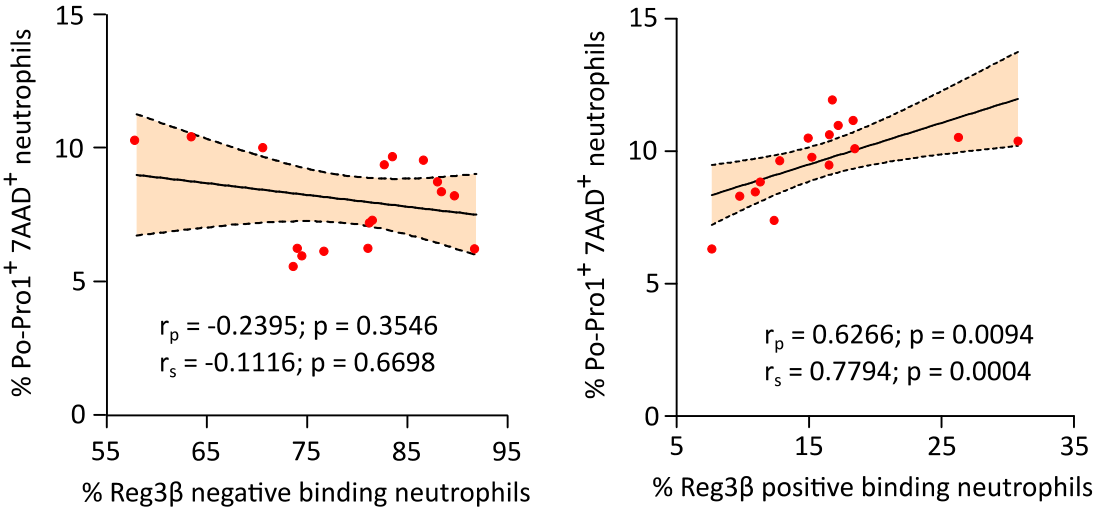

Figure 18: Reg3β binding correlated with the induction of aponecrosis in neutrophils
Reg3β negative and positive binding neutrophils obtained from infarcted hearts of WT mice at day 1, 2, 4 and 7 post-MI were plotted against Po-Pro1^{pos} / 7AAD^{pos} aponecrotic neutrophils. Pearson's correlation coefficient r_p and Spearman's rank correlation coefficient r_s were calculated by linear regression with 95 % confidence band of the best-fit line.

Based on the findings of an increasing Reg3β positive-binding neutrophil population, it can be concluded that the proportion of aponecrotic neutrophils also increases over time and thus Reg3β directly contributes to the removal of neutrophils during cardiac healing.

Considering the correlation between cell death and Reg3β binding, neutrophil cell death was studied in mice deficient for Reg3β compared to WT mice after the onset of MI using the same apoptotic and necrotic cell death marker as described before (Figure 19). With regard to apoptosis (Po-Pro1^{pos} / 7AAD^{neg}) both mouse strains displayed the same kinetics over time post-

MI, strengthening the assumption that Reg3β induced neutrophil cell death is different from apoptosis. The percentage of apoptotic cells slightly increased from ~10 % apoptotic cells at day 1 to ~ 17 % at day 2 followed by a constant decrease back to ~12 % until day 7. Aponecrotic cell death events, however, constantly increased from ~10 % at day 1 up to ~ 20 % at day 7 in WT mice but remained nearly at the same level between 11 % and 14 % in *Reg3b*$^{-/-}$ mice demonstrating a significant reduced neutrophil cell death in Reg3β deficient mice after LAD ligation.

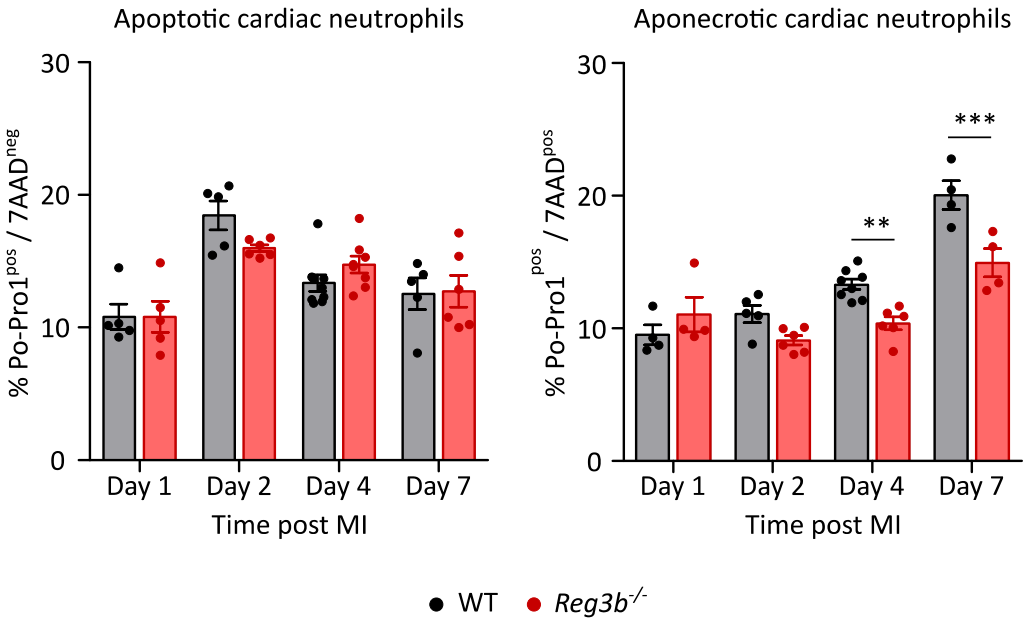

Figure 19: Loss of Reg3β coincides with a reduced aponecrotic cell death in cardiac neutrophils
Infarcted hearts of WT and *Reg3b*$^{-/-}$ mice were enzymatically digested at day 1, 2, 4 and 7 post-MI and analyzed for apoptotic and aponecrotic cell death events in cardiac neutrophils using Po-Pro1 and 7AAD. Neutrophils were identified as CD45^{hi} CD11b^{hi} CD64^{lo} Ly6G^{hi}. Percentage of Po-Pro1^{pos} / 7AAD^{neg} apoptotic and Po-Pro1^{pos} / 7AAD^{neg} aponecrotic cardiac neutrophils are shown as mean ± SEM of four independent experiments. WT, *Reg3b*$^{-/-}$ n = 4 - 6. **p ≤ 0.01, ***p ≤ 0.001 was determined using regular two-way ANOVA followed by Bonferroni post-test.

In summary, loss of Reg3β results in the persistence of neutrophils restricted to the heart after the onset of LAD ligation. Neutrophils of *Reg3b*$^{-/-}$ mice mainly accumulated in the RZ within the ischemic heart presumably leading to destabilization of the left ventricular wall. Additionally, Reg3β co-localizes and binds to a subpopulation of cardiac neutrophils inducing aponecrotic cell death, hence, contributing to neutrophil clearance from the site of inflammation.

6.2.2 Reg3β has a direct cytotoxic effect on inflammatory active neutrophils

Based on the findings in vivo, the direct impact of Reg3β on neutrophil clearance was further examined by different in vitro cytotoxicity assays with primary neutrophils from the peritoneum. The usage of peritoneal neutrophils instead of cardiac cells provides the advantage of a very large cell yield that can be used simultaneously for several assays. Furthermore, the induction of a peritonitis by casein injections mainly enriches inflammatory active cells reflecting the situation in the infarcted heart.

Peritoneal neutrophils, labeled with the cyanine nucleic acid dye Cytotox Green, were stimulated with Reg3β in different doses and neutrophil viability was assessed. The relative number of Cytotox green positive dead cells was measured every hour using life imaging (Figure 20A). Surprisingly, the highest concentration of Reg3β with 1000 ng/ml exhibited the weakest cytotoxicity. On the other hand, the lower Reg3β concentrations of 10 and 100 ng/ml revealed a similar progress with a strong increase of dead cells within the first 60 minutes followed by a continuous but moderate increase in the next hours. However, only stimulation with 100 ng/ml Reg3β demonstrated a significant cytotoxicity in the first hours post stimulation, suggesting this concentration as optimum for the induction of neutrophil cell death. Hence, all further in vitro experiments were conducted with 100 ng/ml Reg3β.

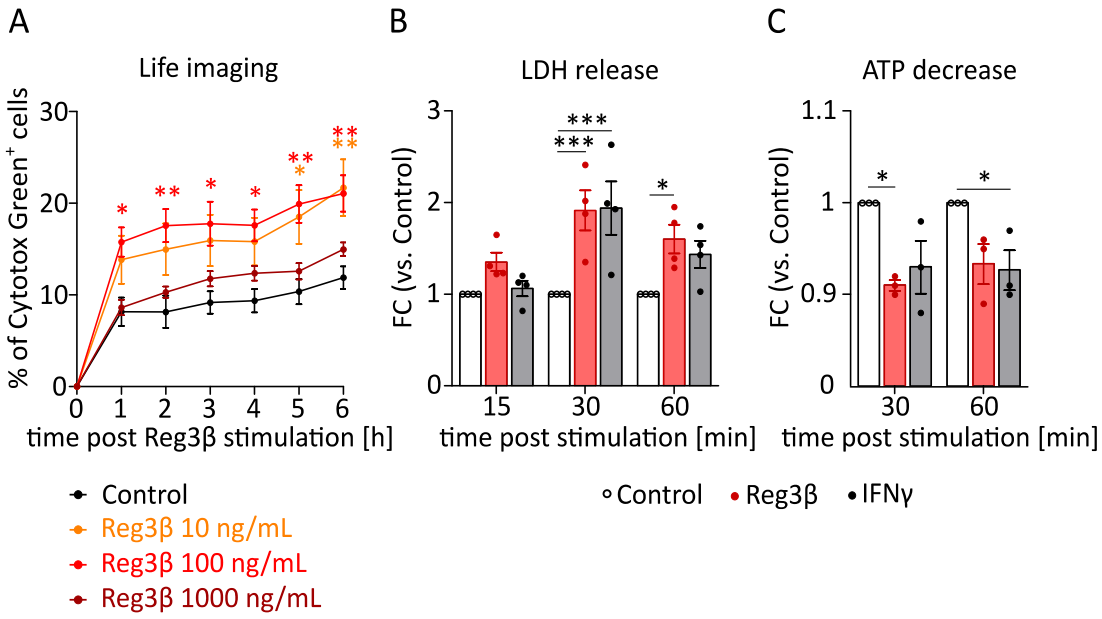

Figure 20: Reg3β has a direct and fast cytotoxic effect on neutrophils
(A) Casein-elicited peritoneal neutrophils were cultivated and stimulated with Reg3β in different concentrations (10, 100 and 1000 ng/ml), control cells were treated equally with PBS. Cell death was determined by counting the relative number of Cytotox Green positive cells every hour in a total of 6 hours using life imaging. Percentage of dead cells is shown as mean ± SEM of three independent experiments. N = 4. (B) LDH release of peritoneal neutrophils was measured after Reg3β (100 ng/ml) treatment for 15, 30 and 60 minutes. (C) Decrease of cell viability was determined based on intracellular ATP levels after 30 and 60 minutes of Reg3β (100 ng/ml) stimulation. IFNγ (100 ng/ml) was used as positive control. Cell death is represented as fold change of treated to control cells and shown as mean ± SEM of two independent experiments. Control, Reg3β, IFNγ n = 3-4. *p ≤ 0.05, **p ≤ 0.01, ***p ≤ 0.001 was determined using regular two-way ANOVA followed by Bonferroni post-test.

Life imaging of dead cells over time revealed an extensive increase within the first hour. Therefore, the following cytotoxicity assays focused on early cell death events that take place within 60 minutes.

LDH, a soluble cytosolic enzyme, is present in most eukaryotic cells. A key feature of cells undergoing apoptosis, necrosis or other forms of cellular death constitutes the release of this enzyme into the extracellular milieu (Decker & Lohmann-Matthes, 1988; Korzeniewski & Callewaert, 1983). Assessment of LDH release demonstrated a significant increase of neutrophil death after 30 minutes (~1.8 fold) and 60 minutes (~1.6 fold) of Reg3β stimulation. (Figure 20B). Next, the cell viability assay based on the measurement of intracellular ATP was applied. Cytosolic ATP, a hallmark of healthy cells, is decreasing during cell death (Maehara, Anai, Tamada, & Sugimachi, 1987). In concurrence with the LDH assay, neutrophils treated with Reg3β for 30 minutes displayed a significant decrease of intracellular ATP levels (~ 0.9 fold) (Figure 20C). All three assays demonstrated a direct cytotoxicity of Reg3β to peritoneal neutrophils in

vitro comparable to the positive control IFNγ (Nandi & Behar, 2011). Noteworthy, Reg3β-mediated induction of neutrophil cell death is a very fast process that occurs within 30 minutes post stimulation.

Previous results displayed a neutrophil persistence in Reg3β deficient mice restricted to the heart (Figure 10). However, after the onset of myocardial infarction Reg3β expression is upregulated in the ischemic heart but also in the serum of mice (Lörchner, Widera, et al., 2018) assuming peripheral neutrophils, that differ in their maturation and activation status, might also be targeted by Reg3β. Thus, the impact of Reg3β on cell viability of resting neutrophils from the bone marrow (Itou, Collins, Thoren, Dahlgren, & Karlsson, 2006), mature but inactive or unprimed neutrophils from the blood (Mayadas, Cullere, & Lowell, 2014) and mature neutrophils from the reservoir in the spleen (Deniset, Surewaard, Lee, & Kubes, 2017; Puga et al., 2011) were further examined using the LDH assay. Remarkably, none of the neutrophil populations were responsive to Reg3β and exhibited similar levels of cell death as control cells over time except for splenic neutrophils, which showed a slight but not significant increase of LDH release after 15 minutes. Bone marrow-derived, splenic and blood neutrophils treated with IFNγ though, died within 60 minutes as expected (Figure 21).

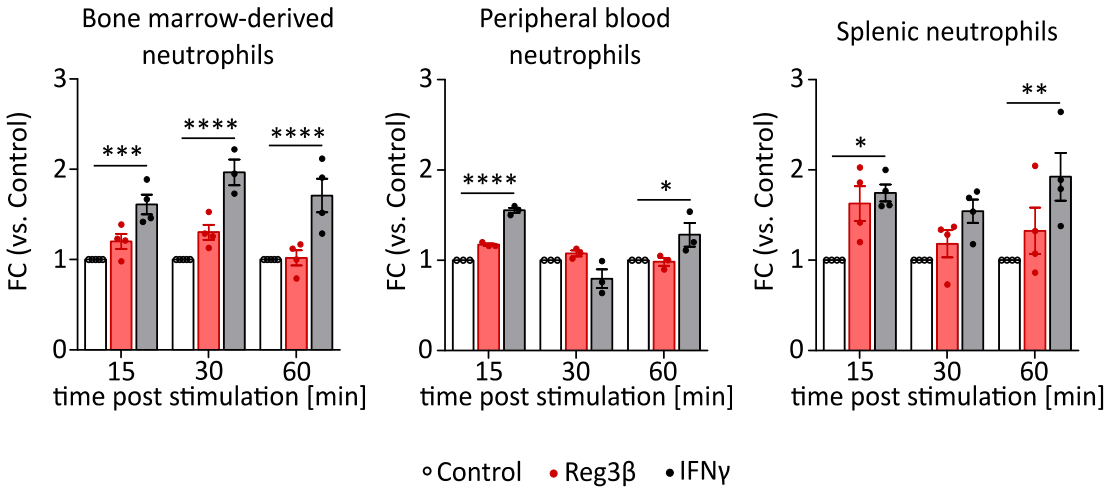

Figure 21: Resting and inactive neutrophils are not responsive to Reg3β
Neutrophils from the bone marrow, blood and spleen were treated with Reg3β (100 ng/ml) and INFγ (100 ng/ml) as positive control. Cell death was monitored by analyzing LDH release after 15, 30 and 60 minutes. Data represent the fold change of treated to control cells and are shown as mean ± SEM of two individual experiments. Control, Reg3β, IFNγ n = 3-4. *p ≤ 0.05, **p ≤ 0.01, ***p ≤ 0.001, ****p ≤ 0.0001 was determined using regular two-way ANOVA followed by Bonferroni post-test.

In contrast to casein-elicited neutrophils from the peritoneum, bone marrow-derived, peripheral blood and splenic neutrophils are not fully active (Devi, Laning, Luo, & Dorf, 1995; Tansho, Abe, & Yamaguchi, 1994) indicating that Reg3β exerts cytotoxic effects only on inflammatory active neutrophils.

Since the cytotoxicity of Reg3β is manifested in its binding to neutrophils, the binding capacities of Reg3β to bone marrow-derived, blood, and splenic neutrophils were analyzed by flow cytometry. As expected, Reg3β did not bind to any neutrophils populations neither in mice post-MI nor in healthy mice providing an explanation for the lack of cytotoxicity (Figure 22).

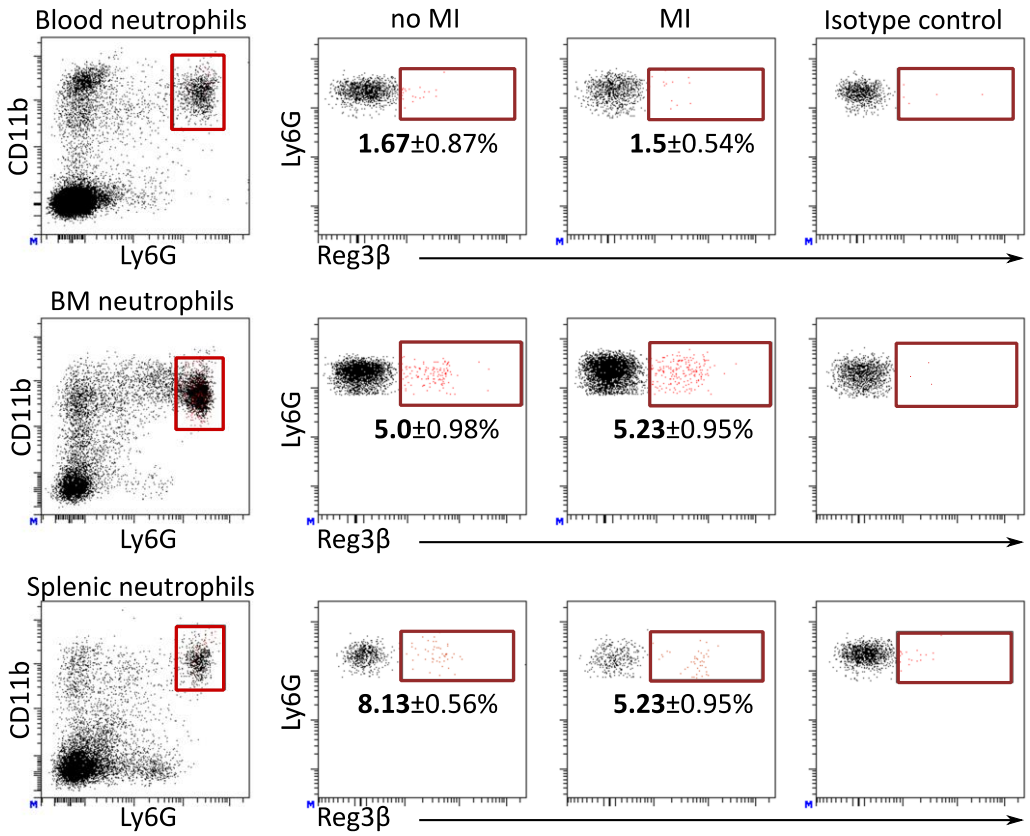

Figure 22: Reg3β does not bind to blood, bone marrow and splenic neutrophils post-MI
Neutrophils from the peripheral blood, bone marrow and spleen was harvested from WT mice 4 days post-MI and stained for Reg3β. Blood, bone marrow-derived and splenic neutrophils from mice without MI were used as controls. Neutrophils were identified as $CD45^+$ $CD11b^+$ and $Ly6G^+$ populations. The gate for the Reg3β binding neutrophil population was set according to the isotype controls. Dot plots are representative of three individual experiments. Percentages of the Reg3β positive neutrophil populations are shown as mean ± SEM.

In addition to the in vitro cytotoxicity assays, morphological changes after Reg3β treatment were assessed over time using transmission electron microscopy (TEM) and scanning electron microscopy (SEM). Unstimulated control cells from the peritoneum displayed the typical phenotype of mature and activated neutrophils including a highly granular cytosol filled with vesicles, a segmented or multilobulated nucleus (Fliedner, Cronkite, Killmann, & Bond, 1964; Schudel, 1965) and an amoeboid-like morphology with extended pseudopods (Ekpenyong, Toepfner, Chilvers, & Guck, 2015; Fernández-Segura, García, Santos, & Campos, 1995; Yap & Kamm, 2005). Immature and inactive bone-marrow neutrophils appeared more round, filled with less granules and no extended pseudopods demonstrating the phenotypical diversity of neutrophils during maturation and activation (Figure 23) (L. G. Ng et al., 2019). Upon Reg3β stimulation, however, there were prominent changes in the morphology of peritoneal neutrophils. Already after 15 minutes, the cells featured cytoplasmic vacuolization, a nearly complete loss of granules and membrane ruffling. The longer the stimulation time, the more dramatic the phenotypic changes became. After 60 minutes of Reg3β stimulation, the intracellular content appeared dissolved but membrane integrity was still maintained (Figure 23).

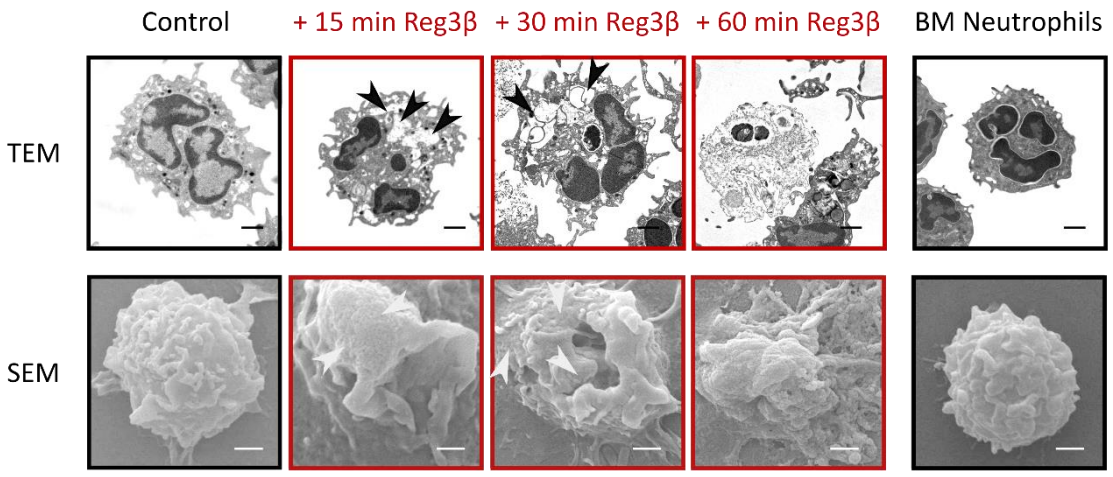

Figure 23: Reg3β treatment of peritoneal neutrophils causes morphological changes
Transmission electron microscopy (TEM) and scanned electron microscopy (SEM) of peritoneal neutrophils after 15, 30 and 60 minutes of Reg3β (100 ng/ml) stimulation. Compared to unstimulated control cells (black frame), Reg3β stimulated cells (red frame) exhibited a decrease in cytosolic granules, formation of cytoplasmic vacuolization (black arrows) and membrane ruffling (white arrows) until complete collapse of intracellular structures without losing membrane integrity. Bone marrow-derived neutrophils were isolated from femur and tibia of WT mice. Images are representative of two individual experiments. Scale bar = 1 µm.

Summarized, Reg3β-mediated cell death is characterized by cytoplasmic changes as vacuolization and loss of intracellular content with a sustained membrane integrity. Yet, the cells do not exhibit key characteristics of apoptosis as the formation of apoptotic bodies (Falcieri et al., 2000; Gorczyca, Melamed, & Darzynkiewicz, 1993), rounding of the nucleus and condensation of nuclear heterochromatin (Kennedy & DeLeo, 2009; Savill et al., 1989) confirming the results regarding apoptotic cell death in peritoneal and cardiac neutrophils by flow cytometry.

6.2.3 Reg3β does not activate common cell death pathways

Although morphological analysis assumed a Reg3β-mediated cell death mechanism different from apoptosis, neutrophils are known to undergo different cell death pathways including necroptosis, NETosis, pyroptosis and autophagy (Dąbrowska, Jabłońska, Iwaniuk, & Garley, 2019). Therefore, the expression of various markers specific for distinct cell death pathways was analyzed in cultured neutrophils post Reg3β stimulation. Namely, the expression of caspase-8, cleaved caspase-3 and -7 to detect the activation of apoptosis (Savill et al., 1989; Yamashita et al., 1999), the phosphorylation of MLKL and RIP3 during necroptosis (X. Wang, He, Liu, Yousefi, & Simon, 2016), cleaved caspase-1 (Miao et al., 2010; Ryu et al., 2017) and caspase-11 (Sun et al., 2018) for the induction of pyroptosis and microtubule-associated protein 1A/1B-light chain 3 (LC3) (Mitroulis et al., 2010) and Beclin-1 (Lv et al., 2017; Sharma, Simonson, Jondle, Mishra, & Sharma, 2017) for autophagy. Finally, citrullinated histone H4 and H3 were detected in the supernatant of neutrophil cultures for the detection of NETosis (Brinkmann et al., 2004) (Figure 24).

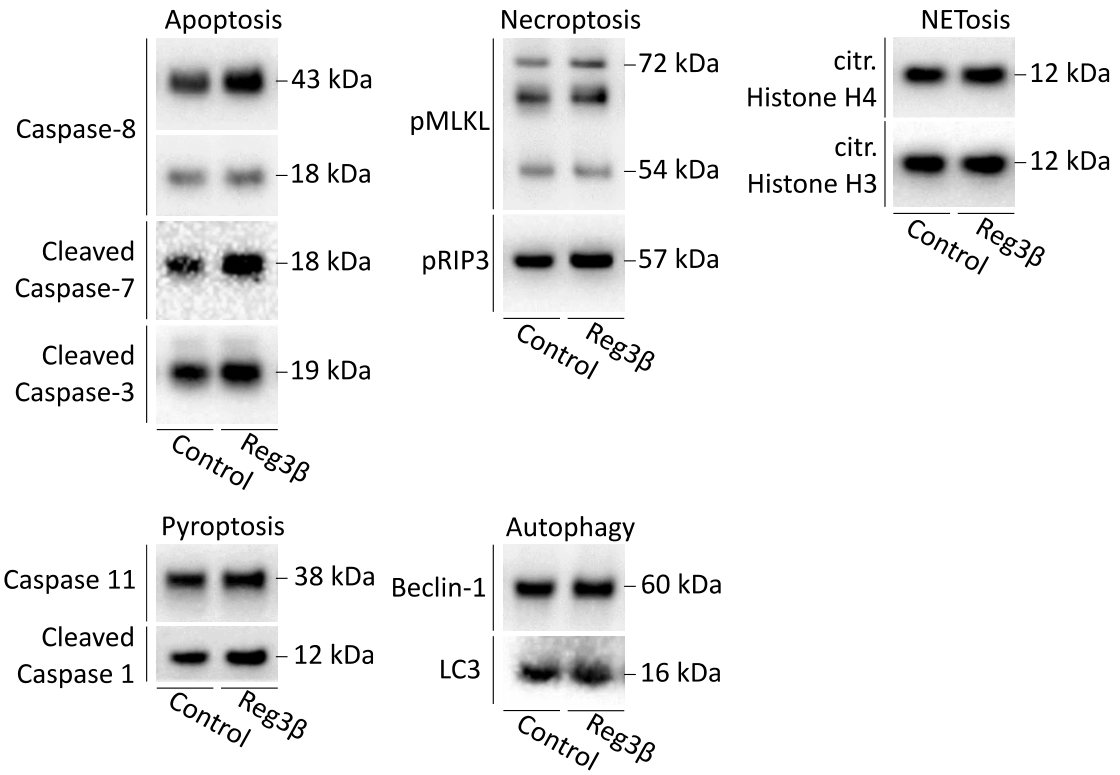

Figure 24: Common neutrophil cell death mechanisms are not activated upon Reg3β treatment
Western blot analysis of cell death markers for apoptosis, necroptosis, pyroptosis, autophagy and NETosis in lysates of peritoneal neutrophils after 60 minutes of Reg3β (100 ng/ml) stimulation. Blots are representative of two individual experiments.

Unexpectedly, none of the cell death pathways appeared to be regulated upon Reg3β stimulation, assuming a different mechanism for the induction of cell death than apoptosis, necroptosis, NETosis, pyroptosis or autophagy.

Necrosis was long thought to be a non-regulated cell death thereby disadvantageous for tissue homeostasis and wound healing. New findings could show that necrosis comprises signs of regulated processes such as ATP depletion, increased ROS generation, proteolysis of calpains and cathepsins and mitochondrial dysfunction (Festjens, Vanden Berghe, & Vandenabeele, 2006). Both, in vivo and in vitro data suggest a neutrophil cell death different from apoptosis with morphological signs for a regulated necrosis by means of the incorporation of the cell impermeant dye 7AAD of neutrophils binding to Reg3β and the rapid cell death induction 30 minutes after Reg3β stimulation associated with cytoplasmic vacuolization and dissolving of intracellular content. Consequently, the cells were examined for additional characteristics, which further substantiate and define the necrotic cell death.

6.2.4 Reg3β does not induce cell lysis by pore formation in the plasma membrane of neutrophils

Lectins of the Reg3 family in the intestine are bactericidal proteins for Gram-positive bacteria providing a spatial segregation of the gut microbiota and the intestinal epithelium (Vaishnava et al., 2011). The human Reg3β orthologue HIP/PAP recognizes the bacteria by binding peptidoglycan carbohydrates (Vaishnava et al., 2011) and kills the bacteria by the formation of a membrane permeabilizing pore (Mukherjee et al., 2014). Our data revealed a fast and necrotic-like cell death of neutrophils after Reg3β treatment. Hence, potential pore formation in neutrophil membrane vesicles obtained by nitrogen cavitation was investigated by negative stain EM (Figure 25). Although some structures resembled pores (dashed circles) they were equally found on Reg3β stimulated (red box) and untreated control vesicles (black box). The pore formation of HIP/PAP was shown on synthetic liposomes whose composition was similar to the bacterial cell surface (Mukherjee et al., 2014). However, when using the same liposomes as control, identical pore-like structures were observed in both, control and Reg3β stimulated conditions.

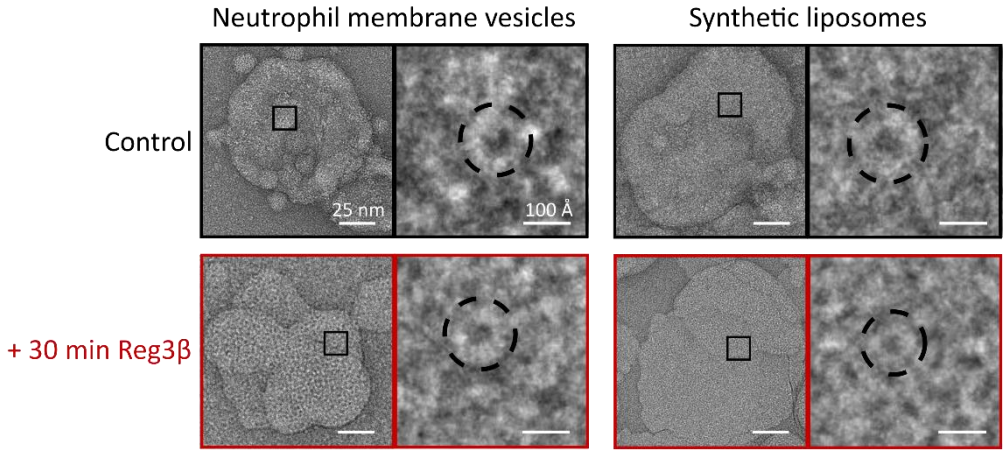

Figure 25: Negative stain EM did not reveal pore formation by Reg3β on neutrophil membranes
Neutrophil membrane vesicles were obtained by nitrogen cavitation of casein-elicited peritoneal neutrophils. The vesicles were purified by size exclusion chromatography prior to Reg3β stimulation (300 ng) for 30 minutes. Control vesicles remained untreated. Synthetic liposomes with the composition of 85 % zwitterionic phospholipid (PC) and 15 % acidic phospholipid (PS) were equally stimulated. For imaging, the vesicles or rather liposomes were placed on a carbon grid and stained with uranyl acetate. Individual pore-like structures are shown in the dashed circles of the right panel. Imaging was performed with Tecnai™ Spirit TEM from FEI™. Scale bars as indicated.

Neutrophil membrane vesicles as well as synthetic liposomes displayed no discernible pore formation upon Reg3β treatment, assuming the detected pore-like structures were normal irregularities of the membrane or rather liposome surface. Additionally, these results suggest a different killing mechanism of Reg3β for neutrophils than inducing cell lysis via pore formation in the plasma membrane.

6.2.5 Reg3β-mediated cytotoxicity is based on a ROS-dependent lysosomal destabilization

The generation of ROS by NOX2 (Chanock et al., 1994) represents a major defense mechanism of neutrophil immune response but is also associated with the induction of neutrophil cell death (Akahoshi et al., 1997; Blomgran et al., 2007; Geering & Simon, 2011; Mihalache et al., 2011; von Gunten et al., 2005). On this account, the kinetics of ROS generation after Reg3β stimulation was analyzed in peritoneal neutrophils. WT peritoneal neutrophils exhibited a significant increase of intracellular ROS levels after 45 minutes (~ 3 fold) and 60 minutes (~ 3.6 fold). In contrast, pre-treatment with the NOX2 inhibitor DPI (Buck et al., 2019) or cells deficient for NOX2 did not show an enhanced ROS generation upon Reg3β stimulation similar to the unstimulated control cells. (Figure 26A). The increase of intracellular ROS generation in peritoneal neutrophils from WT mice in response to Reg3β could be confirmed by measuring ROS levels using a different compound than DHR123, but based on the same principle, called CM-H_2DCFDA (Figure 26B).

The question whether NOX2-derived ROS is involved in the initiation of Reg3β-mediated cell death, was addressed by analyzing cell death based on LDH release in NOX2 deficient (*Nox2*$^{-/-}$) peritoneal neutrophils. Compared to the positive control IFNγ, the cells did not demonstrate a decreased viability in response to Reg3β over time assuming that Reg3β-mediated neutrophil cell death is dependent on NOX2-derived ROS generation (Figure 26C).

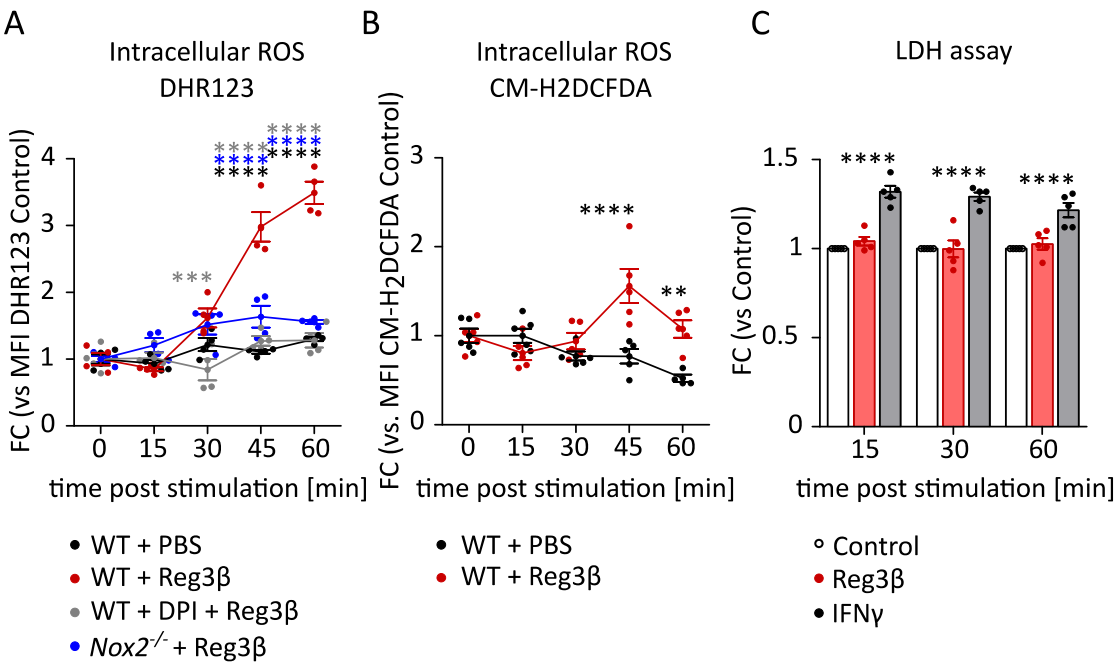

Figure 26: Reg3β-mediated cell death is dependent on enhanced intracellular ROS generation by NOX2

(A) Intracellular ROS generation was analyzed in peritoneal neutrophils of WT mice and *Nox2*$^{-/-}$ mice, as well as in WT neutrophils pre-treated with the NOX2 inhibitor DPI (1 µM) at indicated time points post Reg3β (100 ng/ml) stimulation. Cells were labeled with DHR123 (150 µM) for ROS detection using flow cytometry. Data are shown as fold change of Reg3β treated to control cells as mean ± SEM of four individual experiments. n = 4 for all groups. (B) Intracellular ROS generation was analyzed in peritoneal neutrophils of WT mice at indicated time points post Reg3β (100 ng/ml) stimulation. Control cells were treated with PBS. Cells were labeled with CM-H_2DCFDA (1 µM) for ROS detection using flow cytometry. Data are shown as fold change of Reg3β treated to control cells as mean ± SEM of four independent experiments. WT+PBS, WT+Reg3β n = 5. (C) Peritoneal neutrophils of *Nox2*$^{-/-}$ mice were stimulated with Reg3β (100 ng/ml) and IFNγ (100 ng/ml) as positive control. Cell death was determined based on LDH release after 15, 30 and 60 minutes post Reg3β treatment. Data display the fold change of treated to control cells and are shown as mean ± SEM of three individual experiments. Control, Reg3β, IFNγ n = 5. **p ≤ 0.01, ***p ≤ 0.001, ****p ≤ 0.0001 was determined using regular two-way ANOVA followed by Bonferroni post-test.

In vivo analysis regarding Reg3β-mediated cell death to neutrophils implied a necrotic-like cell death different from apoptosis. Nevertheless, the expression analysis of various cell death marker did not display any changes in response to Reg3β. Based on the morphological changes of Reg3β treated neutrophils, the cells appeared to be degraded from the inside. In that sense, it has been demonstrated that increased ROS generation is also linked to lysosomal membrane destabilization (Cai et al., 2018; Nilsson, Ghassemifar, & Brunk, 1997; Terman, Kurz, Gustafsson, & Brunk, 2006). Subsequent release of lysosomal enzymes as cathepsins into the cytosol (Repnik, Stoka, Turk, & Turk, 2012) results in lysosomal-dependent cell death (LDCD) due to the

degradation of intracellular components and cytosolic acidification (De Duve, 1965). In neutrophils, the lysosomal enzymes cathepsin B and D are located in azurophilic granules (Levy, Kolski, & Douglas, 1989; Tufet, 2008) also known as primary lysosomes (Bainton, 1999).

To investigate the integrity of primary lysosomes, neutrophils from WT and *Nox2*$^{-/-}$ mice were labeled with the lysosomal stain A/O and stimulated with Reg3β. Subsequently, pale cells that lost their lysosomal staining were quantified with flow cytometry. In WT mice that actively generate NOX2-derived ROS, the relative number of pale cells significantly increased up to ~30 % after 45 minutes and to ~50 % after 60 minutes. In contrast, in cells deficient for NOX2, the primary lysosomes mainly remained intact with continuous Reg3β stimulation with around 10 % of pale cells after 60 minutes. (Figure 27A). The sharp increase of pale cells in WT mice assumes an extensive loss of primary lysosomes in neutrophils upon Reg3β treatment, which in turn can lead to necrosis (Yu, Persson, Eaton, Brunk, & Medicine, 2003). Further evidence for lysosomal membrane permeabilization provided the translocation of cytosolic galectin to leaky lysosomes clearly visible in the dot like pattern of galectin-1 in stimulated neutrophils. In unstimulated control cells galectin remained ubiquitously distributed in the cytosol (Figure 27B). Moreover, Reg3β treatment resulted in the release of lysosomal cathepsin B and D into the cytosol whereas in the control cells the cathepsins remained co-localized with primary lysosomes (white arrows, Figure 27B).

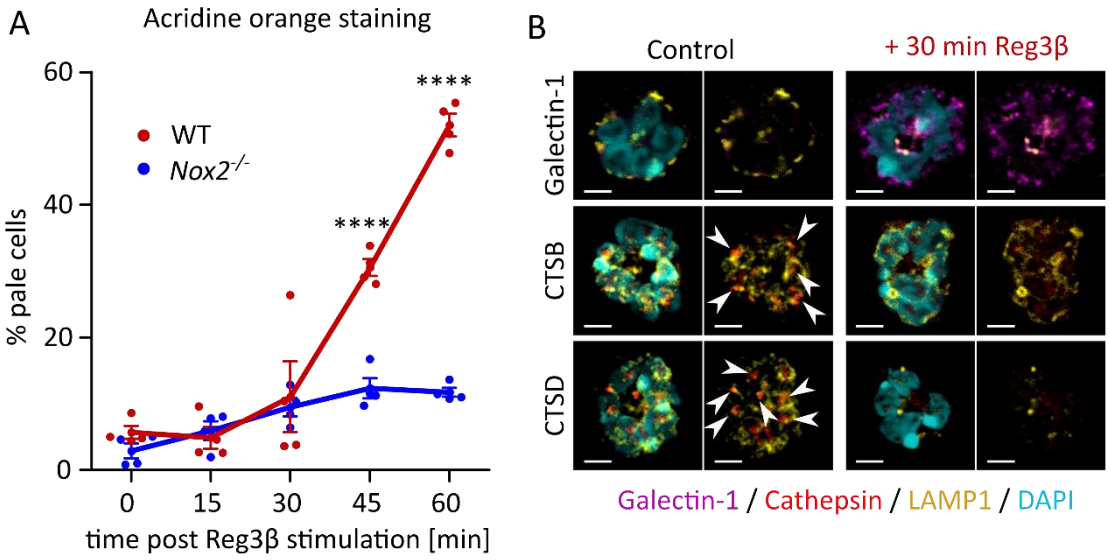

Figure 27: The lysosomal membrane is permeabilized upon Reg3β stimulation of peritoneal neutrophils

(A) Peritoneal neutrophils from WT and *Nox2*$^{-/-}$ mice were labeled with the lysosomotropic dye A/O (5 µg/ml) and increase of pale cells was quantified at indicated time points post Reg3β (100 ng/ml) stimulation with flow cytometry. Percentage of pale cells are shown as mean ± SEM of two individual experiments. WT, *Nox2*$^{-/-}$ n = 4. ****p ≤ 0.0001 was determined using two-way ANOVA followed by Bonferroni post-test. (B) Peritoneal neutrophils were stained for Galectin-1 (magenta), the lysosomal marker LAMP1 (yellow) and DAPI (cyan) for the Galectin puncta assay. Assessment of cathepsin release into the cytosol was conducted by immunohistochemical staining of cathepsin B (CTSB) and D (CTSD) (red), LAMP1 (yellow) and DAPI (cyan) in Reg3β (100 ng/ml) treated neutrophils. White arrows indicate co-localized cathepsins and lysosomes. Images are representative for three individual experiments. Scale bar = 3 µm.

Following the evaluation of Reg3β-mediated destabilization of primary lysosomes in vitro, the effect of Reg3β on primary lysosomes of cardiac tissue neutrophils over time post-MI was examined. Cardiac neutrophils of WT and *Reg3b*$^{-/-}$ mice were labeled with A/O as shown before and additionally with LTR. The relative number of pale cells at day 1 and 2 post-MI was equal in both mouse strains with ~40 % at day 1 and ~30 % at day 2. At day 4 and 7 the relative number of neutrophils with destabilized lysosomes significantly increased up to ~60 % at day 4 and ~50 % at day 7 in WT mice compared to ~20 % pale cells in Reg3β deficient mice. These observations were confirmed by the quantification of LTR positive neutrophils post-MI. Cardiac neutrophils of WT mice displayed a substantial decrease of lysosomal staining at day 4 (~85 % decrease) and at day 7 (~100 % decrease) compared to *Reg3b*$^{-/-}$ mice with around 60 % decrease at day 4 and 7 (Figure 28).

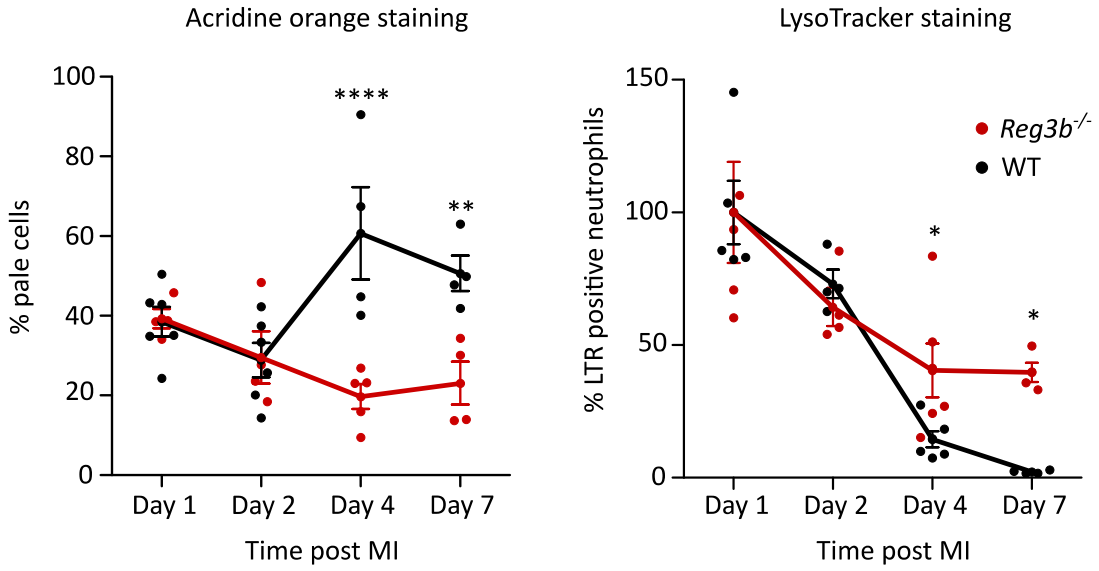

Figure 28: Lysosomal membrane permeabilization occurs in cardiac neutrophils of WT mice post-MI
Cardiac neutrophils isolated from WT and *Reg3b*$^{-/-}$ mice were labeled with the lysosomal dyes A/O (5 µg/ml) and LTR Green (50 nM) to monitor the degradation of lysosomes at day 1, 2, 4 and 7 post LAD ligation. Neutrophils were identified as CD45^{hi} CD11b^{hi} CD64^{lo} Ly6G^{hi}. The percentage of pale cells and LTR positive neutrophils are shown as mean ± SEM of four individual experiments each. WT, *Reg3b*$^{-/-}$ n = 4-5. *p ≤ 0.05, **p ≤ 0.01 and ****p ≤ 0.0001 were determined using regular two-way ANOVA followed by Bonferroni post-test.

Summarized, the in vitro data revealed a Reg3β-mediated necrotic cell death to inflammatory active neutrophils, which was characterized by the release of LDH, decrease of intracellular ATP (Figure 20), cytoplasmic vacuolization and degradation of cytoplasmic components (Figure 23), without activating any common cell death pathways (Figure 24). Yet, neutrophils exhibited enhanced NOX2-derived intracellular ROS levels (Figure 26) resulting in the destabilization of primary lysosomes and cytosolic release of lysosomal enzymes (Figure 27) which could also be confirmed in vivo in cardiac neutrophils post-MI (Figure 28).

6.2.6 Reg3β binds to glycoproteins on neutrophil membranes

Light sheet microscopy and flow cytometry based analysis indicated a direct binding of Reg3β to neutrophils (Figure 14 and Figure 15), yet leaving out the identity of the Reg3β binding site. Reg3β belongs to the C-type lectin family, which was shown to bind carbohydrate residues of glycoproteins on the cell surface of bacteria (Lehotzky et al., 2010). Therefore, treating peritoneal neutrophils with different deglycosidases to catalyze the removal of terminal carbohydrate residues from N- and O-linked glycans (Figure 8) provided information about potential binding partners for Reg3β. The importance of carbohydrate residues of

peptidoglycans for Reg3β binding was confirmed by the positive control Protein Deglycosylation Mix II from NEB. The enzyme mix removed all N-linked and many common O-linked glycoproteins and protected the cells from Reg3β-mediated cell death. The exoglycosidases galactosidase, N-acetylhexosaminidase, that removes terminal N-acetylglucosamine and N-acetylgalactosamine residues, as well as mannosidase were also able to rescue the cells from Reg3β cytotoxicity whereas pre-treatment with neuraminidase did not alter the cytotoxic effect of Reg3β (Figure 29).

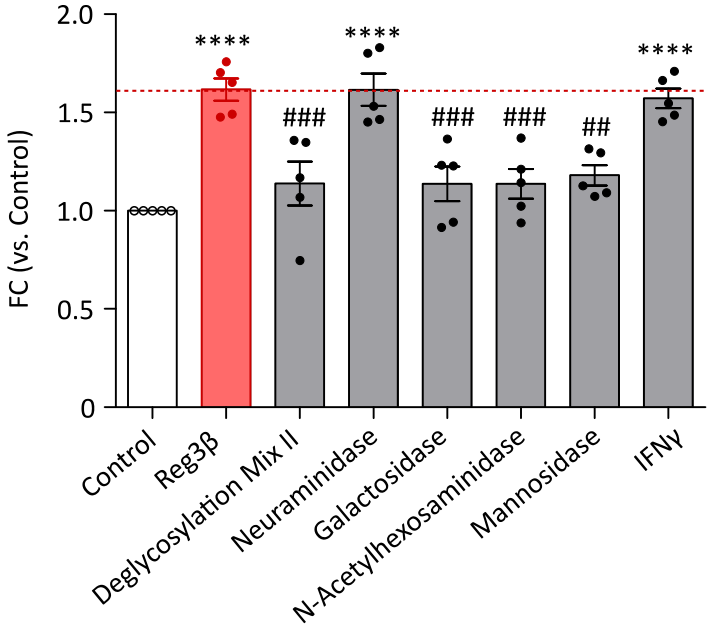

Figure 29: Reg3β-binding depends on carbohydrate residues of glycoproteins on the cell surface of neutrophils

Casein-elicited neutrophils from the peritoneum were pre-treated with different deglycosidases as indicated for 30 minutes prior to Reg3β (100 ng/ml) stimulation for 30 minutes at 37 °C. Cell death was estimated by LDH release of pre-treated cells compared to cells stimulated with Reg3β only (red bar) and untreated control cells (white bar). IFNγ (100 ng/ml) was used as positive control. Basal cytotoxic effects of enzymes were excluded by former dose-response studies. Data represent the fold change of treated cells vs control cells and are shown as mean ± SEM. N = 5 for all groups. ****p ≤ 0.0001 (vs. control), ##p ≤ 0.01, ###p ≤ 0.001 (vs. Reg3β) were determined by one way ANOVA followed by Bonferroni's post test.

To confirm galactose-, N-acetylglucosamine-, N-acetylgalactosamine- and mannan-containing glycoproteins as potential binding sites for Reg3β, a competition assay with soluble carbohydrates was performed (Figure 30). Several mono-, di- and polysaccharides were

pre-incubated with Reg3β, before added to cultured neutrophils. Subsequently, cell death was monitored by analyzing LDH release.

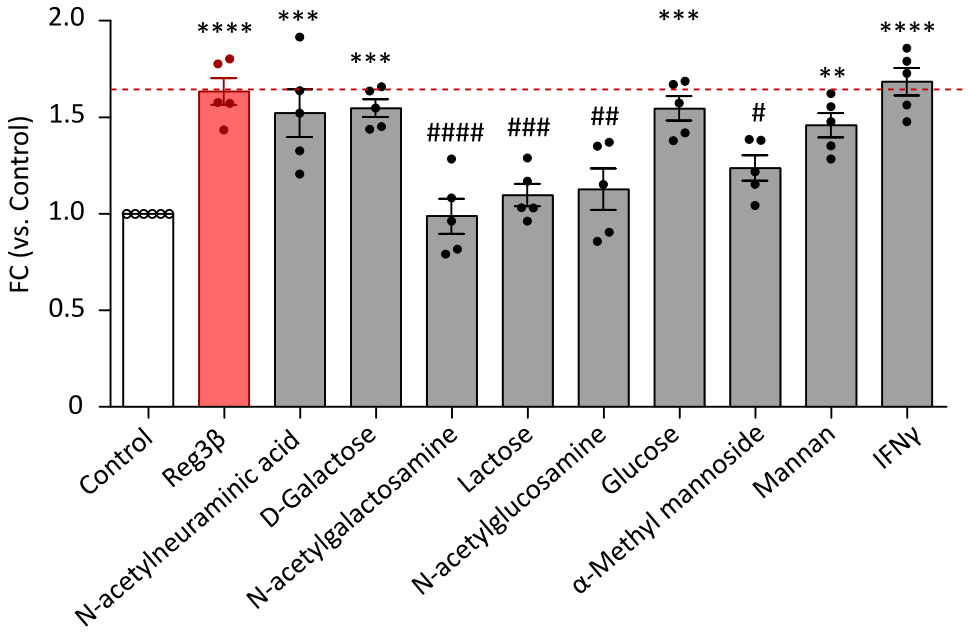

Figure 30: Reg3β-mediated neutrophil cell death is blocked in the presence of N-acetylgalactosamine, lactose, N-acetylglucosamine and mannose

Reg3β (100 ng/ml) was incubated with the indicated soluble carbohydrates for 30 minutes at 37 °C each. Casein-elicited peritoneal neutrophils were stimulated with the pre-incubated Reg3β for 30 minutes at 37 °C. Cell death was monitored by LDH release compared to unstimulated control cells (white bar) and cells treated with Reg3β only (red bar). IFNγ (100 ng/ml) was used as positive control. Basal cytotoxic effects of the soluble glycans were excluded by former dose-response studies. Data represent the fold change of treated cells vs control cells and are shown as mean ± SEM. N=5 for all groups. . **p ≤ 0.01, ***p ≤ 0.001, ****p ≤ 0.0001 (vs. control), #p ≤ 0.05, ##p ≤ 0.01, ###p ≤ 0.001 (vs. Reg3β) were determined by one way ANOVA followed by Bonferroni's post test.

N-acetylneuraminic acid did not prevent Reg3β-mediated cell death confirming the results of pre-treatment with neuraminidase. In contrast to soluble galactose, lactose and N-acetylgalactosamine blocked Reg3β cytotoxicity assuming the acetyl-group or the combination of glucose and galactose is additionally required for Reg3β binding. N-acetylglucosamine but not glucose rescued the cells from Reg3β-mediated cell death verifying the positive results of pre-treatment with N-acetylhexosaminidase. The last carbohydrate mannose promoted neutrophil survival as did the corresponding enzyme mannosidase whereas the polymeric form mannan could not decrease neutrophil death. Both assays suggest the

peptidoglycan residues N-acetylgalactosamine, N-acetylglucosamine and mannose as binding site for Reg3β.

6.2.7 The neutrophil cytotoxicity of Reg3β is based on clathrin-mediated endocytosis

Upon binding of Reg3β to specific peptidoglycan residues (Figure 30), primary lysosomes of neutrophils are rapidly destabilized in a ROS-dependent manner (Figure 26 - Figure 28). To evaluate whether Reg3β directly interacts with the primary lysosomes, endocytosis and subsequent transport to the lysosomes was investigated.

Initial flow cytometry based analysis revealed an enhanced binding of Reg3β to permeabilized neutrophils relative to unpermeabilized neutrophils supporting the concept of Reg3β being internalized (Figure 31). Additionally, both neutrophils subsets, Reg3β^{low} and Reg3β^{high} binding neutrophils, followed the same progress as shown after detection of surface bound Reg3β. The Reg3β^{high} binding neutrophils population was increasing over time with around 43 % positive neutrophils at day 1 and around 55 % positive neutrophils at day 7. The Reg3β^{low} binding population was decreasing from ~54 % at day 1 to ~ 42 % at day 7.

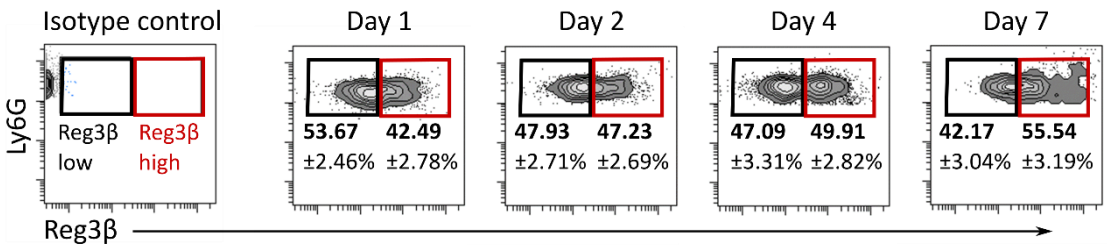

Figure 31: Reg3β is detected intracellular in cardiac neutrophils post-MI
Infarcted hearts of WT mice were digested at indicated time-points post-MI and analyzed with flow cytometry for intracellular Reg3β. Neutrophils were identified as CD45^{hi} CD11b^{hi} CD64^{lo} Ly6G^{hi} and fixed and permeabilized prior to Reg3β staining. Representative dot plots display the Reg3β low (black) and high (red) binding neutrophil populations over time post-MI. The gate determining the Ly6G^{hi} and Reg3β-binding population was set according to the corresponding isotype control of the Reg3β antibody. Percentage of cells are shown as mean ± SEM of four independent experiments.

Endocytosis describes the engulfment of extracellular fluids, particles or microorganisms by invagination of the plasma membrane and subsequent formation of endosomes (Huotari & Helenius, 2011). There are three major types of endocytosis (Marsh, 2002). Phagocytosis describes the recognition and ingestion of large particles such as bacteria or dead cells into plasma membrane-derived vesicles called phagosome and is mainly executed by immune cells

(Rosales & Uribe-Querol, 2017). Micropinocytosis is referred to the unspecific uptake of extracellular particles via actin-driven extension of plasma membrane ruffles and appears to be restricted to innate immune cells (Redka, Gütschow, Grinstein, & Canton, 2018). The third type of endocytosis is receptor-mediated endocytosis, which can be further subdivided into clathrin- and caveolae-mediated endocytosis. Ligands are recognized by their specific cell surface receptors and subsequently internalized into clathrin- and caveolae coated membrane vesicles, respectively (Doherty & McMahon, 2009). The formation of these coated vesicles requires several adaptor proteins involved in different steps (Kaksonen & Roux, 2018). As phagocytosis is only referred to the uptake of microorganism and dead cells, the engulfment of Reg3β by neutrophils was examined using specific inhibitors for micropinocytosis (imipramine), clathrin-mediated (chlorpromazine and MDAC) and caveolae-mediated endocytosis (MβCD and nystatin). Reg3β-mediated cell death was solely inhibited after chlorpromazine and MDAC treatment, but not after MβCD, nystatin or imipramine, indicating that Reg3β is endocytosed by neutrophils via the clathrin-mediated pathway (Figure 32).

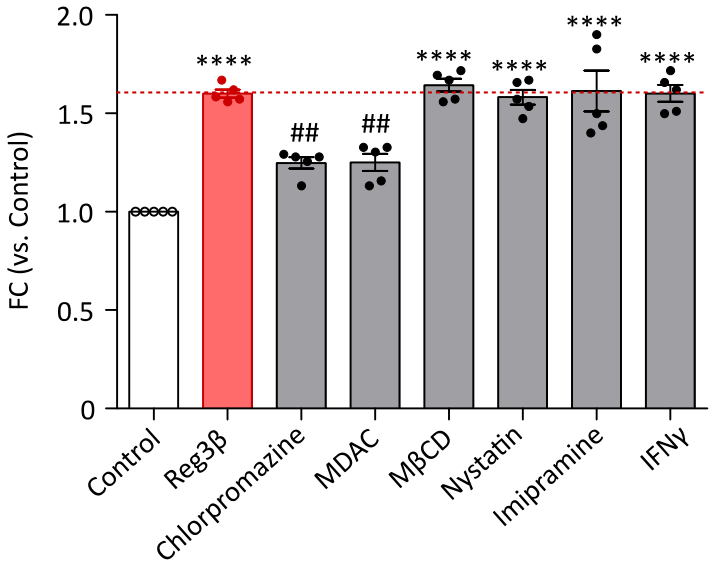

Figure 32: Inhibition of clathrin-mediated endocytosis abrogates the neutrophil cytotoxicity of Reg3β
Casein-elicited neutrophils from the peritoneum were pre-treated with inhibitors for clathrin- and caveolae-mediated endocytosis as well as for micropinocytosis for 30 minutes followed by Reg3β (100 ng/ml) treatment for additional 30 minutes. Cell death was determined using the LDH assay. IFNγ (100 ng/ml) was used as positive control. Basal cytotoxic effects of inhibitors were excluded by former dose-response studies. Data represent the fold change of treated cells (grey bars) vs control cells (white bar) and Reg3β only treated cells (red bar) and are shown as mean ± SEM. N = 5 for all groups. *p ≤ 0.05, **p ≤ 0.01 (vs. control), #p ≤ 0.05 (vs. Reg3β) were determined by one way ANOVA followed by Bonferroni's post test .

Following endocytosis, early endosomes mature into late endosomes (Huotari & Helenius, 2011), and finally fuse with lysosomes (Luzio, Pryor, & Bright, 2007) or in case of neutrophils, with azurophilic and specific granules (Segal, Dorling, & Coade, 1980). Staining for the lysosomal marker LAMP1 and Reg3β in peritoneal neutrophils demonstrated a co-localization of Reg3β and primary lysosomes (white arrows) after Reg3β treatment affirming the transport of internalized Reg3β into lysosomal compartments (Figure 33).

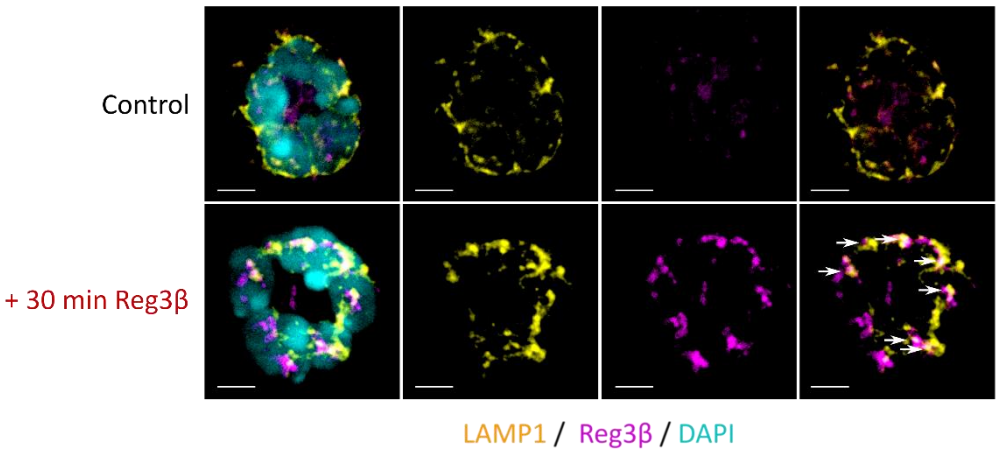

Figure 33: Reg3β co-localizes with primary lysosomes upon entering the cell
Casein-elicited neutrophils from the peritoneum were stained for LAMP1 (yellow), Reg3β (magenta) and DAPI (cyan). Cells were stimulated with Reg3β (100 ng/ml) for 30 minutes, control cells remained untreated. White arrows indicate co-localized lysosomes and Reg3β in treated cells. Images are representative for two individual experiments. Scale bar = 3 µm

Based on these findings, Reg3β binds specific carbohydrate residues of glycoproteins (N-acetylgalactosamine, N-acetylglucosamine and mannose) on the cell membrane of neutrophils and enters the cell via clathrin-mediated endocytosis. Once internalized, Reg3β is transported to primary lysosomes followed by a destabilization of the lysosomal membrane eventually leading to lysosomal dependent cell death.

6.2.8 Reg3β facilitates efferocytosis of dying neutrophils by macrophages

The clearance of dead neutrophils, a hallmark for the resolution of inflammation, is generally executed via efferocytosis by macrophages. The main function is to prevent secondary necrosis resulting in unwanted release of harmful intracellular contents and triggering an immune response (Haslett, 1997; Savill et al., 1989). To elucidate the fate of dying neutrophils after Reg3β treatment, peritoneal neutrophils labeled with a pH sensitive fluorophore were injected into the peritoneum of WT mice 4 days post thioglycollate treatment to accumulate inflammatory active

macrophages. Efferocytosis by macrophages in vivo was quantified based on the increased fluorescence intensity within the acidic environment of the phagosome. Without additional Reg3β stimulation, around 46 % of labeled neutrophils were engulfed by macrophages. The number of efferocytosed neutrophils, however, significantly increased up to 66 % when pre-treated with Reg3β (Figure 34A).

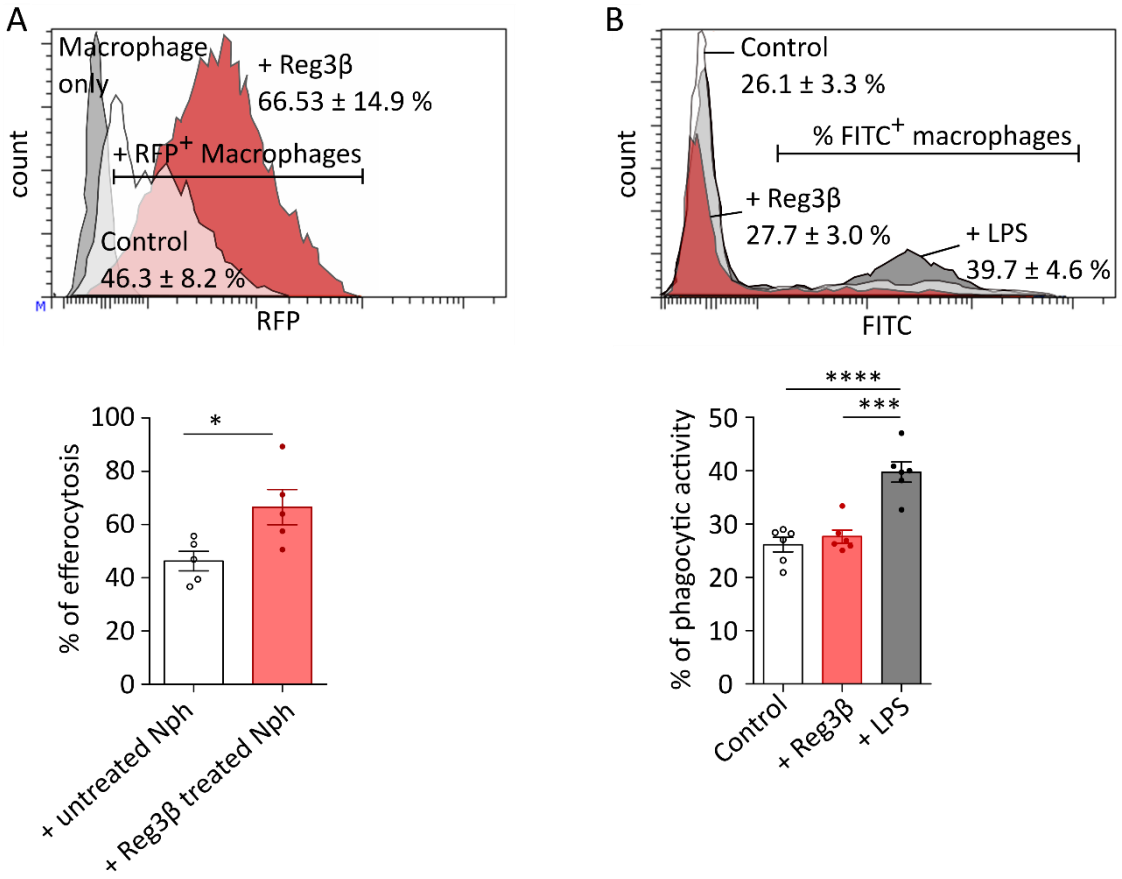

Figure 34: Efferocytosis of neutrophils by macrophages is enhanced after Reg3β pre-treatment
(A) Casein-elicited neutrophils from the peritoneum were labeled with the pH sensitive dye pHrodo Red™ (1 µg/ml) for 30 minutes followed by Reg3β (100 ng/ml) treatment for 30 minutes. Control cells remained untreated. Labeled neutrophils were injected into the peritoneum of WT mice 4 days post thioglycollate injection. After one hour, the peritoneal cells were harvested and stained for CD11b and F4/80 to identify macrophages. The number of engulfed neutrophils was determined by means of $CD11b^+$ $F4/80^+$ RFP^+ macrophages by flow cytometry. Representative histograms and corresponding quantification display the number of RFP^+ macrophages with and without Reg3β pre-treatment. Data are shown as mean ± SEM of three individual experiments. Untreated, treated n = 5. *p ≤ 0.05 was determined by two-tailed Welch's t-test. (B) Thioglycollate-elicited macrophages were cultivated and incubated with IgG-FITC for 2.5 hours. The phagocytic activity in response to Reg3β (100 ng/ml) and LPS (1 µg/ml) compared to untreated control cells was analyzed by flow cytometry. Tryphan blue was added to the cells to quench cell surface bound IgG-FITC before measuring. Representative histograms and corresponding quantifications display the percentage of $FITC^+$ macrophages as mean ± SEM of three individual experiments. Control, Reg3β, LPS n = 6. *p ≤ 0.05 was determined by one-way ANOVA followed by Bonferroni's post test.

Additionally, the effect of Reg3β on the phagocytic activity of macrophages was examined using IgG-FITC particles. In response to LPS around 40 % of macrophages ingested IgG particles whereas unstimulated control cells displayed a phagocytic activity of around 26 %. Stimulation with Reg3β did not increase the number of phagocytosed IgG-FITC particles compared to the control cells (Figure 34B) demonstrating that Reg3β has an impact on the efferocytosis of neutrophils but not on the phagocytic activity of macrophages itself.

The cardiomyocyte-derived C-type lectin Reg3β is released after the onset of MI and represents a new player in the resolution of inflammation by directly regulating the clearance of neutrophils from the site of injury. Reg3β binds to a specific subpopulation of inflammatory active neutrophils in the ischemic heart and enters the cell via clathrin-mediated endocytosis. Subsequently, destabilization of primary lysosomes accompanied with increased ROS production causes an aponecrotic, lysosomal cell death characterized by cathepsin release and cytoplasmic vacuolization. Furthermore, Reg3β enhances the efferocytosis of dying neutrophils by macrophages that are recruited by Reg3β. In conclusion, Reg3β prevents the accumulation of inflammatory active neutrophils in the healthy myocardium and thereby a destabilization of the left ventricular wall resulting in heart failure.

7 Discussion

The output of cardiac remodeling after injury is mainly affected by the immune-inflammatory response, which is dominated by the infiltration of neutrophils and monocytes or rather macrophages (Y. Ma et al., 2013; Prabhu & Frangogiannis, 2016; Swirski & Nahrendorf, 2018). In this context, Reg3β, a cardiomyocyte derived C-type like-lectin was initially identified as a novel regulator for macrophage trafficking within the ischemic myocardium. Its role on restricting neutrophil persistence at the site of injury, however, remained unknown (Loerchner et al., 2015). In this work, a novel feature of Reg3β was determined that is the temporal and spatial restriction of the accumulation of neutrophils at the site of injury. Upon infiltration into the heart, Reg3β bound to a subset of inflammatory active neutrophils. Consequently, a ROS-dependent lysosomal cell death was initiated and resulted in a rapid decline of neutrophil numbers at day 4 post-MI (Figure 35). Regarding the importance of a tightly regulated inflammatory response of neutrophils for cardiac healing, this study identified a novel mechanism for neutrophil clearance from the infarcted heart by Reg3β contributing to the resolution of inflammation. In conclusion, Reg3β represents a novel key player in the early immune response after the onset of myocardial infarction by simultaneously modulating the recruitment macrophages and the removal of neutrophils.

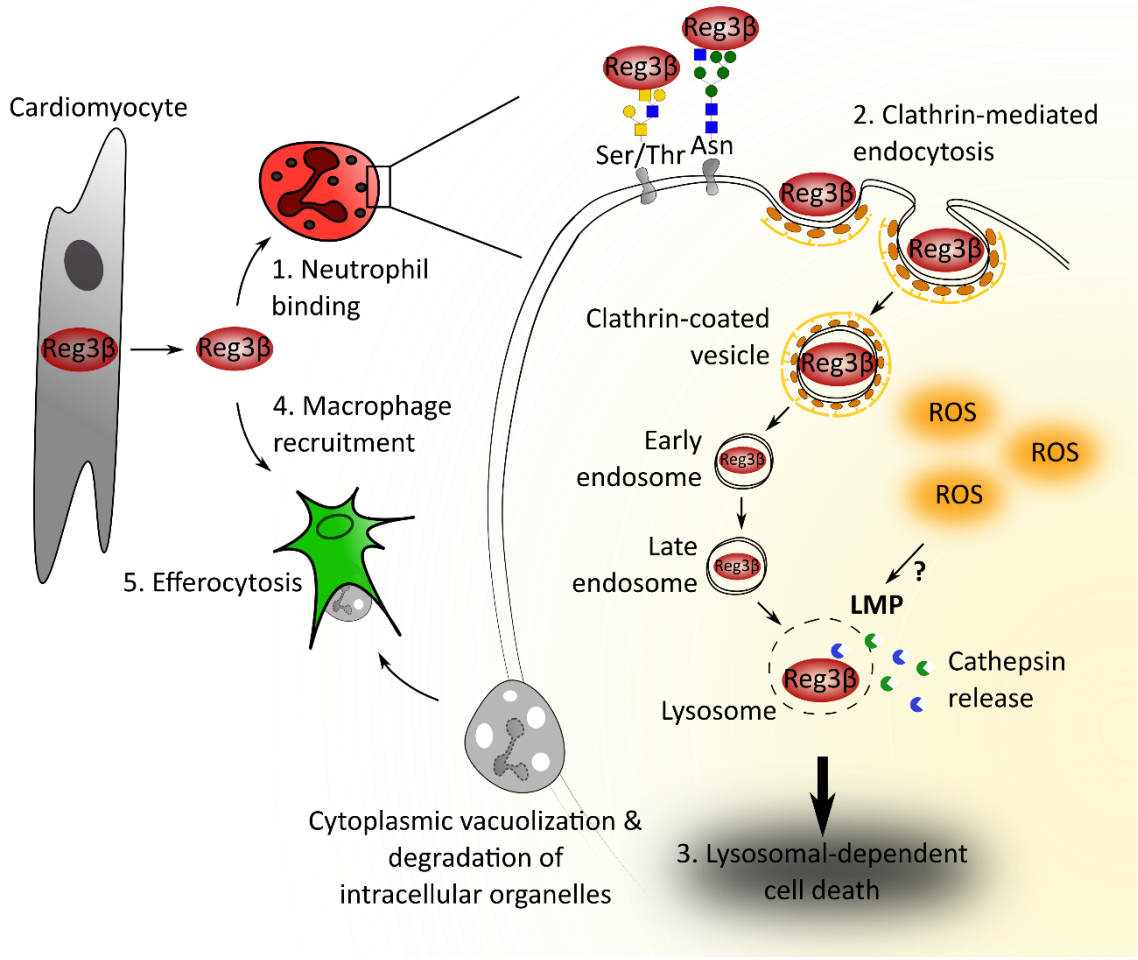

Figure 35: Model of Reg3β-mediated neutrophil removal via the induction of a ROS-dependent lysosomal cell death

Reg3β is secreted by stressed cardiomyocytes after the onset of MI and binds to infiltrating neutrophils via the recognition of specific carbohydrate residues on the cell surface. Upon binding, Reg3β is internalized via clathrin-mediated endocytosis and transported to the lysosomal like azurophilic granules. Simultaneously, intracellular ROS generation is increased and the lysosomal membrane is destabilized. LMP results in the release of cathepsins into the cytosol and finally to lysosomal-dependent cell death of neutrophils characterized by cytoplasmic vacuolization and degradation of intracellular organelles. In addition to neutrophil elimination, Reg3β recruits macrophages to the site of injury and facilitates the efferocytosis of dying neutrophils. Reg3β represents an important key factor for cardiac remodeling by directly restricting the accumulation and inflammatory activity of neutrophils via the induction of a ROS-dependent lysosomal cell death.

7.1 The critical role of Reg3β-mediated neutrophil clearance for cardiac healing

The accumulation of neutrophils into the injured heart peaked at day 2 post-MI and rapidly declined from day 4. Accordingly, the resolution of neutrophil infiltrates from the heart is essential for cardiac healing and functional recovery after the onset of MI. The underlying

mechanisms of neutrophil removal from the site of cardiac injury are not fully understood, yet. It is assumed that the majority of neutrophils undergo spontaneous apoptosis, though the initial trigger remain unclear (Fox, Leitch, Duffin, Haslett, & Rossi, 2010). More recent findings could prove a reverse migration of neutrophils from the site of inflammation back to the circulation by the upregulation of the surface marker CXCR4 (J. Wang et al., 2017). CXCR4 was also found to be upregulated on neutrophils migrating into lymph nodes that drain the inflammatory site (Gorlino et al., 2014). A delayed removal of neutrophils from the site of infarction, however, promotes an excessive inflammation and tissue injury. On this account, mice deficient for Reg3β suffered from an adverse cardiac remodeling due to a transient persistence of cardiac neutrophils at day 4 post-MI. The prolonged accumulation of neutrophils was not observed in the bone marrow, blood and spleen but restricted to the heart indicating the critical role of Reg3β for a timely clearance of neutrophils from the site of cardiac injury.

This study provided evidence for the co-localization and direct binding of Reg3β on a subset of infiltrating neutrophils. Reg3β binding was correlated with the induction of a necrotic-like cell death, different from apoptosis, termed aponecrosis. Therefore, the data suggest a novel removal mechanism, which involves the direct induction of a necrotic-like cell death by Reg3β binding thereby promoting resolution of inflammation. To investigate the effect of neutrophil persistence on cardiac remodeling, the spatial distribution of immune cells in the infarcted heart was assessed using light sheet microscopy according to a recently published protocol of Merz et al. (Merz et al., 2019). The group revealed an accumulation of neutrophils in the heart after ischemia reperfusion (I/R) injury rather in the border zone of the infarction area than in the damaged heart tissue itself (Merz et al., 2019). Although a permanent LAD Ligation (instead of transient occlusion) was used in this study, the results of Merz et al. could be confirmed in WT mice. Upon the loss of Reg3β, neutrophil infiltrates in the *Reg3b*$^{-/-}$ strain displayed an increased accumulation in the healthy myocardium around day 4 post-MI. In contrast to macrophages, Reg3β did not exhibit any chemotactic effects on neutrophils, which might be the reason why the persisting neutrophils in *Reg3b*$^{-/-}$ mice were able to migrate in the non-infarcted RZ. Moreover, the cells exhibited a sustained inflammatory activity suggesting a suppressive role of Reg3β on neutrophil motility and activity. The prolonged secretion of degrading enzymes in the non-infarcted RZ by neutrophils may presumably be associated with the increased mortality due to cardiac rupture in *Reg3b*$^{-/-}$ mice. Hence, by directly modulating the accumulation, inflammatory activity and removal of neutrophils after the onset of MI, Reg3β represent a novel key player for cardiac healing mechanism.

7.2 Reg3β binds to a specific subset of inflammatory active neutrophils

The fact that Reg3β only bound to a small population of cardiac neutrophils followed by the induction of cell death raised the question of a defined neutrophil subset with distinct functions in the infarcted heart. Under inflammatory conditions, granulopoiesis in the bone marrow is increased and high numbers of fresh neutrophils are released into the circulation and recruited to the site of inflammation where they get primed and activated by inflammatory mediators (Evrard et al., 2018; Kolaczkowska & Kubes, 2013). Beside the bone marrow and blood, the spleen also serves as reservoir for neutrophils (Deniset et al., 2017). Consistent with this, Reg3β binding was not observed on unprimed and inactive neutrophils from the bone marrow, blood and spleen, suggesting the specific Reg3β binding neutrophil subset is defined by an inflammatory active status. Furthermore, the persistence of neutrophils in *Reg3b*$^{-/-}$ mice results in an impaired cardiac healing (Loerchner et al., 2015), implying the Reg3β-binding subset possesses pro-inflammatory features. Interestingly, the lectin galectin 1 triggers intracellular ROS production upon binding to specific glycoproteins of primed neutrophils i.e. after transmigration into the inflamed tissue (Almkvist, Dahlgren, Leffler, & Karlsson, 2002; Carlsson et al., 2007; Karlsson, Follin, Leffler, & Dahlgren, 1998) but not to inactive blood neutrophils (Almkvist et al., 2002). Neutrophil priming is concomitant with degranulation, defined by the mobilization of secretory vesicles to the surface. The vesicles do not contain antimicrobial proteins but rather a reservoir of membrane receptors. Thus, the fusion of the secretory vesicles with the plasma membrane results in the appearance of new receptors on the cell surface allowing the cells to interact with chemokines, cytokines and adhesion molecules at the site of inflammation (Borregaard, Sørensen, & Theilgaard-Mönch, 2007; Sengeløv et al., 1993). This might give an explanation why Reg3β cannot bind to unprimed neutrophils from the bone marrow, blood and spleen, followed by the induction of cell death comparable to galectin 1. After the onset of myocardial infarction, neutrophils are recruited to the site of inflammation from the circulation. If Reg3β was able to bind and eliminate blood neutrophils, the initial immune response in the heart would no longer emerge. As shown in the study by Horckmans et al. on antibody depletion of neutrophils in the early phase of the immune response this leads to an increased fibrosis and enhanced mortality (Horckmans et al., 2017).

Recent studies determined a phenotypic heterogeneity and functional diversity of neutrophils under both homeostatic and inflammatory conditions (Christoffersson & Phillipson, 2018). The bone marrow harbors a CD101^{neg} immature neutrophil population as well as CD101^{pos} mature neutrophils (Evrard et al., 2018). Of them, the CD101^{pos} population is released into the circulation under homeostatic conditions. However, an increasing number of CD101^{neg}

immature neutrophils was detected in the blood of tumor bearing mice contributing to tumor progression (Evrard et al., 2018). The identification of disease progressing neutrophils in different pathological settings might serve as a basis for new therapeutic strategies. CXCR4 on the other hand represents a surface marker that is associated with an anti-inflammatory and reparative phenotype of neutrophils. To maintain homeostasis under basal conditions, aged neutrophils in the circulation are guided back to the bone marrow by the upregulation of CD11b and CXCR4 and downregulation of CD62L (Adrover et al., 2016; Casanova-Acebes et al., 2013). Regarding resolution of inflammation, CXCR4 was expressed on neutrophils that migrated out of the inflamed tissue either back to the circulation (J. Wang et al., 2017) or to the draining lymph nodes (Gorlino et al., 2014). Another distinct neutrophil subset actively promoting angiogenesis in the inflamed tissue has been identified as $CD49d^{+}CXCR4^{+}VEGFR1^{+}$ (Massena et al., 2015). Therefore, the phenotypical and functional characterization of neutrophil subsets, as the Reg3β-binding subset, is critical for the design of a cell-specific therapy. A targeted modulation of pro- and anti-inflammatory neutrophils may optimize cardiac healing and prevent heart failure.

7.3 Neutrophils die via necrotic-like cell death

Flow cytometry and electron microscopy revealed an aponecrotic cell death in neutrophils upon Reg3β binding. 7AAD, a cell impermeant dye, was able to enter Reg3β binding cells, indicating an irreversible damage to the plasma membrane. Moreover, the number of apoptotic neutrophils in the ischemic heart did not differ between WT and *Reg3b*$^{-/-}$ mice, indicating Reg3β does not activate the apoptotic machinery. Although members of the Reg3 group, to which Reg3β belongs to, were shown to be bactericidal in relation to Gram-negative and –positive bacteria (Miki et al., 2012) a cytotoxic effect of Reg proteins on eukaryotic cells has not been described, so far. Yet, in addition to the in vivo data, in vitro cytotoxicity assays revealed a direct and fast induction of neutrophil cell death upon Reg3β treatment. However, the highest concentration of 1000 ng/mL used in this setting did not affect the cell viability. This ineffectiveness of Reg3β at higher concentrations might be explained by other findings, in which the bactericidal activity of Reg3γ was inhibited when added in high concentration to the bacterial cells due to filament formation (Mukherjee et al., 2014). The formation of fibrils or filaments was also shown in the pancreas, allowing Reg proteins to resist digestion by pancreatic proteases (Ho et al., 2010).

The antibacterial mechanism of the human Reg3 protein HIP/PAP on Gram-negative bacteria was demonstrated by Mukherjee et al. by using synthetic liposomes and negative stain EM. They

provided evidence of a pore formation in the bacterial membrane leading to cell lysis (Mukherjee et al., 2014). Here, the same method was used to investigate a potential pore formation upon Reg3β treatment on synthetic liposomes according to the protocol of Mukherjee et al. (Mukherjee et al., 2014) but also on neutrophils membrane vesicles obtained from nitrogen cavitation. Since neither the synthetic liposomes nor the membrane vesicles displayed any pore-like structures, the underlying mechanism of Reg3β-mediated induction of neutrophil cell death appears to be different from the Reg3 protein mediated killing of bacteria via cell lysis. The type of cell death can have different immunological consequences. Cells undergoing apoptosis are engulfed by phagocytes without triggering any inflammatory reactions (Ortega-Gómez et al., 2013). Efferocytosis of apoptotic cells can even suppress the immune response and contribute to the resolution of inflammation (D. R. Green, Ferguson, Zitvogel, & Kroemer, 2009). Apoptosis is a programmed cell death with signaling cascades, several effector proteins and morphological characteristics as cell rounding, nuclear condensation and the formation of apoptotic bodies (Kerr, Wyllie, & Currie, 1972).

Necrosis on the other hand has long been considered as a non-regulated, accidental cell death, defined by cell swelling and the uncontrolled release of intracellular content resulting in the activation of the immune system (Douglas R. Green & Llambi, 2015). Nowadays, there is knowledge about the existence of several pathways of regulated necrosis. Of them, NETosis (Brinkmann et al., 2004), necroptosis (X. Wang, Yousefi, & Simon, 2018), pyroptosis (X. Chen et al., 2016), autophagy dependent and LDCD (Conus et al., 2008; Loison et al., 2014) are known to occur in neutrophils.

Although, the known cell death pathways overlap and share a substantial degree of interconnectivity (Lorenzo Galluzzi et al., 2018), the individual pathways can be defined or rather modulated by specific morphological characteristics and effector molecules. TEM and SEM analysis of primary neutrophils treated with Reg3β displayed morphological resemblance to autophagy owing to cytoplasmic vacuolization (Denton, Kumar, & Differentiation, 2019) and NETosis based on the degradation of intracellular organelles (Brinkmann et al., 2004), but no apoptotic features as chromatin condensation or the formation of apoptotic bodies (Kerr et al., 1972). Of note, none of the effector proteins of apoptosis, necroptosis, NETosis, autophagy and pyroptosis were shown to be upregulated in response to Reg3β suggesting a different type of regulated necrosis with similar features to autophagy and NETosis. To confirm this hypothesis, further investigations such as functional assays for individual effector proteins of each cell death pathway are required. These could include enzyme activity assays (i.e. caspases or protein kinases for apoptosis (McStay & Green, 2014) and necroptosis (Maki & Degterev, 2013)), monitoring the release of intracellular cytokines (i.e. IL-1β for pyroptosis (den Hartigh & Fink,

2018)) and inflammatory mediators (i.e. citrullinated histones for NETosis (Tsourouktsoglou et al., 2020)) or histological analysis of the formation of intracellular organelles (i.e. autophagosomes for autophagy (Yoshii & Mizushima, 2017)). The relevance and impact of regulated necrosis in physiological and pathophysiological conditions is not fully understood as necrotic cells can cause tissue injury and disease progression but may also promote tissue repair and wound healing (L. Galluzzi, Buqué, Kepp, Zitvogel, & Kroemer, 2017). With regard to Reg3β-mediated clearance of cardiac neutrophils, the induction of a necrotic-like cell death seems to be advantageous for cardiac repair since the delayed clearance of neutrophils from the site of inflammation in *Reg3b*$^{-/-}$ mice deteriorates wound healing processes.

7.4 Reg3β induces a ROS-dependent lysosomal neutrophil cell death

In response to inflammatory stimuli such as DAMPs, PAMPs, CXCL8, LPS or GM-CSF, activated neutrophils produce ROS via the NADPH oxidase complex NOX2 (Nguyen et al., 2017). Depending on the subcellular localization of NOX2, ROS can be released extracellular and intracellular (Nguyen et al., 2017). The assembly and activation of NOX2 at the cell membrane results in extracellular ROS production, which represents a highly effective anti-microbial tool for the defense of invading pathogens (Klebanoff, 1970; Rosen & Klebanoff, 1979). Upon phagocytosis of bacteria or fungi, the NOX2 complex is located at the phagosomal membrane enabling the ROS generation into the phagosomal lumen to degrade the engulfed target (Rothe et al., 1988). However, intracellular ROS production is not only activated upon phagocytosis of pathogens, but also associated with intracellular signaling (Lambeth & Neish, 2014). ROS is known to augment the inflammatory activity of neutrophils by stimulating the release of neutrophil granules and pro-inflammatory cytokines and is involved in neutrophil migration towards a chemokine gradient (Veal et al., 2007). This study demonstrated a sharp increase of intracellular ROS levels in activated neutrophils from the peritoneum upon Reg3β stimulation in vitro. Moreover, Reg3β lacked cytotoxic effects on peritoneal *Nox2*$^{-/-}$ neutrophils, which are deficient for ROS production suggesting Reg3β-mediated cell death is dependent on intracellular ROS generation. In this regard, the regulation of cell death of activated neutrophils at the site of inflammation was demonstrated to be linked with intracellular ROS generation (M. B. Hampton, Vissers, Keenan, & Winterbourn, 2002). ROS was shown to be involved or even a potent mediator of several cell death pathways in neutrophils (Xu, Loison, & Luo, 2010), including apoptosis (Kasahara et al., 1997), necroptosis (X. Wang et al., 2018), NETosis (Remijsen et al., 2011) and LDCD (Mannick et al., 2001). Since the expression analysis of effector proteins were not indicative for the activation of apoptosis, necroptosis and NETosis, further analysis focused

on the investigation of ROS-dependent LDCD in activated neutrophils upon Reg3β stimulation. Furthermore, sulfasalazine, a sulfonamide used for the treatment of rheumatic and chronic inflammatory intestinal diseases, is known to induce cell death specifically to neutrophils and not to other leukocytes by an enhanced ROS production (Akahoshi et al., 1997).

LDCD shares morphological features with necrosis, apoptosis, autophagy-dependent cell death and ferroptosis and is known to amplify or initiate these cell death pathways (Aits & Jäättelä, 2013; Kroemer & Jaattela, 2005). This underlines the complexity of this not fully understood cell death mechanism. Nevertheless, the Nomenclature Committee of Cell Death (NCCD) declared the LDCD as an independent form of regulated cell death primarily characterized by LMP, cathepsin release into the cytosol and subsequent degradation of intracellular organelles (De Duve, 1965; Lorenzo Galluzzi et al., 2018). LDCD upon LMP can occur in different cell types. ROS-mediated LDCD was shown in intervertebral disc cells upon bupivacaine treatment characterized by swelling of organelles and severe disruption of plasma membrane (Cai et al., 2018). Similarly, macrophages died through a caspase independent, LMP- mediated cell death in response to mycobacterium tuberculosis (Lee, Remold, Ieong, & Kornfeld, 2006). In neutrophils, cathepsin D release from azurophilic granules, the lysosome-like organelles (Bainton, 1999; Dell'Angelica et al., 2000), was found to directly process caspase 8 resulting in cell death. Importantly, granule permeabilization occurred prior to the caspase activation, indicating LMP as primary inducer of neutrophil cell death (Conus et al., 2008). Upon bacterial ingestion, neutrophils underwent apoptosis, driven by lysosomal disruption and cathepsin D release into the cytosol (Prince et al., 2008). Most of these defined features of LDCD have been proven to occur in neutrophils after Reg3β treatment. The increasing number of neutrophils that lost their lysosomal staining as well as the translocation of galectin-1 to leaky lysosomes indicates a destabilization of primary lysosomes in neutrophils upon Reg3β stimulation. Furthermore, the cytosolic release of cathepsin B and D as well as the collapse of intracellular structures post Reg3β stimulation reflect the morphological changes during LDCD. A direct association between the degradation of intracellular organelles and the release of cathepsins into the cytosol still remains to be examined by enzyme activity assays with cytosolic fractions in future investigations. However, subcellular fractionation of primary neutrophils has only been performed in human cells but not in mice (Udby & Borregaard, 2007). Further studies with human neutrophils might also allow the examination of the enzymatic activity of cytosolic cathepsins after Reg3β treatment.

The degree of lysosomal enzyme release into the cytosol determines the type of cell death. Moderate enzyme release leads to apoptosis (Yu et al., 2003), whereas a strong or complete disruption of lysosomes immediately induces necrosis (Berghe et al., 2010; Li et al., 2000). The sharp increase of pale neutrophils, which lost their lysosomal staining upon exposure to Reg3b,

indicates a strong disruption of lysosomes confirming the previous findings for a necrotic-like cell death. In contrast to WT neutrophils, the primary lysosomes of *Nox2*$^{-/-}$ neutrophils were not degraded upon Reg3β stimulation indicating the destabilization of the lysosomal membrane is driven by intracellular ROS production. ROS is a well-known inducer for LMP by enhanced lipid peroxidation (Terman et al., 2006). Apart from that, lysosomes contain free iron but lack enzymes for H_2O_2 degradation. In the presence of ROS, free iron catalyzes H_2O_2 into hydroxyl radical ($OH^{\cdot -}$), also known as fenton reaction, which destabilizes the lysosomal membranes (Eaton & Qian, 2002). Hence, the in vitro data strongly imply a ROS-dependent LMP followed by the release of hydrolytic enzymes resulting in necrotic cell death after Reg3β treatment. The in vivo data confirmed the degradation of primary lysosomes resulting in regulated necrosis of cardiac neutrophils of WT mice at day 4 post-MI, whereas the lysosomes in neutrophils from Reg3β-deficient mice remained largely intact.

Nevertheless, the underlying mechanism of how Reg3β directly modulates ROS production and lysosomal degradation remains to be investigated. This study demonstrated an enhanced production of intracellular ROS by Reg3β stimulation, but did not provide information about the type of oxidants produced and the localization of NOX2 assembly. The activation site of NOX2 can be assessed by immunohistochemistry (Winterbourn, Kettle, & Hampton, 2016) and might help to understand how and where in the cell ROS is generated. Biochemical studies may identify both the specific oxidants produced in Reg3β-stimulated neutrophils as well as their cellular targets. Finally, a neutrophil-specific NOX2 knockout mouse subjected to permanent LAD Ligation might provide new insights into the role of ROS in Reg3β-mediated neutrophil clearance from the injured heart. The direct impact of Reg3β on lysosomal degradation may be examined by analyzing the membrane integrity of isolated primary lysosomes. The isolation and purification of neutrophil granules has only been conducted in human cells so far, suggesting future analysis should be performed with human neutrophils.

7.5 Specific glycoproteins represent a potential binding site of Reg3β on the neutrophil cell surface

Immunohistochemical and flow cytometric analysis revealed a direct binding of Reg3β on the cell surface of a specific cardiac neutrophil population. Interestingly, Reg3β was not able to bind to neutrophils from the bone marrow, blood and spleen suggesting a distinct profile on the cell membrane of inflammatory active neutrophils. Since Reg3β exerts different effects on macrophages and neutrophils (recruitment vs. induction of cell death), there is also the

assumption of cell-type specific binding sites associated with distinct downstream signaling. Consequently, one key aspect of this project was to identify the recognition mechanism of Reg3b for this particular neutrophil population.

So far, there is no known receptor or binding site for Reg proteins, including Reg3β, except the exostosin-like glycosyltransferase 3 (EXTL3) (Kobayashi et al., 2000), which is still controversially discussed. The glycosyltransferase is responsible for the biosynthesis of heparan sulfate and located at the golgi membrane (Busse et al., 2007). However, Kobayashi et al. identified the EXTL3 receptor for Reg on the cell membrane (Kobayashi et al., 2000). The direct interaction of Reg proteins and EXTL3 has also not sufficiently demonstrated, yet. The analysis of binding partners for Reg1 using a yeast two-hybrid method, could not detect clones homologous to EXTL3 (Mueller, Zhang, & Zenilman, 2008). As part of the C-type lectin family, Reg proteins were shown to bind specific peptidoglycans on bacterial membranes through their CTLD (Lehotzky et al., 2010). The bactericidal activity of murine Reg3γ and human HIP/PAP depends on the binding to polymers of alternating N-acetylglucosamine and N-acetylmuramic acid (N-acetylglucosamine with a phosphoenolpyruvate) and the mannose polymer mannan but not mannose itself (Bonjoch et al., 2017; Cash et al., 2006). Important for peptidoglycan binding and bacterial killing is the EPN motif, which is also present in Reg3β (Lehotzky et al., 2010). The removal of common N- and O-linked glycoproteins from the cell surface of neutrophils using a protein deglycosylation mix blocked the Reg3β-mediated cell death suggesting Reg3β binding is dependent on peptidoglycans on the cell membrane. Subsequent analysis with individual deglycosidases and carbohydrate competitive binding assays revealed a high affinity interaction between Reg3β and neutrophils via terminal N-acetylglucosamine, N-acetylgalactosamine and mannose. The murine Reg3β shares about 70% homologous similarity with Reg3γ or rather human HIP/PAP (Z. Chen et al., 2019), what may explain the differences in their binding affinities to mannose and its polymer mannan. Additionally, the bactericidal effect of human HIP/PAP is different from the neutrophil clearing mechanism mediated by murine Reg3β in that bacteria are directly lysed upon Reg protein binding (Mukherjee et al., 2014) and neutrophils are eliminated via the regulated necrotic cell death LDCD.

Recent findings examined the glycoprotein profiles of granules, secretory vesicles and plasma membrane proteins of human neutrophils using liquid chromatography and tandem mass spectrometry (Venkatakrishnan et al., 2020). The glycopeptide profiling revealed distinct signatures insofar azurophilic granules were characterized by paucimannosidic N-glycans (up to 4 mannose units attached to the N-glycan core) but lacked the presence of O-glycans, whereas specific and gelatinase granules displayed complex N- and O-glycans. In contrast, oligomannose (5 and more mannose units attached to the N-glycan core) and complex type N-glycans with N-

acetyllactosamine repeats, a disaccharide consisting of galactose and N-acetylglucosamine, were predominant on secretory vesicles and the plasma membrane of human neutrophils. Thus, the mobilization of secretory vesicles during degranulation in activated neutrophils is able to alter the carbohydrate profile of the cell surface, which might explain the specific binding of Reg3β to inflammatory active neutrophils. The presence of high mannose oligosaccharides on the human neutrophil membrane was confirmed by analyzing the surface marker CD11b/CD18 using matrix-assisted laser desorption/ionization (MALDI) mass spectrometry (Kelm et al., 2020). Moreover, by selectively targeting these glycans with lectins, transmigration and inflammatory functions such as phagocytosis and ROS production were altered or even inhibited in neutrophils (Kelm et al., 2020) similar to the findings of Reg3β having an impact on neutrophil motility and inflammatory activity.

Glycosylation is critical for the regulation of the immune response by mediating cell-cell and cell-ligand interactions. The neutrophil glycan biology is not fully understood yet. However, technological advances in glycoanalytics provide new insights into the structural and functional diversity of glycoproteins as well as their spatiotemporal expression during the maturation in the bone marrow, movement in the blood circulation and inflammatory activity at the site of injury. Therefore, a MS-based glycome profiling of Reg3β positive and negative binding neutrophils will promote the characterization of the Reg3β binding neutrophil subset. To further determine its specific function for cardiac remodeling, additional comprehensive analysis of structural differences in the cell membrane of Reg3β binding neutrophils such as microvilli, cilia, endocytic pits and tight junctions using scanning ion conductance microscopy (SCIM) should be performed (B.-C. Liu et al., 2013). Here, it is important to include macrophages in the structural analysis of the cell membrane to elaborate the cell specific binding of Reg3β to neutrophils and macrophages.

7.6 Clathrin-mediated endocytosis of Reg3β induces enhanced ROS production and neutrophil cell death

Reg3β binding to the cell surface of neutrophils was demonstrated by flow cytometry using a specific antibody directed against Reg3β. By permeabilizing the cells prior to the antibody staining for Reg3b, the number of cells positive for Reg3β substantially increased, suggesting Reg3β enters the cell after binding to the cell membrane. Inhibition studies for endocytosis revealed an internalization of Reg3β via clathrin-mediated endocytosis upon binding to specific glycoproteins on the cell surface of neutrophils. Subsequent to endocytosis, Reg3β was found to be co-localized with primary lysosomes inside the cell indicating Reg3β is transported through

the endolysosomal pathway. However, the correlation between endocytosis of Reg3β, increased ROS production and LMP-mediated LDCD requires further investigations to elucidate the direct mechanism of Reg3β binding to neutrophils. Phagocytosis of microorganism by neutrophils is ultimately linked to increased ROS production into the endolysosomal lumen and has an impact on neutrophil viability by the induction of apoptosis (Watson, Redmond, Wang, Condron, & Bouchier-Hayes, 1996) or autophagy (Mitroulis et al., 2010). Following endocytosis, early endosomes mature into to late endosomes (Huotari & Helenius, 2011) associated with endosomal acidification (Maxfield & Yamashiro, 1987). Late endosomes fuse with lysosomes (Luzio et al., 2007) or in case of neutrophils with azurophilic and specific granules (Peyron, Maridonneau-Parini, & Stegmann, 2001; Segal et al., 1980), thereby forming the endolysosomal compartment (Luzio et al., 2007). Azurophilic granules carry hydrolytic enzymes and proteases to digest the engulfed cargo (Burgoyne & Morgan, 1993). Specific granules carrying the membrane components of NOX2 (Borregaard et al., 1983) enable the assembly and activation of NOX2 on the endolysosomal membrane resulting in ROS production into the lysosomal lumen (Bylund, Campsall, Ma, Conway, & Speert, 2005; Lamb et al., 2012). Inhibition of NOX2 derived ROS generation was shown to block phagocytosis-induced cell death (PICD) in neutrophils (Watson et al., 1996). In line with that, neutrophils from CGD patients exhibited a reduced PICD following phagocytosis compared to healthy controls (Coxon et al., 1996). Beside the activation of intracellular ROS production during phagocytosis of pathogens, the internalization via clathrin-mediated endocytosis of priming agents such as fMLP and TNFα led to enhanced ROS generation and degranulation in neutrophils (Creed, Tandon, Ward, & McLeish, 2017; McLaughlin et al., 2006). Hence, the binding of immunomodulatory agents on specific carbohydrate residues of primed neutrophils and subsequent internalization via clathrin-mediated endocytosis is associated with enhanced ROS production and cell death supporting the yet undescribed mechanism of Reg3β-mediated neutrophil removal via ROS-dependent lysosomal cell death in the infarcted heart. However, it remains to be investigated whether endocytosis of Reg3β causes intracellular ROS production and if so, whether lysosomal cell death is directly triggered by the increased ROS levels during endocytosis of Reg3β or by the direct interaction between Reg3β and primary lysosomes. The association between increased ROS generation and endocytosis of Reg3β can be further analyzed by monitoring intracellular ROS levels after the inhibition of endocytosis in neutrophils stimulated with Reg3β. Whether LMP is caused by directly binding of Reg3β to the lysosomes or the incorporation into their membranes is yet to be determined i.e. using electron microscopy for ultrastructural analysis.

7.7 Consequences of Reg3β-mediated removal of neutrophils for cardiac healing

The inflammatory response after the onset of MI is dominated by the infiltration of neutrophils within hours (Y. Ma et al., 2013). Here, the number of neutrophils rapidly decreased around day 4 post-MI in WT mice. In this context, the data revealed a direct impact of Reg3β on neutrophil viability associated with the induction of an aponecrotic cell death, which contributed to the suppression of neutrophil activity. It has been shown that dead cells, both apoptotic and necrotic, are capable of amplifying the acute inflammatory response due to the release of DAMPs and intracellular content, if not removed properly (Faouzi et al., 2001; Majno, La Gattuta, & Thompson, 1960). Neutrophils are filled with degrading and toxic components, as DAMPS and proteolytic enzymes, that harm the surrounding tissue and augment inflammation if released uncontrolled. Clearance of apoptotic neutrophils prevents secondary necrosis or cell lysis and subsequent release of noxious factors (Nathan, 2002) and is considered as pro-resolving, by stimulating the production of anti-inflammatory mediators (Ortega-Gómez et al., 2013). Impaired or delayed efferocytosis of dead neutrophils is associated with many inflammatory and autoimmune diseases (Vandivier, Henson, & Douglas, 2006). The accumulation of necrotic or lysed cells stimulates macrophages to produce pro-inflammatory mediators as TNFα, whereas apoptotic cells do not (Fadok, Bratton, Guthrie, & Henson, 2001). On the other hand, some pathogens accelerate neutrophil apoptosis resulting in a sudden cell lysis and triggering immune responses (Greenlee-Wacker et al., 2014). Therefore, it is not only fundamental to understand the mechanism of leukocytic cell death but also its impact on engulfing immune cells.

Following Reg3β-mediated induction of neutrophil cell death, the immune cells seemed to be removed by efferocytosis from the inflamed tissue. Reg3β indirectly modulated the proper removal of Reg3β-treated neutrophils by enhancing the efferocytosis by macrophages without affecting the actual phagocytic activity of macrophages. However, efferocytosis of Reg3β pre-treated neutrophils by macrophages was examined in the peritoneum, as the removal of dead neutrophils by macrophages in the infarcted heart has several limitations. First of all, neutrophils infiltrating the infarcted heart need to be labeled to enable their detection in macrophages afterwards. When using neutrophil reporter mice, the endogenous fluorescence might disappear due to the degradation of the cells upon efferocytosis. Second, ex-vivo labeling of the cells poses the challenge of injecting the cells into the infarcted myocardium post-MI. Most importantly, the optimal time point of neutrophil injection post-MI must be set, to avoid adverse side effects on the given immune response in the heart. Therefore, the exact mechanism of how macrophages recognize the Reg3β binding neutrophil subset remains elusive.

Conclusively, this study demonstrated a complex immunomodulatory function of Reg3β and its relevance for reparative processes after the onset of MI. Moreover, Reg3β was detected in patients with acute coronary syndromes, providing the opportunity for new therapeutic strategies in cardiovascular diseases (Lörchner, Widera, et al., 2018). So far, immunomodulatory clinical studies, targeting neutrophils, have not been successful in humans (Baran et al., 2001). The main challenge is the development of a neutrophil specific therapy in order to avoid unwanted side effects due to their close relationship to other myeloid cells. Additionally, novel treatments should aim to attenuate neutrophil-mediated tissue injury while maintaining the beneficial effects in the early immune response after the onset of MI. By simultaneously regulating macrophage recruitment and neutrophil removal, Reg3β provides evidence for a cell type-specific immunomodulatory function. Further, Reg3β initiates resolution of inflammation by mediating the clearance of a pro-inflammatory neutrophil population at day 4 post-MI without affecting the initial neutrophil immune response. This novel mechanism of a spatiotemporal regulation of cardiac neutrophil accumulation and clearance post-MI prevents excessive inflammation and heart failure while maintaining a balanced and well-coordinated immune response for an optimized cardiac healing and functional recovery after the onset of MI (Panahi et al., 2018).

8 Literature

Abbott, J. D., Huang, Y., Liu, D., Hickey, R., Krause, D. S., & Giordano, F. J. (2004). Stromal Cell-Derived Factor-1alpha; Plays a Critical Role in Stem Cell Recruitment to the Heart After Myocardial Infarction but Is Not Sufficient to Induce Homing in the Absence of Injury. *110*(21), 3300-3305. doi:doi:10.1161/01.CIR.0000147780.30124.CF

Abhirath, P., Anne-Fleur, S., & Emmanuel, S. T. (2012). Regenerating proteins and their expression, regulation, and signaling. *Biomolecular Concepts, 3*(1), 57-70. doi:10.1515/bmc.2011.055

Adrover, J. M., Nicolás-Ávila, J. A., & Hidalgo, A. (2016). Aging: A Temporal Dimension for Neutrophils. *Trends Immunol, 37*(5), 334-345. doi:10.1016/j.it.2016.03.005

Aits, S., & Jäättelä, M. (2013). Lysosomal cell death at a glance. *J Cell Sci, 126*(Pt 9), 1905-1912. doi:10.1242/jcs.091181

Aits, S., Kricker, J., Liu, B., Ellegaard, A. M., Hamalisto, S., Tvingsholm, S., . . . Jaattela, M. (2015). Sensitive detection of lysosomal membrane permeabilization by lysosomal galectin puncta assay. *Autophagy, 11*(8), 1408-1424. doi:10.1080/15548627.2015.1063871

Akahoshi, T., Namai, R., Sekiyama, N., Tanaka, S., Hosaka, S., & Kondo, H. (1997). Rapid induction of neutrophil apoptosis by sulfasalazine: implications of reactive oxygen species in the apoptotic process. *J Leukoc Biol, 62*(6), 817-826. doi:10.1002/jlb.62.6.817

Alard, J. E., Ortega-Gomez, A., Wichapong, K., Bongiovanni, D., Horckmans, M., Megens, R. T., . . . Soehnlein, O. (2015). Recruitment of classical monocytes can be inhibited by disturbing heteromers of neutrophil HNP1 and platelet CCL5. *Sci Transl Med, 7*(317), 317ra196. doi:10.1126/scitranslmed.aad5330

Almkvist, J., Dahlgren, C., Leffler, H., & Karlsson, A. J. T. J. o. I. (2002). Activation of the neutrophil nicotinamide adenine dinucleotide phosphate oxidase by galectin-1. *168*(8), 4034-4041.

Alon, R., Hammer, D. A., & Springer, T. A. (1995). Lifetime of the P-selectin-carbohydrate bond and its response to tensile force in hydrodynamic flow. *Nature, 374*(6522), 539-542. doi:10.1038/374539a0

Anzai, A., Anzai, T., Nagai, S., Maekawa, Y., Naito, K., Kaneko, H., . . . Mochizuki, S. J. C. (2012). Regulatory role of dendritic cells in postinfarction healing and left ventricular remodeling. *125*(10), 1234-1245.

Astorri, E., Guglielmi, C., Bombardieri, M., Alessandri, C., Buzzetti, R., Maggi, D., . . . research, m. (2010). Circulating Reg1α proteins and autoantibodies to Reg1α proteins as biomarkers of β-cell regeneration and damage in type 1 diabetes. *42*(13), 955-960.

Bainton, D. F. (1999). Distinct granule populations in human neutrophils and lysosomal organelles identified by immuno-electron microscopy. *J Immunol Methods, 232*(1-2), 153-168. doi:10.1016/s0022-1759(99)00173-8

Baran, K. W., Nguyen, M., McKendall, G. R., Lambrew, C. T., Dykstra, G., Palmeri, S. T., . . . Barron, H. V. (2001). Double-blind, randomized trial of an anti-CD18 antibody in conjunction with recombinant tissue plasminogen activator for acute myocardial infarction: limitation of myocardial infarction following thrombolysis in acute myocardial infarction (LIMIT AMI) study. *Circulation, 104*(23), 2778-2783. doi:10.1161/hc4801.100236

Bartneck, M., & Wang, J. (2019). Therapeutic Targeting of Neutrophil Granulocytes in Inflammatory Liver Disease. *10*(2257). doi:10.3389/fimmu.2019.02257

Beaumel, S., Picciocchi, A., Debeurme, F., Vivès, C., Hesse, A.-M., Ferro, M., . . . Stasia, M. J. (2017). Down-regulation of NOX2 activity in phagocytes mediated by ATM-kinase dependent phosphorylation. *Free Radical Biology and Medicine, 113*, 1-15. doi:10.1016/j.freeradbiomed.2017.09.007

Becher, B., Schlitzer, A., Chen, J., Mair, F., Sumatoh, H. R., Teng, K. W., . . . Newell, E. W. (2014). High-dimensional analysis of the murine myeloid cell system. *Nature immunology, 15*(12), 1181-1189. doi:10.1038/ni.3006

Bejjani, A. T., Saab, S. A., Muhieddine, D. H., Habeichi, N. J., Booz, G. W., & Zouein, F. A. (2020). Spatiotemporal Dynamics of Immune Cells in Early Left Ventricular Remodeling After Acute Myocardial Infarction in Mice. *75*(2), 112-122. doi:10.1097/fjc.0000000000000777

Berghe, T. V., Vanlangenakker, N., Parthoens, E., Deckers, W., Devos, M., Festjens, N., . . . Vandenabeele, P. (2010). Necroptosis, necrosis and secondary necrosis converge on similar cellular disintegration features. *Cell Death & Differentiation, 17*(6), 922-930. doi:10.1038/cdd.2009.184

Bergmann, O., Bhardwaj, R. D., Bernard, S., Zdunek, S., Barnabé-Heider, F., Walsh, S., . . . Frisén, J. (2009). Evidence for cardiomyocyte renewal in humans. *Science, 324*(5923), 98-102. doi:10.1126/science.1164680

Bishop, J. E., Greenbaum, R., Gibson, D. G., Yacoub, M., & Laurent, G. J. (1990). Enhanced deposition of predominantly type I collagen in myocardial disease. *J Mol Cell Cardiol, 22*(10), 1157-1165. doi:10.1016/0022-2828(90)90079-h

Blomgran, R., Zheng, L., & Stendahl, O. (2007). Cathepsin-cleaved Bid promotes apoptosis in human neutrophils via oxidative stress-induced lysosomal membrane permeabilization. *J Leukoc Biol, 81*(5), 1213-1223. doi:10.1189/jlb.0506359

Bonjoch, L., Gironella, M., Iovanna, J. L., & Closa, D. J. S. R. (2017). REG3β modifies cell tumor function by impairing extracellular vesicle uptake. *7*(1), 1-11.

Borregaard, N., & Cowland, J. B. (1997). Granules of the human neutrophilic polymorphonuclear leukocyte. *Blood, 89*(10), 3503-3521.

Borregaard, N., Heiple, J. M., Simons, E. R., & Clark, R. A. (1983). Subcellular localization of the b-cytochrome component of the human neutrophil microbicidal oxidase: translocation during activation. *Journal of Cell Biology, 97*(1), 52-61. doi:10.1083/jcb.97.1.52 %J Journal of Cell Biology

Borregaard, N., Kjeldsen, L., Lollike, K., & Sengeløv, H. (1993). Granules and vesicles of human neutrophils. The role of endomembranes as source of plasma membrane proteins. *51*(5), 318-322. doi:10.1111/j.1600-0609.1993.tb01615.x

Borregaard, N., Miller, L. J., & Springer, T. A. (1987). Chemoattractant-regulated mobilization of a novel intracellular compartment in human neutrophils. *Science, 237*(4819), 1204. doi:10.1126/science.3629236

Borregaard, N., Sehested, M., Nielsen, B., Sengelov, H., & Kjeldsen, L. (1995). Biosynthesis of granule proteins in normal human bone marrow cells. Gelatinase is a marker of terminal neutrophil differentiation. *Blood, 85*(3), 812-817. doi:10.1182/blood.V85.3.812.bloodjournal853812 %J Blood

Borregaard, N., Sørensen, O. E., & Theilgaard-Mönch, K. (2007). Neutrophil granules: a library of innate immunity proteins. *Trends Immunol, 28*(8), 340-345. doi:10.1016/j.it.2007.06.002

Boya, P., Andreau, K., Poncet, D., Zamzami, N., Perfettini, J. L., Metivier, D., . . . Kroemer, G. (2003). Lysosomal membrane permeabilization induces cell death in a mitochondrion-dependent fashion. *The Journal of experimental medicine, 197*(10), 1323-1334. doi:10.1084/jem.20021952

Brinkmann, V., Reichard, U., Goosmann, C., Fauler, B., Uhlemann, Y., Weiss, D. S., . . . Zychlinsky, A. (2004). Neutrophil extracellular traps kill bacteria. *Science, 303*(5663), 1532-1535. doi:10.1126/science.1092385

Brown, G. D., Willment, J. A., & Whitehead, L. J. N. R. I. (2018). C-type lectins in immunity and homeostasis. *18*, 374-389.

Buck, A., Sanchez Klose, F. P., Venkatakrishnan, V., Khamzeh, A., Dahlgren, C., Christenson, K., & Bylund, J. (2019). DPI Selectively Inhibits Intracellular NADPH Oxidase Activity in Human Neutrophils. *Immunohorizons, 3*(10), 488-497. doi:10.4049/immunohorizons.1900062

Buckley, C. D., Ross, E. A., McGettrick, H. M., Osborne, C. E., Haworth, O., Schmutz, C., . . . Vohra, R. K. J. J. o. l. b. (2006). Identification of a phenotypically and functionally distinct

population of long-lived neutrophils in a model of reverse endothelial migration. *79*(2), 303-311.

Burchfield, J. S., Xie, M., & Hill, J. A. (2013). Pathological ventricular remodeling: mechanisms: part 1 of 2. *Circulation, 128*(4), 388-400. doi:10.1161/CIRCULATIONAHA.113.001878

Burgoyne, R. D., & Morgan, A. (1993). Regulated exocytosis. *The Biochemical journal, 293 (Pt 2)*(Pt 2), 305-316. doi:10.1042/bj2930305

Buscher, K., Riese, S. B., Shakibaei, M., Reich, C., Dernedde, J., Tauber, R., & Ley, K. (2010). The transmembrane domains of L-selectin and CD44 regulate receptor cell surface positioning and leukocyte adhesion under flow. *J Biol Chem, 285*(18), 13490-13497. doi:10.1074/jbc.m110.102640

Busse, M., Feta, A., Presto, J., Wilén, M., Grønning, M., Kjellén, L., & Kusche-Gullberg, M. (2007). Contribution of EXT1, EXT2, and EXTL3 to heparan sulfate chain elongation. *J Biol Chem, 282*(45), 32802-32810. doi:10.1074/jbc.M703560200

Butcher, E. C. (1991). Leukocyte-endothelial cell recognition: three (or more) steps to specificity and diversity. *Cell, 67*(6), 1033-1036. doi:10.1016/0092-8674(91)90279-8

Bylund, J., Campsall, P. A., Ma, R. C., Conway, B.-A. D., & Speert, D. P. J. T. J. o. I. (2005). Burkholderia cenocepacia induces neutrophil necrosis in chronic granulomatous disease. *174*(6), 3562-3569.

Cai, X., Liu, Y., Hu, Y., Liu, X., Jiang, H., Yang, S., . . . Xiong, L. (2018). ROS-mediated lysosomal membrane permeabilization is involved in bupivacaine-induced death of rabbit intervertebral disc cells. *Redox Biol, 18*, 65-76. doi:10.1016/j.redox.2018.06.010

Cannistra, S. A., & Griffin, J. D. (1988). Regulation of the production and function of granulocytes and monocytes. *Semin Hematol, 25*(3), 173-188.

Carlsson, S., Oberg, C. T., Carlsson, M. C., Sundin, A., Nilsson, U. J., Smith, D., . . . Leffler, H. (2007). Affinity of galectin-8 and its carbohydrate recognition domains for ligands in solution and at the cell surface. *Glycobiology, 17*(6), 663-676. doi:10.1093/glycob/cwm026

Casanova-Acebes, M., Pitaval, C., Weiss, L. A., Nombela-Arrieta, C., Chèvre, R., N, A. G., . . . Hidalgo, A. (2013). Rhythmic modulation of the hematopoietic niche through neutrophil clearance. *Cell, 153*(5), 1025-1035. doi:10.1016/j.cell.2013.04.040

Cash, H. L., Whitham, C. V., Hooper, L. V. J. P. e., & purification. (2006). Refolding, purification, and characterization of human and murine RegIII proteins expressed in Escherichia coli. *48*(1), 151-159.

Cavard, C., Terris, B., Grimber, G., Christa, L., Audard, V., Radenen-Bussiere, B., . . . Perret, C. J. O. (2006). Overexpression of regenerating islet-derived 1 alpha and 3 alpha genes in human primary liver tumors with β-catenin mutations. *25*(4), 599-608.

Chamberlain, A. M., St Sauver, J. L., Gerber, Y., Manemann, S. M., Boyd, C. M., Dunlay, S. M., . . . Roger, V. L. (2015). Multimorbidity in heart failure: a community perspective. *Am J Med, 128*(1), 38-45. doi:10.1016/j.amjmed.2014.08.024

Chanock, S. J., el Benna, J., Smith, R. M., & Babior, B. M. (1994). The respiratory burst oxidase. *J Biol Chem, 269*(40), 24519-24522.

Chen, B., & Frangogiannis, N. G. (2020). Chemokines in Myocardial Infarction. *J Cardiovasc Transl Res*. doi:10.1007/s12265-020-10006-7

Chen, J. W., Murphy, T. L., Willingham, M. C., Pastan, I., & August, J. T. (1985). Identification of two lysosomal membrane glycoproteins. *J Cell Biol, 101*(1), 85-95. doi:10.1083/jcb.101.1.85

Chen, X., He, W. T., Hu, L., Li, J., Fang, Y., Wang, X., . . . Han, J. (2016). Pyroptosis is driven by non-selective gasdermin-D pore and its morphology is different from MLKL channel-mediated necroptosis. *Cell Res, 26*(9), 1007-1020. doi:10.1038/cr.2016.100

Chen, Z., Downing, S., & Tzanakakis, E. S. (2019). Four Decades After the Discovery of Regenerating Islet-Derived (Reg) Proteins: Current Understanding and Challenges. *7*(235). doi:10.3389/fcell.2019.00235

Christia, P., & Frangogiannis, N. G. (2013). Targeting inflammatory pathways in myocardial infarction. *Eur J Clin Invest, 43*(9), 986-995. doi:10.1111/eci.12118

Christoffersson, G., & Phillipson, M. (2018). The neutrophil: one cell on many missions or many cells with different agendas? *Cell and Tissue Research, 371*(3), 415-423. doi:10.1007/s00441-017-2780-z

Cochain, C., Channon, K. M., & Silvestre, J.-S. (2013). Angiogenesis in the infarcted myocardium. *Antioxidants & redox signaling, 18*(9), 1100-1113. doi:10.1089/ars.2012.4849

Cohn, J. N., Ferrari, R., & Sharpe, N. (2000). Cardiac remodeling--concepts and clinical implications: a consensus paper from an international forum on cardiac remodeling. Behalf of an International Forum on Cardiac Remodeling. *J Am Coll Cardiol, 35*(3), 569-582. doi:10.1016/s0735-1097(99)00630-0

Colotta, F., Re, F., Polentarutti, N., Sozzani, S., & Mantovani, A. (1992). Modulation of granulocyte survival and programmed cell death by cytokines and bacterial products. *Blood, 80*(8), 2012-2020.

Conus, S., Perozzo, R., Reinheckel, T., Peters, C., Scapozza, L., Yousefi, S., & Simon, H. U. (2008). Caspase-8 is activated by cathepsin D initiating neutrophil apoptosis during the resolution of inflammation. *The Journal of experimental medicine, 205*(3), 685-698. doi:10.1084/jem.20072152

Coxon, A., Rieu, P., Barkalow, F. J., Askari, S., Sharpe, A. H., von Andrian, U. H., . . . Mayadas, T. N. (1996). A novel role for the beta 2 integrin CD11b/CD18 in neutrophil apoptosis: a homeostatic mechanism in inflammation. *Immunity, 5*(6), 653-666. doi:10.1016/s1074-7613(00)80278-2

Creed, T. M., Tandon, S., Ward, R. A., & McLeish, K. R. (2017). Endocytosis is required for exocytosis and priming of respiratory burst activity in human neutrophils. *Inflamm Res, 66*(10), 891-899. doi:10.1007/s00011-017-1070-2

Creemers, E. E., Cleutjens, J. P., Smits, J. F., & Daemen, M. J. J. C. r. (2001). Matrix metalloproteinase inhibition after myocardial infarction: a new approach to prevent heart failure? *, 89*(3), 201-210.

Dąbrowska, D., Jabłońska, E., Iwaniuk, A., & Garley, M. (2019). Many Ways-One Destination: Different Types of Neutrophils Death. *Int Rev Immunol, 38*(1), 18-32. doi:10.1080/08830185.2018.1540616

Dalen, J. E., Gore, J. M., Braunwald, E., Borer, J., Goldberg, R. J., Passamani, E. R., . . . Knatterud, G. (1988). Six- and twelve-month follow-up of the phase I Thrombolysis in Myocardial Infarction (TIMI) trial. *Am J Cardiol, 62*(4), 179-185. doi:10.1016/0002-9149(88)90208-1

Dancey, J. T., Deubelbeiss, K. A., Harker, L. A., & Finch, C. A. (1976). Neutrophil kinetics in man. *J Clin Invest, 58*(3), 705-715. doi:10.1172/jci108517

Daseke, M. J., Valerio, F. M., Kalusche, W. J., Ma, Y., DeLeon-Pennell, K. Y., & Lindsey, M. L. (2019). Neutrophil proteome shifts over the myocardial infarction time continuum. *Basic Research in Cardiology, 114*(5), 37. doi:10.1007/s00395-019-0746-x

de Buhr, N., & Köckritz-Blickwede, M. (2016). How Neutrophil Extracellular Traps Become Visible. *Journal of Immunology Research, 2016*, 1-13. doi:10.1155/2016/4604713

De Caro, A., Lohse, J., Sarles, H. J. B., & communications, b. r. (1979). Characterization of a protein isolated from pancreatic calculi of men suffering from chronic calcifying pancreatitis. *87*(4), 1176-1182.

De Duve, C. J. H. l. (1965). The separation and characterization of subcellular particles. *59*, 49.

deCathelineau, A. M., & Henson, P. M. (2003). The final step in programmed cell death: phagocytes carry apoptotic cells to the grave. *Essays Biochem, 39*, 105-117. doi:10.1042/bse0390105

Decker, T., & Lohmann-Matthes, M. L. (1988). A quick and simple method for the quantitation of lactate dehydrogenase release in measurements of cellular cytotoxicity and tumor necrosis factor (TNF) activity. *J Immunol Methods, 115*(1), 61-69. doi:10.1016/0022-1759(88)90310-9

Dehn, S., & Thorp, E. B. (2018). Myeloid receptor CD36 is required for early phagocytosis of myocardial infarcts and induction of Nr4a1-dependent mechanisms of cardiac repair. *Faseb j, 32*(1), 254-264. doi:10.1096/fj.201700450R

Dell'Angelica, E. C., Mullins, C., Caplan, S., & Bonifacino, J. S. (2000). Lysosome-related organelles. *Faseb j, 14*(10), 1265-1278. doi:10.1096/fj.14.10.1265

den Hartigh, A. B., & Fink, S. L. (2018). Pyroptosis Induction and Detection. *Current protocols in immunology*, e52-e52. doi:10.1002/cpim.52

Deniset, J. F., Surewaard, B. G., Lee, W.-Y., & Kubes, P. (2017). Splenic Ly6G(high) mature and Ly6G(int) immature neutrophils contribute to eradication of S. pneumoniae. *The Journal of experimental medicine, 214*(5), 1333-1350. doi:10.1084/jem.20161621

Denton, D., Kumar, S. J. C. D., & Differentiation. (2019). Autophagy-dependent cell death. *26*(4), 605-616.

Desmoulière, A., Geinoz, A., Gabbiani, F., & Gabbiani, G. (1993). Transforming growth factor-beta 1 induces alpha-smooth muscle actin expression in granulation tissue myofibroblasts and in quiescent and growing cultured fibroblasts. *Journal of Cell Biology, 122*(1), 103-111. doi:10.1083/jcb.122.1.103 %J Journal of Cell Biology

Deten, A., Hölzl, A., Leicht, M., Barth, W., Zimmer, H.-G. J. J. o. m., & cardiology, c. (2001). Changes in extracellular matrix and in transforming growth factor beta isoforms after coronary artery ligation in rats. *33*(6), 1191-1207.

Devi, S., Laning, J., Luo, Y., & Dorf, M. E. (1995). Biologic activities of the beta-chemokine TCA3 on neutrophils and macrophages. *154*(10), 5376-5383.

Dewald, O., Ren, G., Duerr, G. D., Zoerlein, M., Klemm, C., Gersch, C., . . . Frangogiannis, N. G. (2004). Of Mice and Dogs: Species-Specific Differences in the Inflammatory Response Following Myocardial Infarction. *Am J Pathol, 164*(2), 665-677. doi:10.1016/S0002-9440(10)63154-9

Dewas, C., Dang, P. M., Gougerot-Pocidalo, M. A., & El-Benna, J. (2003). TNF-alpha induces phosphorylation of p47(phox) in human neutrophils: partial phosphorylation of p47phox is a common event of priming of human neutrophils by TNF-alpha and granulocyte-macrophage colony-stimulating factor. *J Immunol, 171*(8), 4392-4398. doi:10.4049/jimmunol.171.8.4392

Dhalla, N. S., Elmoselhi, A. B., Hata, T., & Makino, N. (2000). Status of myocardial antioxidants in ischemia–reperfusion injury. *Cardiovascular Research, 47*(3), 446-456. doi:10.1016/S0008-6363(00)00078-X %J Cardiovascular Research

Dhandapani, P. K., Begines-Moreno, I. M., Brea-Calvo, G., Gärtner, U., Graeber, T. G., Javier Sanchez, G., . . . Szibor, M. (2019). Hyperoxia but not AOX expression mitigates pathological cardiac remodeling in a mouse model of inflammatory cardiomyopathy. *Scientific Reports, 9*(1), 12741-12741. doi:10.1038/s41598-019-49231-9

Dieckgraefe, B. K., Crimmins, D. L., Landt, V., Houchen, C., Anant, S., Porche-Sorbet, R., & Ladenson, J. H. J. J. o. i. m. (2002). Expression of the regenerating gene family in inflammatory bowel disease mucosa: Reg Iα upregulation, processing, and antiapoptotic activity. *50*(6), 421-434.

Dobaczewski, M., Gonzalez-Quesada, C., & Frangogiannis, N. G. (2010). The extracellular matrix as a modulator of the inflammatory and reparative response following myocardial infarction. *J Mol Cell Cardiol, 48*(3), 504-511. doi:10.1016/j.yjmcc.2009.07.015

Doerfler, M. E., Danner, R. L., Shelhamer, J. H., & Parrillo, J. E. (1989). Bacterial lipopolysaccharides prime human neutrophils for enhanced production of leukotriene B4. *J Clin Invest, 83*(3), 970-977. doi:10.1172/jci113983

Doherty, G. J., & McMahon, H. T. (2009). Mechanisms of endocytosis. *Annu Rev Biochem, 78*, 857-902. doi:10.1146/annurev.biochem.78.081307.110540

Drickamer, K. (1999). C-type lectin-like domains. *Curr Opin Struct Biol, 9*(5), 585-590. doi:10.1016/s0959-440x(99)00009-3

Duplan, L., Michel, B., Boucraut, J., Barthellémy, S., Desplat-Jego, S., Marin, V., . . . Alescio-Lautier, B. J. N. o. a. (2001). Lithostathine and pancreatitis-associated protein are involved in the very early stages of Alzheimer's disease. *22*(1), 79-88.

Eaton, J. W., & Qian, M. (2002). Molecular bases of cellular iron toxicity. *Free Radic Biol Med, 32*(9), 833-840. doi:10.1016/s0891-5849(02)00772-4

Ekpenyong, A. E., Toepfner, N., Chilvers, E. R., & Guck, J. (2015). Mechanotransduction in neutrophil activation and deactivation. *Biochimica et Biophysica Acta (BBA) - Molecular Cell Research, 1853*(11, Part B), 3105-3116. doi:10.1016/j.bbamcr.2015.07.015

Esmann, L., Idel, C., Sarkar, A., Hellberg, L., Behnen, M., Möller, S., . . . Laskay, T. (2010). Phagocytosis of apoptotic cells by neutrophil granulocytes: diminished proinflammatory neutrophil functions in the presence of apoptotic cells. *J Immunol, 184*(1), 391-400. doi:10.4049/jimmunol.0900564

Eszter, T., Gabrielle, D. B., & Zsolt, J. B. (2017). The Role of Neutrophil Extracellular Traps in Post-Injury Inflammation. doi:10.5772/intechopen.68906

Evrard, M., Kwok, I. W. H., Chong, S. Z., Teng, K. W. W., Becht, E., Chen, J., . . . Ng, L. G. (2018). Developmental Analysis of Bone Marrow Neutrophils Reveals Populations Specialized in Expansion, Trafficking, and Effector Functions. *Immunity, 48*(2), 364-379.e368. doi:10.1016/j.immuni.2018.02.002

Fadok, V. A., Bratton, D. L., Guthrie, L., & Henson, P. M. (2001). Differential effects of apoptotic versus lysed cells on macrophage production of cytokines: role of proteases. *J Immunol, 166*(11), 6847-6854. doi:10.4049/jimmunol.166.11.6847

Falcieri, E., Luchetti, F., Burattini, S., Canonico, B., Santi, S., & Papa, S. (2000). Lineage-related sensitivity to apoptosis in human tumor cells undergoing hyperthermia. *Histochemistry and Cell Biology, 113*(2), 135-144. doi:10.1007/s004180050016

Fan, K., Ruan, Q., Sensenbrenner, L., & Chen, B. (1992). Transforming growth factor-beta 1 bifunctionally regulates murine macrophage proliferation. *Blood, 79*(7), 1679-1685.

Faouzi, S., Burckhardt, B. E., Hanson, J. C., Campe, C. B., Schrum, L. W., Rippe, R. A., & Maher, J. J. (2001). Anti-Fas induces hepatic chemokines and promotes inflammation by an NF-kappa B-independent, caspase-3-dependent pathway. *J Biol Chem, 276*(52), 49077-49082. doi:10.1074/jbc.M109791200

Farinholt, T., Dinh, C., & Kuspa, A. (2019). Microbiome management in the social amoeba Dictyostelium discoideum compared to humans. *Int J Dev Biol, 63*(8-9-10), 447-450. doi:10.1387/ijdb.190240ak

Faurschou, M., & Borregaard, N. (2003). Neutrophil granules and secretory vesicles in inflammation. *Microbes Infect, 5*(14), 1317-1327. doi:10.1016/j.micinf.2003.09.008

Faxon, D. P., Gibbons, R. J., Chronos, N. A., Gurbel, P. A., & Sheehan, F. (2002). The effect of blockade of the CD11/CD18 integrin receptor on infarct size in patients with acute myocardial infarction treated with direct angioplasty: the results of the HALT-MI study. *J Am Coll Cardiol, 40*(7), 1199-1204. doi:10.1016/s0735-1097(02)02136-8

Fernández-Segura, E., García, J. M., Santos, J. L., & Campos, A. (1995). Shape, F-actin, and surface morphology changes during chemotactic peptide-induced polarity in human neutrophils. *241*(4), 519-528. doi:10.1002/ar.1092410410

Ferraro, B., Leoni, G., Hinkel, R., Ormanns, S., Paulin, N., Ortega-Gomez, A., . . . Soehnlein, O. (2019). Pro-Angiogenic Macrophage Phenotype to Promote Myocardial Repair. *J Am Coll Cardiol, 73*(23), 2990-3002. doi:10.1016/j.jacc.2019.03.503

Festjens, N., Vanden Berghe, T., & Vandenabeele, P. (2006). Necrosis, a well-orchestrated form of cell demise: Signalling cascades, important mediators and concomitant immune response. *Biochimica et Biophysica Acta (BBA) - Bioenergetics, 1757*(9), 1371-1387. doi:10.1016/j.bbabio.2006.06.014

Fliedner, T. M., Cronkite, E. P., Killmann, S. A., & Bond, V. P. (1964). GRANULOCYTOPOIESIS. II. EMERGENCE AND PATTERN OF LABELING OF NEUTROPHILIC GRANULOCYTES IN HUMANS. *Blood, 24*, 683-700.

Fox, S., Leitch, A. E., Duffin, R., Haslett, C., & Rossi, A. G. (2010). Neutrophil apoptosis: relevance to the innate immune response and inflammatory disease. *J Innate Immun, 2*(3), 216-227. doi:10.1159/000284367

Frangogiannis, N. G. (2012). Regulation of the inflammatory response in cardiac repair. *Circ Res, 110*(1), 159-173. doi:10.1161/circresaha.111.243162

Frangogiannis, N. G. (2014). The inflammatory response in myocardial injury, repair, and remodelling. *Nature reviews. Cardiology, 11*(5), 255-265. doi:10.1038/nrcardio.2014.28

Frangogiannis, N. G., Lindsey, M. L., Michael, L. H., Youker, K. A., Bressler, R. B., Mendoza, L. H., . . . Entman, M. L. (1998). Resident Cardiac Mast Cells Degranulate and Release Preformed TNF-α, Initiating the Cytokine Cascade in Experimental Canine Myocardial Ischemia/Reperfusion. *98*(7), 699-710. doi:doi:10.1161/01.CIR.98.7.699

Frangogiannis, N. G., Mendoza, L. H., Lindsey, M. L., Ballantyne, C. M., Michael, L. H., Smith, C. W., & Entman, M. L. (2000). IL-10 is induced in the reperfused myocardium and may modulate the reaction to injury. *J Immunol, 165*(5), 2798-2808. doi:10.4049/jimmunol.165.5.2798

Frangogiannis, N. G., Mendoza, L. H., Smith, C. W., Michael, L. H., & Entman, M. L. (2000). Induction of the synthesis of the C-X-C chemokine interferon-γ-inducible protein-10 in experimental canine endotoxemia. *Cell and Tissue Research, 302*(3), 365-376. doi:10.1007/s004410000274

Fridlender, Z. G., Sun, J., Kim, S., Kapoor, V., Cheng, G., Ling, L., . . . Albelda, S. M. (2009). Polarization of tumor-associated neutrophil phenotype by TGF-beta: "N1" versus "N2" TAN. *Cancer Cell, 16*(3), 183-194. doi:10.1016/j.ccr.2009.06.017

Furze, R. C., & Rankin, S. M. (2008). The role of the bone marrow in neutrophil clearance under homeostatic conditions in the mouse. *22*(9), 3111-3119. doi:10.1096/fj.08-109876

Galluzzi, L., Buqué, A., Kepp, O., Zitvogel, L., & Kroemer, G. (2017). Immunogenic cell death in cancer and infectious disease. *Nat Rev Immunol, 17*(2), 97-111. doi:10.1038/nri.2016.107

Galluzzi, L., Vitale, I., Aaronson, S. A., Abrams, J. M., Adam, D., Agostinis, P., . . . Kroemer, G. (2018). Molecular mechanisms of cell death: recommendations of the Nomenclature Committee on Cell Death 2018. *Cell death and differentiation, 25*(3), 486-541. doi:10.1038/s41418-017-0012-4

Gamble, J. R., & Vadas, M. A. (1988). Endothelial adhesiveness for blood neutrophils is inhibited by transforming growth factor-beta. *Science, 242*(4875), 97-99. doi:10.1126/science.3175638

Gaudron, P., Kugler, I., Hu, K., Bauer, W., Eilles, C., & Ertl, G. (2001). Time course of cardiac structural, functional and electrical changes in asymptomatic patients after myocardial infarction: their inter-relation and prognostic impact. *J Am Coll Cardiol, 38*(1), 33-40. doi:10.1016/s0735-1097(01)01319-5

Geering, B., & Simon, H. U. (2011). Peculiarities of cell death mechanisms in neutrophils. *Cell Death Differ, 18*(9), 1457-1469. doi:10.1038/cdd.2011.75

Geering, B., Stoeckle, C., Conus, S., & Simon, H. U. (2013). Living and dying for inflammation: neutrophils, eosinophils, basophils. *Trends Immunol, 34*(8), 398-409. doi:10.1016/j.it.2013.04.002

Giugliano, G. R., Giugliano, R. P., Gibson, C. M., & Kuntz, R. E. (2003). Meta-analysis of corticosteroid treatment in acute myocardial infarction. *Am J Cardiol, 91*(9), 1055-1059. doi:10.1016/s0002-9149(03)00148-6

Gorczyca, W., Melamed, M. R., & Darzynkiewicz, Z. (1993). [Programmed death of cells (apoptosis)]. *Patol Pol, 44*(3), 113-119.

Gordon, J. W., Shaw, J. A., & Kirshenbaum, L. A. (2011). Multiple facets of NF-κB in the heart: to be or not to NF-κB. *Circ Res, 108*(9), 1122-1132. doi:10.1161/circresaha.110.226928

Gorlino, C. V., Ranocchia, R. P., Harman, M. F., García, I. A., Crespo, M. I., Morón, G., . . . Pistoresi-Palencia, M. C. J. T. J. o. I. (2014). Neutrophils exhibit differential requirements for

homing molecules in their lymphatic and blood trafficking into draining lymph nodes. *193*(4), 1966-1974.

Graf, R., Schiesser, M., Scheele, G. A., Marquardt, K., Frick, T. W., Ammann, R. W., & Bimmler, D. J. J. o. B. C. (2001). A family of 16-kDa pancreatic secretory stress proteins form highly organized fibrillar structures upon tryptic activation. *276*(24), 21028-21038.

Green, D. R., Ferguson, T., Zitvogel, L., & Kroemer, G. (2009). Immunogenic and tolerogenic cell death. *Nat Rev Immunol, 9*(5), 353-363. doi:10.1038/nri2545

Green, D. R., & Llambi, F. (2015). Cell Death Signaling. *Cold Spring Harbor perspectives in biology, 7*(12), a006080. doi:10.1101/cshperspect.a006080

Greenlee-Wacker, M. C., Rigby, K. M., Kobayashi, S. D., Porter, A. R., DeLeo, F. R., & Nauseef, W. M. (2014). Phagocytosis of Staphylococcus aureus by human neutrophils prevents macrophage efferocytosis and induces programmed necrosis. *J Immunol, 192*(10), 4709-4717. doi:10.4049/jimmunol.1302692

Groemping, Y., & Rittinger, K. (2005). Activation and assembly of the NADPH oxidase: a structural perspective. *The Biochemical journal, 386*(Pt 3), 401-416. doi:10.1042/bj20041835

Guthrie, L. A., McPhail, L. C., Henson, P. M., & Johnston, R. B., Jr. (1984). Priming of neutrophils for enhanced release of oxygen metabolites by bacterial lipopolysaccharide. Evidence for increased activity of the superoxide-producing enzyme. *The Journal of experimental medicine, 160*(6), 1656-1671. doi:10.1084/jem.160.6.1656

Gwechenberger, M., Mendoza, L. H., Youker, K. A., Frangogiannis, N. G., Smith, C. W., Michael, L. H., & Entman, M. L. (1999). Cardiac myocytes produce interleukin-6 in culture and in viable border zone of reperfused infarctions. *Circulation, 99*(4), 546-551. doi:10.1161/01.cir.99.4.546

Hampton, H. R., Bailey, J., Tomura, M., Brink, R., & Chtanova, T. (2015). Microbe-dependent lymphatic migration of neutrophils modulates lymphocyte proliferation in lymph nodes. *Nat Commun, 6*, 7139. doi:10.1038/ncomms8139

Hampton, M. B., Vissers, M. C., Keenan, J. I., & Winterbourn, C. C. (2002). Oxidant-mediated phosphatidylserine exposure and macrophage uptake of activated neutrophils: possible impairment in chronic granulomatous disease. *J Leukoc Biol, 71*(5), 775-781.

Harlan, J. M., & Winn, R. K. (2002). Leukocyte-endothelial interactions: clinical trials of anti-adhesion therapy. *Crit Care Med, 30*(5 Suppl), S214-219. doi:10.1097/00003246-200205001-00007

Hartupee, J., Zhang, H., Bonaldo, M., Soares, M., Dieckgraefe, B. J. B. e. B. A.-G. S., & Expression. (2001). Isolation and characterization of a cDNA encoding a novel member of the human regenerating protein family: Reg IV. *1518*(3), 287-293.

Haslett, C. (1992). Resolution of acute inflammation and the role of apoptosis in the tissue fate of granulocytes. *Clinical Science, 83*(6), 639-648. doi:10.1042/cs0830639

Haslett, C. (1997). Granulocyte apoptosis and inflammatory disease. *Br Med Bull, 53*(3), 669-683. doi:10.1093/oxfordjournals.bmb.a011638

Hervieu, V., Christa, L., Gouysse, G., Bouvier, R., Chayvialle, J.-A., Bréchot, C., & Scoazec, J.-Y. J. H. p. (2006). HIP/PAP, a member of the reg family, is expressed in glucagon-producing enteropancreatic endocrine cells and tumors. *37*(8), 1066-1075.

Hilgendorf, I., Gerhardt, L. M., Tan, T. C., Winter, C., Holderried, T. A., Chousterman, B. G., . . . Swirski, F. K. (2014). Ly-6Chigh monocytes depend on Nr4a1 to balance both inflammatory and reparative phases in the infarcted myocardium. *Circ Res, 114*(10), 1611-1622. doi:10.1161/circresaha.114.303204

Hill, J. H., & Ward, P. A. (1971). The phlogistic role of C3 leukotactic fragments in myocardial infarcts of rats. *The Journal of experimental medicine, 133*(4), 885-900. doi:10.1084/jem.133.4.885

Ho, M.-R., Lou, Y.-C., Wei, S.-Y., Luo, S.-C., Lin, W.-C., Lyu, P.-C., & Chen, C. J. J. o. m. b. (2010). Human RegIV protein adopts a typical C-type lectin fold but binds mannan with two calcium-independent sites. *402*(4), 682-695.

Hochman, J. S., & Bulkley, B. H. (1982). Expansion of acute myocardial infarction: an experimental study. *Circulation, 65*(7), 1446-1450. doi:10.1161/01.cir.65.7.1446

Hofmann, U., Beyersdorf, N., Weirather, J., Podolskaya, A., Bauersachs, J., Ertl, G., . . . Frantz, S. (2012). Activation of CD4+ T lymphocytes improves wound healing and survival after experimental myocardial infarction in mice. *Circulation, 125*(13), 1652-1663. doi:10.1161/circulationaha.111.044164

Holmes, D. R., Jr., Savage, M., LaBlanche, J. M., Grip, L., Serruys, P. W., Fitzgerald, P., . . . Poland, M. (2002). Results of Prevention of REStenosis with Tranilast and its Outcomes (PRESTO) trial. *Circulation, 106*(10), 1243-1250. doi:10.1161/01.cir.0000028335.31300.da

Holz, R. W. (1974). THE EFFECTS OF THE POLYENE ANTIBIOTICS NYSTATIN AND AMPHOTERICIN B ON THIN LIPID MEMBRANES. *235*(1), 469-479. doi:10.1111/j.1749-6632.1974.tb43284.x

Hong, C., Kidani, Y., N, A. G., Phung, T., Ito, A., Rong, X., . . . Bensinger, S. J. (2012). Coordinate regulation of neutrophil homeostasis by liver X receptors in mice. *J Clin Invest, 122*(1), 337-347. doi:10.1172/jci58393

Horckmans, M., Ring, L., Duchene, J., Santovito, D., Schloss, M. J., Drechsler, M., . . . Steffens, S. (2017). Neutrophils orchestrate post-myocardial infarction healing by polarizing macrophages towards a reparative phenotype. *Eur Heart J, 38*(3), 187-197. doi:10.1093/eurheartj/ehw002

Humeres, C., & Frangogiannis, N. G. (2019). Fibroblasts in the Infarcted, Remodeling, and Failing Heart. *JACC. Basic to translational science, 4*(3), 449-467. doi:10.1016/j.jacbts.2019.02.006

Huotari, J., & Helenius, A. (2011). Endosome maturation. *The EMBO journal, 30*(17), 3481-3500. doi:10.1038/emboj.2011.286

Idziorek, T., Estaquier, J., De Bels, F., & Ameisen, J.-C. (1995). YOPRO-1 permits cytofluorometric analysis of programmed cell death (apoptosis) without interfering with cell viability. *Journal of Immunological Methods, 185*(2), 249-258. doi:10.1016/0022-1759(95)00172-7

Imlay, J. A. (2008). Cellular defenses against superoxide and hydrogen peroxide. *Annu Rev Biochem, 77*, 755-776. doi:10.1146/annurev.biochem.77.061606.161055

Infanger, D. W., Cao, X., Butler, S. D., Burmeister, M. A., Zhou, Y., Stupinski, J. A., . . . Davisson, R. L. (2010). Silencing nox4 in the paraventricular nucleus improves myocardial infarction-induced cardiac dysfunction by attenuating sympathoexcitation and periinfarct apoptosis. *Circ Res, 106*(11), 1763-1774. doi:10.1161/circresaha.109.213025

Itou, T., Collins, L. V., Thoren, F. B., Dahlgren, C., & Karlsson, A. (2006). Changes in activation states of murine polymorphonuclear leukocytes (PMN) during inflammation: a comparison of bone marrow and peritoneal exudate PMN. *Clin Vaccine Immunol, 13*(5), 575-583. doi:10.1128/CVI.13.5.575-583.2006

Ivey, C. L., Williams, F. M., Collins, P. D., Jose, P. J., & Williams, T. J. (1995). Neutrophil chemoattractants generated in two phases during reperfusion of ischemic myocardium in the rabbit. Evidence for a role for C5a and interleukin-8. *J Clin Invest, 95*(6), 2720-2728. doi:10.1172/jci117974

Jennings, R. B., Sommers, H. M., Smyth, G. A., Flack, H. A., & Linn, H. (1960). Myocardial necrosis induced by temporary occlusion of a coronary artery in the dog. *Arch Pathol, 70*, 68-78.

Kaksonen, M., & Roux, A. (2018). Mechanisms of clathrin-mediated endocytosis. *Nat Rev Mol Cell Biol, 19*(5), 313-326. doi:10.1038/nrm.2017.132

Karlsson, A., Follin, P., Leffler, H., & Dahlgren, C. J. B., The Journal of the American Society of Hematology. (1998). Galectin-3 activates the NADPH-oxidase in exudated but not peripheral blood neutrophils. *91*(9), 3430-3438.

Kasahara, Y., Iwai, K., Yachie, A., Ohta, K., Konno, A., Seki, H., . . . Taniguchi, N. (1997). Involvement of reactive oxygen intermediates in spontaneous and CD95 (Fas/APO-1)-mediated apoptosis of neutrophils. *Blood, 89*(5), 1748-1753.

Keeley, E. C., & Hillis, L. D. (2007). Primary PCI for myocardial infarction with ST-segment elevation. *N Engl J Med, 356*(1), 47-54. doi:10.1056/NEJMct063503

Keim, V., Rohr, G., Stöckert, H. G., & Haberich, F. J. (1984). An additional secretory protein in the rat pancreas. *Digestion, 29*(4), 242-249. doi:10.1159/000199041

Kelm, M., Lehoux, S., Azcutia, V., Cummings, R. D., Nusrat, A., Parkos, C. A., & Brazil, J. C. (2020). Regulation of neutrophil function by selective targeting of glycan epitopes expressed on the integrin CD11b/CD18. *34*(2), 2326-2343. doi:10.1096/fj.201902542R

Kennedy, A. D., & DeLeo, F. R. (2009). Neutrophil apoptosis and the resolution of infection. *Immunologic Research, 43*(1), 25-61. doi:10.1007/s12026-008-8049-6

Keppner, L., Heinrichs, M., Rieckmann, M., Demengeot, J., Frantz, S., Hofmann, U., & Ramos, G. (2018). Antibodies aggravate the development of ischemic heart failure. *Am J Physiol Heart Circ Physiol, 315*(5), H1358-h1367. doi:10.1152/ajpheart.00144.2018

Kerr, J. F., Wyllie, A. H., & Currie, A. R. (1972). Apoptosis: a basic biological phenomenon with wide-ranging implications in tissue kinetics. *Br J Cancer, 26*(4), 239-257. doi:10.1038/bjc.1972.33

Kilsdonk, E. P., Yancey, P. G., Stoudt, G. W., Bangerter, F. W., Johnson, W. J., Phillips, M. C., & Rothblat, G. H. (1995). Cellular cholesterol efflux mediated by cyclodextrins. *J Biol Chem, 270*(29), 17250-17256. doi:10.1074/jbc.270.29.17250

Klebanoff, S. J. (1970). Myeloperoxidase: contribution to the microbicidal activity of intact leukocytes. *Science, 169*(3950), 1095-1097. doi:10.1126/science.169.3950.1095

Knorr, M., Münzel, T., & Wenzel, P. (2014). Interplay of NK cells and monocytes in vascular inflammation and myocardial infarction. *Frontiers in physiology, 5*, 295. doi:10.3389/fphys.2014.00295

Kobayashi, S., Akiyama, T., Nata, K., Abe, M., Tajima, M., Shervani, N. J., . . . Okamoto, H. (2000). Identification of a receptor for reg (regenerating gene) protein, a pancreatic beta-cell regeneration factor. *J Biol Chem, 275*(15), 10723-10726. doi:10.1074/jbc.275.15.10723

Kolaczkowska, E., & Kubes, P. (2013). Neutrophil recruitment and function in health and inflammation. *Nature Reviews Immunology, 13*(3), 159-175. doi:10.1038/nri3399

Kono, H., Karmarkar, D., Iwakura, Y., & Rock, K. L. (2010). Identification of the cellular sensor that stimulates the inflammatory response to sterile cell death. *J Immunol, 184*(8), 4470-4478. doi:10.4049/jimmunol.0902485

Korzeniewski, C., & Callewaert, D. M. (1983). An enzyme-release assay for natural cytotoxicity. *J Immunol Methods, 64*(3), 313-320. doi:10.1016/0022-1759(83)90438-6

Kroemer, G., & Jaattela, M. (2005). Lysosomes and autophagy in cell death control. *Nat Rev Cancer, 5*(11), 886-897. doi:10.1038/nrc1738

Kumar, A. G., Ballantyne, C. M., Michael, L. H., Kukielka, G. L., Youker, K. A., Lindsey, M. L., . . . Entman, M. L. (1997). Induction of monocyte chemoattractant protein-1 in the small veins of the ischemic and reperfused canine myocardium. *Circulation, 95*(3), 693-700. doi:10.1161/01.cir.95.3.693

Lamb, F. S., Hook, J. S., Hilkin, B. M., Huber, J. N., Volk, A. P., & Moreland, J. G. (2012). Endotoxin priming of neutrophils requires endocytosis and NADPH oxidase-dependent endosomal reactive oxygen species. *J Biol Chem, 287*(15), 12395-12404. doi:10.1074/jbc.M111.306530

Lambeth, J. D., & Neish, A. S. (2014). Nox enzymes and new thinking on reactive oxygen: a double-edged sword revisited. *Annual review of pathology, 9*, 119-145. doi:10.1146/annurev-pathol-012513-104651

Lämmermann, T., Afonso, P. V., Angermann, B. R., Wang, J. M., Kastenmüller, W., Parent, C. A., & Germain, R. N. (2013). Neutrophil swarms require LTB4 and integrins at sites of cell death in vivo. *Nature, 498*(7454), 371-375. doi:10.1038/nature12175

Lasky, L. A. (1992). Selectins: interpreters of cell-specific carbohydrate information during inflammation. *Science, 258*(5084), 964. doi:10.1126/science.1439808

Lasserre, C., Christa, L., Simon, M. T., Vernier, P., & Bréchot, C. (1992). A novel gene (HIP) activated in human primary liver cancer. *Cancer Res, 52*(18), 5089-5095.

LeBlanc, S. (2020). Review: Relationships between metabolism and neutrophil function in dairy cows in the peripartum period. *animal, 14*, s44-s54. doi:10.1017/S1751731119003227

Lee, J., Remold, H. G., Ieong, M. H., & Kornfeld, H. (2006). Macrophage apoptosis in response to high intracellular burden of Mycobacterium tuberculosis is mediated by a novel caspase-independent pathway. *J Immunol, 176*(7), 4267-4274. doi:10.4049/jimmunol.176.7.4267

Lefer, D. J., & Granger, D. N. (2000). Oxidative stress and cardiac disease. *Am J Med, 109*(4), 315-323. doi:10.1016/S0002-9343(00)00467-8

Lehotzky, R. E., Partch, C. L., Mukherjee, S., Cash, H. L., Goldman, W. E., Gardner, K. H., & Hooper, L. V. (2010). Molecular basis for peptidoglycan recognition by a bactericidal lectin. *Proc Natl Acad Sci U S A, 107*(17), 7722-7727. doi:10.1073/pnas.0909449107

Leuschner, F., Rauch, P. J., Ueno, T., Gorbatov, R., Marinelli, B., Lee, W. W., . . . Nahrendorf, M. (2012). Rapid monocyte kinetics in acute myocardial infarction are sustained by extramedullary monocytopoiesis. *The Journal of experimental medicine, 209*(1), 123-137. doi:10.1084/jem.20111009

Levy, J., Kolski, G. B., & Douglas, S. D. (1989). Cathepsin D-like activity in neutrophils and monocytes. *Infect Immun, 57*(5), 1632-1634.

Li, W., Yuan, X., Nordgren, G., Dalen, H., Dubowchik, G. M., Firestone, R. A., & Brunk, U. T. J. F. l. (2000). Induction of cell death by the lysosomotropic detergent MSDH. *470*(1), 35-39.

Liehn, E. A., Postea, O., Curaj, A., & Marx, N. (2011). Repair After Myocardial Infarction, Between Fantasy and Reality: The Role of Chemokines. *J Am Coll Cardiol, 58*(23), 2357-2362. doi:10.1016/j.jacc.2011.08.034

Lieu, H.-T., Simon, M.-T., Nguyen-Khoa, T., Kebede, M., Cortes, A., Tebar, L., . . . Christa, L. (2006). Reg2 inactivation increases sensitivity to Fas hepatotoxicity and delays liver regeneration post-hepatectomy in mice. *44*(6), 1452-1464. doi:10.1002/hep.21434

Lin, H. P., Singla, B., Ghoshal, P., Faulkner, J. L., Cherian-Shaw, M., O'Connor, P. M., . . . Csányi, G. (2018). Identification of novel macropinocytosis inhibitors using a rational screen of Food and Drug Administration-approved drugs. *Br J Pharmacol, 175*(18), 3640-3655. doi:10.1111/bph.14429

Lin, M., Jackson, P., Tester, A. M., Diaconu, E., Overall, C. M., Blalock, J. E., & Pearlman, E. (2008). Matrix metalloproteinase-8 facilitates neutrophil migration through the corneal stromal matrix by collagen degradation and production of the chemotactic peptide Pro-Gly-Pro. *Am J Pathol, 173*(1), 144-153. doi:10.2353/ajpath.2008.080081

Lindsey, M. L., Mann, D. L., Entman, M. L., & Spinale, F. G. (2003). Extracellular matrix remodeling following myocardial injury. *Annals of Medicine, 35*(5), 316-326. doi:10.1080/07853890310001285

Liu, B.-C., Lu, X.-Y., Song, X., Lei, K.-Y., Alli, A. A., Bao, H.-F., . . . Ma, H.-P. J. F. i. p. (2013). Scanning ion conductance microscopy: a nanotechnology for biological studies in live cells. *3*, 483.

Liu, X., Ma, B., Malik, A. B., Tang, H., Yang, T., Sun, B., . . . Zhao, Y. J. N. i. (2012). Bidirectional regulation of neutrophil migration by mitogen-activated protein kinases. *13*(5), 457-464.

Liu, Y., Fang, S., Li, X., Feng, J., Du, J., Guo, L., . . . Liu, Y. (2017). Aspirin inhibits LPS-induced macrophage activation via the NF-κB pathway. *Scientific Reports, 7*(1), 11549. doi:10.1038/s41598-017-10720-4

Loerchner, H., Poling, J., Gajawada, P., Hou, Y., Polyakova, V., Kostin, S., . . . Braun, T. (2015). Myocardial healing requires Reg3beta-dependent accumulation of macrophages in the ischemic heart. *Nat Med, 21*(4), 353-362. doi:10.1038/nm.3816

Loison, F., Zhu, H., Karatepe, K., Kasorn, A., Liu, P., Ye, K., . . . Luo, H. R. (2014). Proteinase 3-dependent caspase-3 cleavage modulates neutrophil death and inflammation. *J Clin Invest, 124*(10), 4445-4458. doi:10.1172/jci76246

Lörchner, H., Hou, Y., Adrian-Segarra, J. M., Kulhei, J., Detzer, J., Günther, S., . . . Braun, T. (2018). Reg proteins direct accumulation of functionally distinct macrophage subsets after myocardial infarction. *Cardiovasc Res, 114*(12), 1667-1679. doi:10.1093/cvr/cvy126

Lörchner, H., Widera, C., Hou, Y., Elsässer, A., Warnecke, H., Giannitsis, E., . . . Pöling, J. (2018). Reg3β is associated with cardiac inflammation and provides prognostic information in patients with acute coronary syndrome. *Int J Cardiol, 258*, 7-13. doi:10.1016/j.ijcard.2018.01.043

Lou, O., Alcaide, P., Luscinskas, F. W., & Muller, W. A. (2007). CD99 is a key mediator of the transendothelial migration of neutrophils. *J Immunol, 178*(2), 1136-1143. doi:10.4049/jimmunol.178.2.1136

Luzio, J. P., Pryor, P. R., & Bright, N. A. (2007). Lysosomes: fusion and function. *Nat Rev Mol Cell Biol, 8*(8), 622-632. doi:10.1038/nrm2217

Lv, X. X., Liu, S. S., Li, K., Cui, B., Liu, C., & Hu, Z. W. (2017). Cigarette smoke promotes COPD by activating platelet-activating factor receptor and inducing neutrophil autophagic death in mice. *Oncotarget, 8*(43), 74720-74735. doi:10.18632/oncotarget.20353

Ma, Q., Jones, D., & Springer, T. A. (1999). The chemokine receptor CXCR4 is required for the retention of B lineage and granulocytic precursors within the bone marrow microenvironment. *Immunity, 10*(4), 463-471. doi:10.1016/s1074-7613(00)80046-1

Ma, Y., Yabluchanskiy, A., Iyer, R. P., Cannon, P. L., Flynn, E. R., Jung, M., . . . Lindsey, M. L. (2016). Temporal neutrophil polarization following myocardial infarction. *Cardiovascular Research, 110*(1), 51-61. doi:10.1093/cvr/cvw024

Ma, Y., Yabluchanskiy, A., & Lindsey, M. L. (2013). Neutrophil roles in left ventricular remodeling following myocardial infarction. *Fibrogenesis Tissue Repair, 6*(1), 11. doi:10.1186/1755-1536-6-11

Maehara, Y., Anai, H., Tamada, R., & Sugimachi, K. (1987). The ATP assay is more sensitive than the succinate dehydrogenase inhibition test for predicting cell viability. *European Journal of Cancer and Clinical Oncology, 23*(3), 273-276. doi:10.1016/0277-5379(87)90070-8

Majno, G., La Gattuta, M., & Thompson, T. E. (1960). Cellular death and necrosis: chemical, physical and morphologic changes in rat liver. *Virchows Arch Pathol Anat Physiol Klin Med, 333*, 421-465. doi:10.1007/bf00955327

Maki, J. L., & Degterev, A. (2013). Activity assays for receptor-interacting protein kinase 1:a key regulator of necroptosis. *Methods Mol Biol, 1004*, 31-42. doi:10.1007/978-1-62703-383-1_3

Mann, D. L., McMurray, J. J., Packer, M., Swedberg, K., Borer, J. S., Colucci, W. S., . . . Fleming, T. (2004). Targeted anticytokine therapy in patients with chronic heart failure: results of the Randomized Etanercept Worldwide Evaluation (RENEWAL). *Circulation, 109*(13), 1594-1602. doi:10.1161/01.Cir.0000124490.27666.B2

Mannick, J. B., Schonhoff, C., Papeta, N., Ghafourifar, P., Szibor, M., Fang, K., & Gaston, B. (2001). S-Nitrosylation of mitochondrial caspases. *J Cell Biol, 154*(6), 1111-1116. doi:10.1083/jcb.200104008

Markis, J. E., Malagold, M., Parker, J. A., Silverman, K. J., Barry, W. H., Als, A. V., . . . Braunwald, E. (1981). Myocardial salvage after intracoronary thrombolysis with streptokinase in acute myocardial infarction. *N Engl J Med, 305*(14), 777-782. doi:10.1056/nejm198110013051401

Marsh, M. (2002). *Endocytosis. Edited by Mark Marsh* (Vol. 77): The University of Chicago Press.

Martin, C., Burdon, P. C., Bridger, G., Gutierrez-Ramos, J. C., Williams, T. J., & Rankin, S. M. (2003). Chemokines acting via CXCR2 and CXCR4 control the release of neutrophils from the bone marrow and their return following senescence. *Immunity, 19*(4), 583-593. doi:10.1016/s1074-7613(03)00263-2

Massena, S., Christoffersson, G., Vågesjö, E., Seignez, C., Gustafsson, K., Binet, F., . . . Phillipson, M. (2015). Identification and characterization of VEGF-A-responsive neutrophils

expressing CD49d, VEGFR1, and CXCR4 in mice and humans. *Blood, 126*(17), 2016-2026. doi:10.1182/blood-2015-03-631572

Mathias, J. R., Perrin, B. J., Liu, T. X., Kanki, J., Look, A. T., & Huttenlocher, A. J. J. o. l. b. (2006). Resolution of inflammation by retrograde chemotaxis of neutrophils in transgenic zebrafish. *80*(6), 1281-1288.

Maxfield, F. R., & Yamashiro, D. J. (1987). Endosome acidification and the pathways of receptor-mediated endocytosis. *Adv Exp Med Biol, 225*, 189-198. doi:10.1007/978-1-4684-5442-0_16

Mayadas, T. N., Cullere, X., & Lowell, C. A. (2014). The multifaceted functions of neutrophils. *Annual review of pathology, 9*, 181-218. doi:10.1146/annurev-pathol-020712-164023

McDonald, B., Pittman, K., Menezes, G. B., Hirota, S. A., Slaba, I., Waterhouse, C. C. M., . . . Kubes, P. (2010). Intravascular Danger Signals Guide Neutrophils to Sites of Sterile Inflammation. *Science, 330*(6002), 362. doi:10.1126/science.1195491

McEver, R. P., Moore, K. L., & Cummings, R. D. (1995). Leukocyte trafficking mediated by selectin-carbohydrate interactions. *J Biol Chem, 270*(19), 11025-11028. doi:10.1074/jbc.270.19.11025

McKay, R. G., Pfeffer, M. A., Pasternak, R. C., Markis, J. E., Come, P. C., Nakao, S., . . . Grossman, W. (1986). Left ventricular remodeling after myocardial infarction: a corollary to infarct expansion. *Circulation, 74*(4), 693-702. doi:10.1161/01.cir.74.4.693

McLaughlin, N. J., Banerjee, A., Kelher, M. R., Gamboni-Robertson, F., Hamiel, C., Sheppard, F. R., . . . Silliman, C. C. (2006). Platelet-activating factor-induced clathrin-mediated endocytosis requires beta-arrestin-1 recruitment and activation of the p38 MAPK signalosome at the plasma membrane for actin bundle formation. *J Immunol, 176*(11), 7039-7050. doi:10.4049/jimmunol.176.11.7039

McStay, G. P., & Green, D. R. J. C. S. H. P. (2014). Measuring apoptosis: caspase inhibitors and activity assays. *2014*(8), pdb. top070359.

Merz, S. F., Korste, S., Bornemann, L., Michel, L., Stock, P., Squire, A., . . . Totzeck, M. (2019). Contemporaneous 3D characterization of acute and chronic myocardial I/R injury and response. *Nat Commun, 10*(1), 2312. doi:10.1038/s41467-019-10338-2

Miao, E. A., Leaf, I. A., Treuting, P. M., Mao, D. P., Dors, M., Sarkar, A., . . . Aderem, A. (2010). Caspase-1-induced pyroptosis is an innate immune effector mechanism against intracellular bacteria. *Nature immunology, 11*(12), 1136-1142. doi:10.1038/ni.1960

Mihalache, C. C., Yousefi, S., Conus, S., Villiger, P. M., Schneider, E. M., & Simon, H. U. (2011). Inflammation-associated autophagy-related programmed necrotic death of human neutrophils characterized by organelle fusion events. *J Immunol, 186*(11), 6532-6542. doi:10.4049/jimmunol.1004055

Miki, T., Holst, O., & Hardt, W.-D. (2012). The bactericidal activity of the C-type lectin RegIIIβ against Gram-negative bacteria involves binding to lipid A. *J Biol Chem, 287*(41), 34844-34855. doi:10.1074/jbc.M112.399998

Miller, L. S., O'Connell, R. M., Gutierrez, M. A., Pietras, E. M., Shahangian, A., Gross, C. E., . . . Modlin, R. L. (2006). MyD88 mediates neutrophil recruitment initiated by IL-1R but not TLR2 activation in immunity against Staphylococcus aureus. *Immunity, 24*(1), 79-91. doi:10.1016/j.immuni.2005.11.011

Mishra, J., Dent, C., Tarabishi, R., Mitsnefes, M. M., Ma, Q., Kelly, C., . . . Bean, J. J. T. L. (2005). Neutrophil gelatinase-associated lipocalin (NGAL) as a biomarker for acute renal injury after cardiac surgery. *365*(9466), 1231-1238.

Mitroulis, I., Kourtzelis, I., Kambas, K., Rafail, S., Chrysanthopoulou, A., Speletas, M., & Ritis, K. (2010). Regulation of the autophagic machinery in human neutrophils. *Eur J Immunol, 40*(5), 1461-1472. doi:10.1002/eji.200940025

Moran, A. E., Forouzanfar, M. H., Roth, G. A., Mensah, G. A., Ezzati, M., Flaxman, A., . . . Naghavi, M. (2014). The global burden of ischemic heart disease in 1990 and 2010: the Global

Burden of Disease 2010 study. *Circulation, 129*(14), 1493-1501. doi:10.1161/circulationaha.113.004046

Morimoto, H., Takahashi, M., Izawa, A., Ise, H., Hongo, M., Kolattukudy, P. E., & Ikeda, U. (2006). Cardiac Overexpression of Monocyte Chemoattractant Protein-1 in Transgenic Mice Prevents Cardiac Dysfunction and Remodeling After Myocardial Infarction. *99*(8), 891-899. doi:doi:10.1161/01.RES.0000246113.82111.2d

Mozaffarian, D., Benjamin, E. J., Go, A. S., Arnett, D. K., Blaha, M. J., Cushman, M., . . . Turner, M. B. (2015). Heart disease and stroke statistics--2015 update: a report from the American Heart Association. *Circulation, 131*(4), e29-322. doi:10.1161/cir.0000000000000152

Mueller, C. M., Zhang, H., & Zenilman, M. E. J. J. o. S. R. (2008). Pancreatic reg I binds MKP-1 and regulates cyclin D in pancreatic-derived cells. *150*(1), 137-143.

Mukherjee, S., Zheng, H., Derebe, M. G., Callenberg, K. M., Partch, C. L., Rollins, D., . . . Jiang, Q.-X. J. N. (2014). Antibacterial membrane attack by a pore-forming intestinal C-type lectin. *505*(7481), 103-107.

Nahrendorf, M., Swirski, F. K., Aikawa, E., Stangenberg, L., Wurdinger, T., Figueiredo, J. L., . . . Pittet, M. J. (2007). The healing myocardium sequentially mobilizes two monocyte subsets with divergent and complementary functions. *The Journal of experimental medicine, 204*(12), 3037-3047. doi:10.1084/jem.20070885

Nandi, B., & Behar, S. M. (2011). Regulation of neutrophils by interferon-γ limits lung inflammation during tuberculosis infection. *The Journal of experimental medicine, 208*(11), 2251-2262. doi:10.1084/jem.20110919

Nathan, C. (2002). Points of control in inflammation. *Nature, 420*(6917), 846-852. doi:10.1038/nature01320

Ng, L. G., Ostuni, R., & Hidalgo, A. (2019). Heterogeneity of neutrophils. *Nature Reviews Immunology, 19*(4), 255-265. doi:10.1038/s41577-019-0141-8

Ng, L. L., Khan, S. Q., Narayan, H., Quinn, P., Squire, I. B., & Davies, J. E. (2011). Proteinase 3 and prognosis of patients with acute myocardial infarction. *Clin Sci (Lond), 120*(6), 231-238. doi:10.1042/cs20100366

Nguyen, G. T., Green, E. R., & Mecsas, J. (2017). Neutrophils to the ROScue: Mechanisms of NADPH Oxidase Activation and Bacterial Resistance. *Front Cell Infect Microbiol, 7*, 373. doi:10.3389/fcimb.2017.00373

Nian, M., Lee, P., Khaper, N., & Liu, P. (2004). Inflammatory Cytokines and Postmyocardial Infarction Remodeling. *94*(12), 1543-1553. doi:doi:10.1161/01.RES.0000130526.20854.fa

Nichols, M., Townsend, N., Scarborough, P., & Rayner, M. (2014). Cardiovascular disease in Europe 2014: epidemiological update. *Eur Heart J, 35*(42), 2929. doi:10.1093/eurheartj/ehu378

Nilsson, E., Ghassemifar, R., & Brunk, U. T. (1997). Lysosomal heterogeneity between and within cells with respect to resistance against oxidative stress. *The Histochemical Journal, 29*(11), 857-865. doi:10.1023/A:1026441907803

Nourshargh, S., Renshaw, S. A., & Imhof, B. A. (2016). Reverse Migration of Neutrophils: Where, When, How, and Why? *Trends Immunol, 37*(5), 273-286. doi:10.1016/j.it.2016.03.006

Nozawa, H., Chiu, C., & Hanahan, D. (2006). Infiltrating neutrophils mediate the initial angiogenic switch in a mouse model of multistage carcinogenesis. *Proc Natl Acad Sci U S A, 103*(33), 12493-12498. doi:10.1073/pnas.0601807103

Okamoto, H. J. J. o. h.-b.-p. s. (1999). The Reg gene family and Reg proteins: with special attention to the regeneration of pancreatic β-cells. *6*(3), 254-262.

Ong, S.-B., Hernández-Reséndiz, S., Crespo-Avilan, G. E., Mukhametshina, R. T., Kwek, X.-Y., Cabrera-Fuentes, H. A., & Hausenloy, D. J. (2018). Inflammation following acute myocardial infarction: Multiple players, dynamic roles, and novel therapeutic opportunities. *Pharmacology & therapeutics, 186*, 73-87. doi:10.1016/j.pharmthera.2018.01.001

Ortega-Gómez, A., Perretti, M., & Soehnlein, O. (2013). Resolution of inflammation: an integrated view. *EMBO Mol Med, 5*(5), 661-674. doi:10.1002/emmm.201202382

Panahi, M., Papanikolaou, A., Torabi, A., Zhang, J.-G., Khan, H., Vazir, A., . . . Sattler, S. (2018). Immunomodulatory interventions in myocardial infarction and heart failure: a systematic review of clinical trials and meta-analysis of IL-1 inhibition. *Cardiovascular Research, 114*(11), 1445-1461. doi:10.1093/cvr/cvy145

Panizzi, P., Swirski, F. K., Figueiredo, J.-L., Waterman, P., Sosnovik, D. E., Aikawa, E., . . . Nahrendorf, M. (2010). Impaired infarct healing in atherosclerotic mice with Ly-6C(hi) monocytosis. *J Am Coll Cardiol, 55*(15), 1629-1638. doi:10.1016/j.jacc.2009.08.089

Peyron, P., Maridonneau-Parini, I., & Stegmann, T. (2001). Fusion of Human Neutrophil Phagosomes with Lysosomes in Vitro : INVOLVEMENT OF TYROSINE KINASES OF THE Src FAMILY AND INHIBITION BY MYCOBACTERIA. *Journal of Biological Chemistry, 276*(38), 35512-35517.

Pfeffer, J. M., Pfeffer, M. A., Fletcher, P. J., & Braunwald, E. (1991). Progressive ventricular remodeling in rat with myocardial infarction. *Am J Physiol, 260*(5 Pt 2), H1406-1414. doi:10.1152/ajpheart.1991.260.5.H1406

Phillipson, M., Heit, B., Colarusso, P., Liu, L., Ballantyne, C. M., & Kubes, P. (2006). Intraluminal crawling of neutrophils to emigration sites: a molecularly distinct process from adhesion in the recruitment cascade. *The Journal of experimental medicine, 203*(12), 2569-2575. doi:10.1084/jem.20060925

Pillay, J., den Braber, I., Vrisekoop, N., Kwast, L. M., de Boer, R. J., Borghans, J. A. M., . . . Koenderman, L. (2010). In vivo labeling with 2H2O reveals a human neutrophil lifespan of 5.4 days. *Blood, 116*(4), 625-627. doi:10.1182/blood-2010-01-259028 %J Blood

Pollock, J. D., Williams, D. A., Gifford, M. A., Li, L. L., Du, X., Fisherman, J., . . . Dinauer, M. C. (1995). Mouse model of X-linked chronic granulomatous disease, an inherited defect in phagocyte superoxide production. *Nat Genet, 9*(2), 202-209. doi:10.1038/ng0295-202

Prabhu, S. D., & Frangogiannis, N. G. (2016). The Biological Basis for Cardiac Repair After Myocardial Infarction: From Inflammation to Fibrosis. *Circ Res, 119*(1), 91-112. doi:10.1161/CIRCRESAHA.116.303577

Prince, L. R., Bianchi, S. M., Vaughan, K. M., Bewley, M. A., Marriott, H. M., Walmsley, S. R., . . . Whyte, M. K. B. (2008). Subversion of a lysosomal pathway regulating neutrophil apoptosis by a major bacterial toxin, pyocyanin. *J Immunol, 180*(5), 3502-3511. doi:10.4049/jimmunol.180.5.3502

Puga, I., Cols, M., Barra, C. M., He, B., Cassis, L., Gentile, M., . . . Cerutti, A. (2011). B cell-helper neutrophils stimulate the diversification and production of immunoglobulin in the marginal zone of the spleen. *Nature immunology, 13*(2), 170-180. doi:10.1038/ni.2194

Rankin, S. M. (2010). The bone marrow: a site of neutrophil clearance. *88*(2), 241-251. doi:10.1189/jlb.0210112

Rather, L. J. (1970). Lectures on the Comparative Pathology of Inflammation. *Medical History, 14*(4), 409-412.

Ray, A., & Dittel, B. N. (2010). Isolation of Mouse Peritoneal Cavity Cells. *JoVE*(35), e1488. doi:doi:10.3791/1488

Redka, D. y. S., Gütschow, M., Grinstein, S., & Canton, J. J. M. b. o. t. c. (2018). Differential ability of proinflammatory and anti-inflammatory macrophages to perform macropinocytosis. *29*(1), 53-65.

Reimer, K. A., Lowe, J. E., Rasmussen, M. M., & Jennings, R. B. (1977). The wavefront phenomenon of ischemic cell death. 1. Myocardial infarct size vs duration of coronary occlusion in dogs. *Circulation, 56*(5), 786-794. doi:10.1161/01.cir.56.5.786

Remijsen, Q., Vanden Berghe, T., Wirawan, E., Asselbergh, B., Parthoens, E., De Rycke, R., . . . Vandenabeele, P. (2011). Neutrophil extracellular trap cell death requires both autophagy and superoxide generation. *Cell Res, 21*(2), 290-304. doi:10.1038/cr.2010.150

Renshaw, S. A., Timmons, S. J., Eaton, V., Usher, L. R., Akil, M., Bingle, C. D., & Whyte, M. K. (2000). Inflammatory neutrophils retain susceptibility to apoptosis mediated via the Fas death receptor. *J Leukoc Biol, 67*(5), 662-668. doi:10.1002/jlb.67.5.662

Repnik, U., Česen, M. H., & Turk, B. (2016). The Use of Lysosomotropic Dyes to Exclude Lysosomal Membrane Permeabilization. *Cold Spring Harb Protoc, 2016*(5). doi:10.1101/pdb.prot087106

Repnik, U., Stoka, V., Turk, V., & Turk, B. (2012). Lysosomes and lysosomal cathepsins in cell death. *Biochim Biophys Acta, 1824*(1), 22-33. doi:10.1016/j.bbapap.2011.08.016

Root, R. K., Metcalf, J., Oshino, N., & Chance, B. (1975). H2O2 release from human granulocytes during phagocytosis. I. Documentation, quantitation, and some regulating factors. *J Clin Invest, 55*(5), 945-955. doi:10.1172/JCI108024

Rosales, C., & Uribe-Querol, E. (2017). Phagocytosis: A Fundamental Process in Immunity. *BioMed research international, 2017*, 9042851-9042851. doi:10.1155/2017/9042851

Rosen, H., & Klebanoff, S. J. (1979). Bactericidal activity of a superoxide anion-generating system. A model for the polymorphonuclear leukocyte. *The Journal of experimental medicine, 149*(1), 27-39. doi:10.1084/jem.149.1.27

Roth, G. A., Abate, D., Abate, K. H., Abay, S. M., Abbafati, C., Abbasi, N., . . . Murray, C. J. L. (2018). Global, regional, and national age-sex-specific mortality for 282 causes of death in 195 countries and territories, 1980–2017: a systematic analysis for the Global Burden of Disease Study 2017. *The Lancet, 392*(10159), 1736-1788. doi:10.1016/S0140-6736(18)32203-7

Rothe, G., Oser, A., & Valet, G. (1988). Dihydrorhodamine 123: a new flow cytometric indicator for respiratory burst activity in neutrophil granulocytes. *Naturwissenschaften, 75*(7), 354-355. doi:10.1007/BF00368326

Ryu, J. C., Kim, M. J., Kwon, Y., Oh, J. H., Yoon, S. S., Shin, S. J., . . . Ryu, J. H. (2017). Neutrophil pyroptosis mediates pathology of P. aeruginosa lung infection in the absence of the NADPH oxidase NOX2. *Mucosal Immunology, 10*(3), 757-774. doi:10.1038/mi.2016.73

Sanz, M. J., & Kubes, P. (2012). Neutrophil-active chemokines in in vivo imaging of neutrophil trafficking. *Eur J Immunol, 42*(2), 278-283. doi:10.1002/eji.201142231

Savill, J. S., Wyllie, A. H., Henson, J. E., Walport, M. J., Henson, P. M., & Haslett, C. (1989). Macrophage phagocytosis of aging neutrophils in inflammation. Programmed cell death in the neutrophil leads to its recognition by macrophages. *J Clin Invest, 83*(3), 865-875. doi:10.1172/jci113970

Scannell, M., Flanagan, M. B., deStefani, A., Wynne, K. J., Cagney, G., Godson, C., & Maderna, P. (2007). Annexin-1 and peptide derivatives are released by apoptotic cells and stimulate phagocytosis of apoptotic neutrophils by macrophages. *J Immunol, 178*(7), 4595-4605. doi:10.4049/jimmunol.178.7.4595

Schlegel, R., Dickson, R. B., Willingham, M. C., & Pastan, I. H. (1982). Amantadine and dansylcadaverine inhibit vesicular stomatitis virus uptake and receptor-mediated endocytosis of alpha 2-macroglobulin. *Proc Natl Acad Sci U S A, 79*(7), 2291-2295. doi:10.1073/pnas.79.7.2291

Schudel, L. (1965). *Leitfaden der Blutmorphologie* (11. ed.). Stuttgart: Georg Thieme Verlag.

Segal, A. W., Dorling, J., & Coade, S. (1980). Kinetics of fusion of the cytoplasmic granules with phagocytic vacuoles in human polymorphonuclear leukocytes. Biochemical and morphological studies. *J Cell Biol, 85*(1), 42-59. doi:10.1083/jcb.85.1.42

Seger, R. A. (2010). Chronic granulomatous disease: recent advances in pathophysiology and treatment. *Neth J Med, 68*(11), 334-340.

Segers, V. F. M., Brutsaert, D. L., & De Keulenaer, G. W. (2018). Cardiac Remodeling: Endothelial Cells Have More to Say Than Just NO. *Frontiers in physiology, 9*, 382-382. doi:10.3389/fphys.2018.00382

Sellak, H., Franzini, E., Hakim, J., & Pasquier, C. (1994). Reactive oxygen species rapidly increase endothelial ICAM-1 ability to bind neutrophils without detectable upregulation. *Blood, 83*(9), 2669-2677.

Sengeløv, H., Kjeldsen, L., & Borregaard, N. (1993). Control of exocytosis in early neutrophil activation. *The Journal of Immunology, 150*(4), 1535.

Sharma, A., Simonson, T. J., Jondle, C. N., Mishra, B. B., & Sharma, J. (2017). Mincle-Mediated Neutrophil Extracellular Trap Formation by Regulation of Autophagy. *J Infect Dis, 215*(7), 1040-1048. doi:10.1093/infdis/jix072

Shehadul Islam, M., Aryasomayajula, A., & Selvaganapathy, P. R. (2017). A Review on Macroscale and Microscale Cell Lysis Methods. *Micromachines, 8*(3), 83. doi:10.3390/mi8030083

Sheppard, F. R., Kelher, M. R., Moore, E. E., McLaughlin, N. J. D., Banerjee, A., & Silliman, C. C. (2005). Structural organization of the neutrophil NADPH oxidase: phosphorylation and translocation during priming and activation. *78*(5), 1025-1042. doi:10.1189/jlb.0804442

Shi, J., Gilbert, G. E., Kokubo, Y., & Ohashi, T. (2001). Role of the liver in regulating numbers of circulating neutrophils. *Blood, 98*(4), 1226-1230. doi:10.1182/blood.v98.4.1226

Siwik, D. A., Chang, D. L.-F., & Colucci, W. S. J. C. r. (2000). Interleukin-1β and tumor necrosis factor-α decrease collagen synthesis and increase matrix metalloproteinase activity in cardiac fibroblasts in vitro. *86*(12), 1259-1265.

Smith, R. M., Connor, J. A., Chen, L. M., & Babior, B. M. (1996). The cytosolic subunit p67phox contains an NADPH-binding site that participates in catalysis by the leukocyte NADPH oxidase. *J Clin Invest, 98*(4), 977-983. doi:10.1172/jci118882

Smolina, K., Wright, F. L., Rayner, M., & Goldacre, M. J. (2012). Long-term survival and recurrence after acute myocardial infarction in England, 2004 to 2010. *Circ Cardiovasc Qual Outcomes, 5*(4), 532-540. doi:10.1161/circoutcomes.111.964700

Soehnlein, O., Steffens, S., Hidalgo, A., & Weber, C. (2017). Neutrophils as protagonists and targets in chronic inflammation. *Nat Rev Immunol, 17*(4), 248-261. doi:10.1038/nri.2017.10

Sørensen, O. E., Follin, P., Johnsen, A. H., Calafat, J., Tjabringa, G. S., Hiemstra, P. S., & Borregaard, N. (2001). Human cathelicidin, hCAP-18, is processed to the antimicrobial peptide LL-37 by extracellular cleavage with proteinase 3. *Blood, 97*(12), 3951-3959. doi:10.1182/blood.V97.12.3951 %J Blood

Spinale, F. G., Coker, M. L., Heung, L. J., Bond, B. R., Gunasinghe, H. R., Etoh, T., . . . Crumbley, A. J. J. C. (2000). A matrix metalloproteinase induction/activation system exists in the human left ventricular myocardium and is upregulated in heart failure. *102*(16), 1944-1949.

Steenbergen, C., & Frangogiannis, N. G. (2012). Chapter 36 - Ischemic Heart Disease. In J. A. Hill & E. N. Olson (Eds.), *Muscle* (pp. 495-521). Boston/Waltham: Academic Press.

Stelter, C., Käppeli, R., König, C., Krah, A., Hardt, W. D., Stecher, B., & Bumann, D. (2011). Salmonella-induced mucosal lectin RegIIIβ kills competing gut microbiota. *PLoS One, 6*(6), e20749. doi:10.1371/journal.pone.0020749

Sun, Y., Abbondante, S., Karmakar, M., de Jesus Carrion, S., Che, C., Hise, A. G., & Pearlman, E. (2018). Neutrophil Caspase-11 Is Required for Cleavage of Caspase-1 and Secretion of IL-1β in Aspergillus fumigatus Infection. *The Journal of Immunology*, ji1701195. doi:10.4049/jimmunol.1701195

Swamydas, M., Luo, Y., Dorf, M. E., & Lionakis, M. S. (2015). Isolation of Mouse Neutrophils. *Curr Protoc Immunol, 110*, 3 20 21-23 20 15. doi:10.1002/0471142735.im0320s110

Swift, J., Ivanovska, I. L., Buxboim, A., Harada, T., Dingal, P. C., Pinter, J., . . . Discher, D. E. (2013). Nuclear lamin-A scales with tissue stiffness and enhances matrix-directed differentiation. *Science, 341*(6149), 1240104. doi:10.1126/science.1240104

Swirski, F. K., & Nahrendorf, M. (2018). Cardioimmunology: the immune system in cardiac homeostasis and disease. *Nature Reviews Immunology, 18*(12), 733-744. doi:10.1038/s41577-018-0065-8

Takemura, G., Ohno, M., Hayakawa, Y., Misao, J., Kanoh, M., Ohno, A., . . . Fujiwara, H. (1998). Role of Apoptosis in the Disappearance of Infiltrated and Proliferated Interstitial Cells After Myocardial Infarction. *82*(11), 1130-1138. doi:doi:10.1161/01.RES.82.11.1130

Talman, V., & Kivelä, R. (2018). Cardiomyocyte-Endothelial Cell Interactions in Cardiac Remodeling and Regeneration. *Frontiers in cardiovascular medicine, 5*, 101-101. doi:10.3389/fcvm.2018.00101

Tansho, S., Abe, S., & Yamaguchi, H. (1994). Inhibition of Candida albicans growth by murine peritoneal neutrophils and augmentation of the inhibitory activity by bacterial lipopolysaccharide and cytokines. *Microbiol Immunol, 38*(5), 379-383. doi:10.1111/j.1348-0421.1994.tb01794.x

Terazono, K., Yamamoto, H., Takasawa, S., Shiga, K., Yonemura, Y., Tochino, Y., & Okamoto, H. J. J. o. B. C. (1988). A novel gene activated in regenerating islets. *263*(5), 2111-2114.

Terman, A., Kurz, T., Gustafsson, B., & Brunk, U. T. (2006). Lysosomal labilization. *IUBMB Life, 58*(9), 531-539. doi:10.1080/15216540600904885

Truman, L. A., Ford, C. A., Pasikowska, M., Pound, J. D., Wilkinson, S. J., Dumitriu, I. E., . . . Nibbs, R. J. B., The Journal of the American Society of Hematology. (2008). CX3CL1/fractalkine is released from apoptotic lymphocytes to stimulate macrophage chemotaxis. *112*(13), 5026-5036.

Tsourouktsoglou, T.-D., Warnatsch, A., Ioannou, M., Hoving, D., Wang, Q., & Papayannopoulos, V. (2020). Histones, DNA, and Citrullination Promote Neutrophil Extracellular Trap Inflammation by Regulating the Localization and Activation of TLR4. *Cell Rep, 31*(5), 107602. doi:10.1016/j.celrep.2020.107602

Tsuda, Y., Takahashi, H., Kobayashi, M., Hanafusa, T., Herndon, D. N., & Suzuki, F. (2004). Three different neutrophil subsets exhibited in mice with different susceptibilities to infection by methicillin-resistant Staphylococcus aureus. *Immunity, 21*(2), 215-226. doi:10.1016/j.immuni.2004.07.006

Tufet, M. (2008). Killing neutrophils the cathepsin way. *Nature Reviews Immunology, 8*(4), 244-245. doi:10.1038/nri2298

Udby, L., & Borregaard, N. (2007). Subcellular fractionation of human neutrophils and analysis of subcellular markers. *Methods Mol Biol, 412*, 35-56. doi:10.1007/978-1-59745-467-4_4

Uhl, B., Vadlau, Y., Zuchtriegel, G., Nekolla, K., Sharaf, K., Gaertner, F., . . . Reichel, C. A. (2016). Aged neutrophils contribute to the first line of defense in the acute inflammatory response. *Blood, 128*(19), 2327-2337. doi:10.1182/blood-2016-05-718999

Vaishnava, S., Yamamoto, M., Severson, K. M., Ruhn, K. A., Yu, X., Koren, O., . . . Hooper, L. V. J. S. (2011). The antibacterial lectin RegIIIγ promotes the spatial segregation of microbiota and host in the intestine. *334*(6053), 255-258.

van Amerongen, M. J., Harmsen, M. C., van Rooijen, N., Petersen, A. H., & van Luyn, M. J. (2007). Macrophage depletion impairs wound healing and increases left ventricular remodeling after myocardial injury in mice. *Am J Pathol, 170*(3), 818-829. doi:10.2353/ajpath.2007.060547

van den Borne, S. W., van de Schans, V. A., Strzelecka, A. E., Vervoort-Peters, H. T., Lijnen, P. M., Cleutjens, J. P., . . . Blankesteijn, W. M. (2009). Mouse strain determines the outcome of wound healing after myocardial infarction. *Cardiovasc Res, 84*(2), 273-282. doi:10.1093/cvr/cvp207

van Hout, G. P., Arslan, F., Pasterkamp, G., & Hoefer, I. E. (2016). Targeting danger-associated molecular patterns after myocardial infarction. *Expert Opin Ther Targets, 20*(2), 223-239. doi:10.1517/14728222.2016.1088005

van Pee, K., Neuhaus, A., D'Imprima, E., Mills, D. J., Kühlbrandt, W., & Yildiz, Ö. (2017). CryoEM structures of membrane pore and prepore complex reveal cytolytic mechanism of Pneumolysin. *eLife, 6*, e23644. doi:10.7554/eLife.23644

Vandivier, R. W., Henson, P. M., & Douglas, I. S. (2006). Burying the dead: the impact of failed apoptotic cell removal (efferocytosis) on chronic inflammatory lung disease. *Chest, 129*(6), 1673-1682. doi:10.1378/chest.129.6.1673

Veal, E. A., Day, A. M., & Morgan, B. A. (2007). Hydrogen Peroxide Sensing and Signaling. *Molecular Cell, 26*(1), 1-14. doi:10.1016/j.molcel.2007.03.016

Velten, L., Haas, S. F., Raffel, S., Blaszkiewicz, S., Islam, S., Hennig, B. P., . . . Steinmetz, L. M. (2017). Human haematopoietic stem cell lineage commitment is a continuous process. *Nat Cell Biol, 19*(4), 271-281. doi:10.1038/ncb3493

Venkatakrishnan, V., Dieckmann, R., Loke, I., Tjondro, H., Chatterjee, S., Bylund, J., . . . Karlsson-Bengtsson, A. (2020). Glycan analysis of human neutrophil granules implicates a maturation-dependent glycosylation machinery. 2020.2004.2002.021394. doi:10.1101/2020.04.02.021394 %J bioRxiv

Vignais, P. V. (2002). The superoxide-generating NADPH oxidase: structural aspects and activation mechanism. *Cell Mol Life Sci, 59*(9), 1428-1459. doi:10.1007/s00018-002-8520-9

Violette, S., Festor, E., Pandrea-Vasile, I., Mitchell, V., Adida, C., Dussaulx, E., . . . Lesuffleur, T. J. I. j. o. c. (2003). Reg IV, a new member of the regenerating gene family, is overexpressed in colorectal carcinomas. *103*(2), 185-193.

von Gunten, S., Yousefi, S., Seitz, M., Jakob, S. M., Schaffner, T., Seger, R., . . . Simon, H. U. (2005). Siglec-9 transduces apoptotic and nonapoptotic death signals into neutrophils depending on the proinflammatory cytokine environment. *Blood, 106*(4), 1423-1431. doi:10.1182/blood-2004-10-4112

Wang, F., Gómez-Sintes, R., & Boya, P. (2018). Lysosomal membrane permeabilization and cell death. *Traffic, 19*(12), 918-931. doi:10.1111/tra.12613

Wang, J., Hossain, M., Thanabalasuriar, A., Gunzer, M., Meininger, C., & Kubes, P. (2017). Visualizing the function and fate of neutrophils in sterile injury and repair. *Science, 358*(6359), 111-116. doi:10.1126/science.aam9690

Wang, L. H., Rothberg, K. G., & Anderson, R. G. (1993). Mis-assembly of clathrin lattices on endosomes reveals a regulatory switch for coated pit formation. *J Cell Biol, 123*(5), 1107-1117. doi:10.1083/jcb.123.5.1107

Wang, X., He, Z., Liu, H., Yousefi, S., & Simon, H. U. (2016). Neutrophil Necroptosis Is Triggered by Ligation of Adhesion Molecules following GM-CSF Priming. *J Immunol, 197*(10), 4090-4100. doi:10.4049/jimmunol.1600051

Wang, X., Yousefi, S., & Simon, H. U. (2018). Necroptosis and neutrophil-associated disorders. *Cell Death Dis, 9*(2), 111. doi:10.1038/s41419-017-0058-8

Watson, R. W., Redmond, H. P., Wang, J. H., Condron, C., & Bouchier-Hayes, D. (1996). Neutrophils undergo apoptosis following ingestion of Escherichia coli. *J Immunol, 156*(10), 3986-3992.

Wegmann, F., Petri, B., Khandoga, A. G., Moser, C., Khandoga, A., Volkery, S., . . . Vestweber, D. (2006). ESAM supports neutrophil extravasation, activation of Rho, and VEGF-induced vascular permeability. *The Journal of experimental medicine, 203*(7), 1671-1677. doi:10.1084/jem.20060565

Weirather, J., Hofmann, U. D., Beyersdorf, N., Ramos, G. C., Vogel, B., Frey, A., . . . Frantz, S. J. C. r. (2014). Foxp3+ CD4+ T cells improve healing after myocardial infarction by modulating monocyte/macrophage differentiation. *115*(1), 55-67.

Weis, W. I., Drickamer, K., & Hendrickson, W. A. (1992). Structure of a C-type mannose-binding protein complexed with an oligosaccharide. *Nature, 360*(6400), 127-134. doi:10.1038/360127a0

Werner, F., Jain, M. K., Feinberg, M. W., Sibinga, N. E., Pellacani, A., Wiesel, P., . . . Lee, M. E. (2000). Transforming growth factor-beta 1 inhibition of macrophage activation is mediated via Smad3. *J Biol Chem, 275*(47), 36653-36658. doi:10.1074/jbc.M004536200

Westman, P. C., Lipinski, M. J., Luger, D., Waksman, R., Bonow, R. O., Wu, E., & Epstein, S. E. (2016). Inflammation as a Driver of Adverse Left Ventricular Remodeling After Acute Myocardial Infarction. *J Am Coll Cardiol, 67*(17), 2050. doi:10.1016/j.jacc.2016.01.073

Wilbanks, A., Zondlo, S. C., Murphy, K., Mak, S., Soler, D., Langdon, P., . . . Briskin, M. (2001). Expression Cloning of the STRL33/BONZO/TYMSTR Ligand Reveals Elements of CC, CXC, and CX3C Chemokines. *The Journal of Immunology, 166*(8), 5145. doi:10.4049/jimmunol.166.8.5145

Winterbourn, C. C., Kettle, A. J., & Hampton, M. B. (2016). Reactive Oxygen Species and Neutrophil Function. *Annu Rev Biochem, 85*, 765-792. doi:10.1146/annurev-biochem-060815-014442

Wlodkowic, D., Skommer, J., & Pelkonen, J. (2007). Brefeldin A triggers apoptosis associated with mitochondrial breach and enhances HA14-1- and anti-Fas-mediated cell killing in follicular lymphoma cells. *Leukemia Research, 31*(12), 1687-1700. doi:10.1016/j.leukres.2007.03.008

Wlodkowic, D., Telford, W., Skommer, J., & Darzynkiewicz, Z. (2011). Apoptosis and beyond: cytometry in studies of programmed cell death. *Methods Cell Biol, 103*, 55-98. doi:10.1016/B978-0-12-385493-3.00004-8

Wright, H. L., Moots, R. J., Bucknall, R. C., & Edwards, S. W. (2010). Neutrophil function in inflammation and inflammatory diseases. *Rheumatology (Oxford), 49*(9), 1618-1631. doi:10.1093/rheumatology/keq045

Xu, Y., Loison, F., & Luo, H. R. (2010). Neutrophil spontaneous death is mediated by down-regulation of autocrine signaling through GPCR, PI3Kgamma, ROS, and actin. *Proc Natl Acad Sci U S A, 107*(7), 2950-2955. doi:10.1073/pnas.0912717107

Yago, T., Zarnitsyna, V. I., Klopocki, A. G., McEver, R. P., & Zhu, C. (2007). Transport governs flow-enhanced cell tethering through L-selectin at threshold shear. *Biophys J, 92*(1), 330-342. doi:10.1529/biophysj.106.090969

Yamashita, K., Takahashi, A., Kobayashi, S., Hirata, H., Mesner, P. W., Jr., Kaufmann, S. H., . . . Sasada, M. (1999). Caspases mediate tumor necrosis factor-alpha-induced neutrophil apoptosis and downregulation of reactive oxygen production. *Blood, 93*(2), 674-685.

Yan, X., Anzai, A., Katsumata, Y., Matsuhashi, T., Ito, K., Endo, J., . . . Sano, M. (2013). Temporal dynamics of cardiac immune cell accumulation following acute myocardial infarction. *J Mol Cell Cardiol, 62*, 24-35. doi:10.1016/j.yjmcc.2013.04.023

Yang, F., Liu, Y. H., Yang, X. P., Xu, J., Kapke, A., & Carretero, O. A. (2002). Myocardial infarction and cardiac remodelling in mice. *Exp Physiol, 87*(5), 547-555. doi:10.1113/eph8702385

Yap, B., & Kamm, R. D. (2005). Mechanical deformation of neutrophils into narrow channels induces pseudopod projection and changes in biomechanical properties. *98*(5), 1930-1939. doi:10.1152/japplphysiol.01226.2004

Yellon, D. M., & Hausenloy, D. J. (2007). Myocardial reperfusion injury. *N Engl J Med, 357*(11), 1121-1135. doi:10.1056/NEJMra071667

Yipp, B. G., Kim, J. H., Lima, R., Zbytnuik, L. D., Petri, B., Swanlund, N., . . . Kubes, P. (2017). The Lung is a Host Defense Niche for Immediate Neutrophil-Mediated Vascular Protection. *Sci Immunol, 2*(10). doi:10.1126/sciimmunol.aam8929

Yoshii, S. R., & Mizushima, N. (2017). Monitoring and Measuring Autophagy. *International journal of molecular sciences, 18*(9), 1865. doi:10.3390/ijms18091865

Yu, Z., Persson, H. L., Eaton, J. W., Brunk, U. T. J. F. R. B., & Medicine. (2003). Intralysosomal iron: a major determinant of oxidant-induced cell death. *34*(10), 1243-1252.

Yuan, S. Y., Shen, Q., Rigor, R. R., & Wu, M. H. (2012). Neutrophil transmigration, focal adhesion kinase and endothelial barrier function. *Microvascular Research, 83*(1), 82-88. doi:10.1016/j.mvr.2011.06.015

Zarbock, A., Ley, K., McEver, R. P., & Hidalgo, A. (2011). Leukocyte ligands for endothelial selectins: specialized glycoconjugates that mediate rolling and signaling under flow. *Blood, 118*(26), 6743-6751. doi:10.1182/blood-2011-07-343566 %J Blood

Zelensky, A. N., & Gready, J. E. J. T. F. j. (2005). The C-type lectin-like domain superfamily. *272*(24), 6179-6217.

Zhao, W., Zhao, D., Yan, R., & Sun, Y. (2009). Cardiac oxidative stress and remodeling following infarction: role of NADPH oxidase. *Cardiovasc Pathol, 18*(3), 156-166. doi:10.1016/j.carpath.2007.12.013

Zhao, W., Zhao, T., Chen, Y., Ahokas, R. A., & Sun, Y. (2009). Reactive oxygen species promote angiogenesis in the infarcted rat heart. *Int J Exp Pathol, 90*(6), 621-629. doi:10.1111/j.1365-2613.2009.00682.x

Zhou, E., Conejeros, I., Velasquez, Z. D., Munoz-Caro, T., Gartner, U., Hermosilla, C., & Taubert, A. (2019). Simultaneous and Positively Correlated NET Formation and Autophagy in Besnoitia besnoiti Tachyzoite-Exposed Bovine Polymorphonuclear Neutrophils. *Front Immunol, 10*, 1131. doi:10.3389/fimmu.2019.01131

Zhu, Q., Han, X., Peng, J., Qin, H., & Wang, Y. (2012). The role of CXC chemokines and their receptors in the progression and treatment of tumors. *Journal of Molecular Histology, 43*(6), 699-713. doi:10.1007/s10735-012-9435-x

Zimmerli, W., Seligmann, B., & Gallin, J. I. (1986). Exudation primes human and guinea pig neutrophils for subsequent responsiveness to the chemotactic peptide N-formylmethionylleucylphenylalanine and increases complement component C3bi receptor expression. *J Clin Invest, 77*(3), 925-933. doi:10.1172/jci112391

Zouggari, Y., Ait-Oufella, H., Bonnin, P., Simon, T., Sage, A. P., Guérin, C., . . . Mallat, Z. (2013). B lymphocytes trigger monocyte mobilization and impair heart function after acute myocardial infarction. *Nat Med, 19*(10), 1273-1280. doi:10.1038/nm.3284

9 List of figures and tables

10 List of abbreviations

µm	Microgram
3D	Three-dimensional
A/O	Acridine orange
Asp	Asparagine
ATP	Adenosin tri phosphate
BSA	Bovine serum albumin
BW	Body weight
C5a	Complement component 5a
Ca^{2+}	$Calcium^{2+}$
CABG	Thrombolysis and coronary artery bypass graft
CGD	Chronic granulomatous diseases
CM-H_2DCFDA	Chloromethyl derivative of 2',7'-dichlorodihydrofluorescein diacetate
CO_2	Carbon Dioxide
CTLD	C-type-like lectin domain
CXCL	C-X-C motif chemokine ligand
CXCR	C-X-C chemokine receptor
DAMP	Danger associated molecular pattern
DAPI	4’,6-Diamidin-2-phenylindol
DC	Dendritic cells
dH_2O	Destilled water
DHR123	Dihydrorhodamine 123
DMEM	Dulbecco’s modified medium
DMSO	Dimethyl sulfoxide
DPI	Diphenyleneiodonium chloride
DTT	Dithiothreitol
ECi	Ethylcinnamate
ECM	Extracellular matrix
EXTL3	Exostosin-like glycosyltransferase 3
FCS	Fetal calw serum
fMLP	N-formylmethionyl-leucyl-phenylalanine
FSC	Forward scatter
G-CSF	Granulocyte colony-stimulating factor

GM-CSF	Granulocyte-macrophage colony-stimulating factor
h	Hour
HEPES	4-(2-hydroxyethyl)-1-piperazineethanesulfonic acid
HMBG1	High-mobility group box 1
HRP	horseradish peroxidase
HSP	Heat shock protein
i.p.	Intraperitoneal
i.v.	Intravenous
I/R	Ischemia reperfusion
IFNγ	Interferon gamma
IL	Interleukin
IP10	Interferon gamma induced protein 10
IZ	Infarct zone
LAD	Left anterior descending coronary artery
LAMP1	Lysosome-associated membrane protein 1
LAP	Latency-associated peptide
LDCD	Lysosomal-dependent cell death
LDH	Lactate dehydrogenase
LMP	Lysosomal membrane permeabilization
LPS	Lipopolysaccharide
LTB4	Leukotriene B4
LTR	LysoTracker
LV	Left ventricle
MAPK	Mitogen-activated protein kinase
MDAC	Monodansylcadaverine
MerTK	Proto-oncogene tyrosine-protein kinase MER
MFI	Mean fluorescence intensity
mg	Milligram
MI	Myocardial infarction
min	Minutes
MIP-2α	Macrophage inflammatory protein-2 alpha
MMP	Matrix metalloproteinase
MPO	Myeloperoxidase
MβCD	Methyl-β-cyclodextrin

NE	Neutrophil elastase
NET	Neutrophil extracellular trap
NeuAc	Neuraminic acid
ng	Nanogram
NGAL	Neutrophil gelatinase-associated lipocalin
NK cells	Natural killer cells
NOX2	NADPH oxidase 2
O/N	Over night
P/S	Penicillin/Streptavidin
PAMP	Pathogen-associated molecular pattern
PBS	Phosphate-buffered saline
PCI	Percutaneous coronary intervention
PECAM-1	Platelet endothelial cell adhesion molecule 1
PFA	Paraformaldehyde
PICD	Phagocytosis-induced cell death
PKC	Protein kinase C
PMA	Phorbol-12-myristat-13-acetat
PMN	Polymorphonuclear
PS	Phosphatidylserine
PSGL-1	Selectin P ligand 1
Reg3β	Regenerating islet-derived protein 3 beta
ROS	Reactive oxygen species
RT	Room temperature
RZ	Remote zone
SDF-1	Stromal cell-derived factor 1
SDS	Sodium dodecyl sulfate
SEM	Scanning electron microscopy
Ser/Thr	Serine/Threonine
SOD	Sodium dismutase
SSC	Sideward scatter
TEM	Transmission electron microscopy
TGFβ	Transforming growth factor β
TIMP	Tissue inhibitor of metalloproteinase
TNFα	Tumor necrosis factor α

T_{reg}	Regulating T-cells
VEGF-A	Vascular endothelial growth factor A
WGA	Wheat germ agglutinin
WT	Wild-type

11 Selbstständigkeitserklärung

Hiermit versichere ich, die vorgelegte Thesis selbstständig und ohne unerlaubte fremde Hilfe und nur mit den Hilfen angefertigt zu haben, die ich in der Thesis angegeben habe. Alle Textstellen, die wörtlich oder sinngemäß aus veröffentlichten Schriften entnommen sind, und alle Angaben die auf mündlichen Auskünften beruhen, sind als solche kenntlich gemacht. Bei den von mir durchgeführten und in der Thesis erwähnten Untersuchungen habe ich die Grundsätze gute wissenschaftlicher Praxis, wie sie in der ‚Satzung der Justus-Liebig-Universität zur Sicherung guter wissenschaftlicher Praxis' niedergelegt sind, eingehalten. Gemäß § 25 Abs. 6 der Allgemeinen Bestimmungen für modularisierte Studiengänge dulde ich eine Überprüfung der Thesis mittels Anti-Plagiatssoftware.

Bad Nauheim, den 15.10.2020_____

(Julia Detzer)

12 Publications and scientific presentations

12.1 Peer-reviewed publications

Merz SF, Korste S, Bornemann L, Michel L, Stock P, Squire A, Soun C, Engel DR, **Detzer J**, Lörchner H, Hermann DM, Kamler M, Klode J, Hendgen-Cotta UB, Rassaf T, Gunzer M, Totzeck M. (2019). Publisher Correction: Contemporaneous 3D characterization of acute and chronic myocardial I/R injury and response. *Nat Commun, 10(1)*, 2312. doi:10.1038/s41467-019-10804-2

Lörchner H, Hou Y, Adrian-Segarra JM, Kulhei J, **Detzer J**, Günther S, Gajawada P, Warnecke H, Niessen HW, Pöling J, Braun T. (2018). Reg proteins direct accumulation of functionally distinct macrophage subsets after myocardial infarction. *Cardiovasc Res, 114(12)*, 1667-1679. doi: 10.1093/cvr/cvy126

12.2 Scientific presentations

Poster Presentations:

2019 Internal meeting MPI-HLR, Bad Marienberg, Germany

2019 IMPRS graduate school retreat, Hohenroda, Germany

2018 The Neutrophil International Symposium, Quebec City, Canada

2018 Internal meeting MPI-HLR, Bad Marienberg, Germany

2017 IMPRS graduate school retreat, Kreuth, Germany

Oral Presentations:

2019 IMPRS graduate school evaluation, Bad Nauheim, Germany

2018 IMRPS graduate school retreat, Bad Weilburg, Germany

13 Acknowledgment

At first, I would like to express my sincere gratitude to my supervisor Prof. Dr. Dr. Thomas Braun for his invaluable guidance and support throughout the whole time. Special thanks deserve my direct supervisors PD Dr. Jochen Pöling and Dr. Holger Lörchner for their continuous support, encouragement and all of the opportunities they gave me to conduct my research.

I would also like to thank Prof. Dr. Michael Martin for his valuable mentoring in my thesis committee and his insightful comments and support.

I would like to express my appreciation for Ann Atzberger, Kerstin Richter and Kikhi Khrievono for their exceptional assistance and commitment in the FACS facility.

I am very grateful for the excellent collaboration with Prof. Dr. Matthias Gunzer, Dr. Simon Merz and Dr. Sebastian Korste from the university of Duisburg-Essen for the light sheet microscopy, for the collaboration with Dr. Özkan Yildiz and Saskia Mehlmann from the MPI for Biophysics in Frankfurt for the negative stain electron microscopy and for the help of PD Dr. Ulrich Gärtner and Anika Seipp for transmission and scanning electron microscopy.

To all the colleagues and friends from the institute, thank you so much for your support and motivation and the wonderful time we spend together. Special thanks goes to my group, Jochen, Holger, Roxy, Maria and Nathalie, to Kerstin for helping me out with Haribo, and to Melissa, without whom I would not have gotten that far. And of course, I want to thank my family for everything.